

RIVM report 728001022/2002

**Responsibility for past and future global
warming: time horizon and non-linearities in
the climate system**

M.G.J. den Elzen, M. Schaeffer and B. Eickhout

This research was conducted for the Dutch Ministry of Environment as part of the Climate Change Policy Support Project (M/728001 Ondersteuning Klimaatbeleid).

Abstract

The Brazilian proposal for sharing the burden of emissions reductions among Annex-I Parties is based on the relative effect of a country's emissions on the global-mean surface-air temperature. This paper presents calculations of these relative effects, analysing the influence of the time horizon of emissions and of including non-linearities in the global carbon cycle.

The analysis shows that an early start date for historical emissions increases the Annex-I contributions to global warming. Choosing an end date of emissions relatively late in time increases non-Annex-I contributions, giving more weight to their larger share in 21st century emissions. Delayed effects of global warming can be taken into account, if contributions are calculated some time after the emission end date. A calculation date long after the emission end date reduces non-Annex-I contributions, mainly because of their relative large share of relatively short-lived methane in total emissions.

Our proposal for a new 'non-linear', but transparent, approach for attributing CO₂ concentrations generally reduces Annex-I contributions. The impact is larger than that of including non-linearity in radiative forcing ('saturation effect'). The latter effect increases in time, until the two effects almost cancel out near the end of the 21st century.

The analyses were performed for several aggregations of parties in the climate convention (Annex-I/non-Annex-I, 4 IPCC SRES regions, or 17 smaller RIVM IMAGE-regions). We found considerable heterogeneity within aggregated IPCC groups, so that general conclusions drawn for groups as a whole often do not apply to the individual regions within the groups.

Summary

During the Kyoto Protocol negotiations, Brazil presented an approach for sharing the burden of emissions reductions among Annex-I Parties. This sharing is based on the relative effect of a country's emissions on the global-mean surface-air temperature. In UNFCCC context, it was also suggested to use this approach for assigning contributions to a global adaptation fund. This paper describes the RIVM contribution to the UNFCCC project 'Assessment of Contributions to Climate Change', focusing on the time horizon of emissions and the influence of including non-linearities in the global carbon cycle in the calculations.

The analysis presented here shows that an early start date for historical emissions increases the Annex-I contributions to global warming. Choosing an end date of emissions relatively late in time increases non-Annex-I contributions, because of the increasing share in global emissions in the 21st century. If contributions are calculated at a point in time after the emission end date, delayed effects of global warming are accounted for. Choosing an evaluation date long after the emission end date reduces non-Annex-I contributions, mainly because of their relative large share of methane in total emissions, combined with the short atmospheric residence time of methane.

In addition, we propose a new, transparent approach for attributing CO₂ concentrations, which provides a way for attributing (non-linear) global removal processes of CO₂ from the atmosphere to emission regions. Adopting this approach generally increases non-Annex-I contributions. The impact is larger than the impact of including non-linearity in radiative forcing ('saturation effect'). Since the two effects are opposite and the effect of non-linear forcing increases in time, the effects almost cancel out each other near the end of the 21st century.

For the IPCC SRES regions, the strongest influence on contributions to global warming in 2000 is exerted by the choice of emission sources included or excluded (fossil CO₂ only, all anthropogenic CO₂, or all Kyoto gases). The time horizons and choice of indicator for global warming (CO₂ concentrations, radiative forcing, temperature increase, or sea level rise) have the second largest impact. Non-linear attribution of CO₂ concentrations and an alternative historical emissions database also are a major factor, while non-linear attribution of radiative forcing is less important. With the emissions end date set to 2050, non-linearities become much more important, while the impact of historical emissions is reduced. The future emissions scenario emerges as an influential choice. We found considerable heterogeneity within aggregated IPCC groups, so that general conclusions drawn for groups as a whole do not apply to the individual regions within the groups.

Contents

Samenvatting	9
Introduction	11
1. Attributing anthropogenic climate change	13
1.1. <i>Aim and methodology of the analysis</i>	13
1.2. <i>Modelling approach</i>	14
2. Contributions to various climate-change indicators	19
3. Sensitivity analysis of contributions to climate change	25
3.1. <i>The timeframe of emissions</i>	25
3.1.1. <i>The impact of time horizon historical emissions (start date)</i>	28
3.1.2. <i>The impact of time horizon future emissions (end date)</i>	30
3.1.3. <i>The impact of calculation evaluation date</i>	31
3.2. <i>Non-linearities in the climate change cause-and-effect chain</i>	34
3.2.1. <i>The impact of the non-linear approach to attributing CO₂ concentrations</i>	35
3.2.2. <i>The impact of the non-linear approach to attributing radiative forcing</i>	39
3.2.3. <i>Combining alternatives for calculating contribution to radiative forcing and CO₂ concentration</i>	40
4. Conclusions	41
References	45
Appendix A Mailing list	49
Appendix B UNFCCC-ACCC Terms of Reference	51
Appendix C Model description of IMAGE-AOS and ACCC	55
Appendix D Calculation of contributions of emission regions	59
Appendix E RIVM results Phase 1 of UNFCCC-ACCC	61
Appendix F Numerical data	63

Samenvatting

Tijdens de onderhandelingen voor het Kyoto Protocol presenteerde de Braziliaanse delegatie een benadering om totale emissiereducties te verdelen onder Annex-I landen. Het basisidee van de methode is dat elk land een percentage bijdraagt aan de totale emissiereductie, gelijk aan het percentage dat dit land bijdraagt aan de totaal gerealiseerde klimaatverandering. In UNFCCC context is ook voorgesteld om een degelijke berekeningsmethode te gebruiken als basis voor contributies aan een mondiaal adaptatie fonds. Dit rapport beschrijft de RIVM bijdrage aan het UNFCCC project 'Assessment of Contributions to Climate Change', gericht op de evaluatie van de tijdschik van de analyse en op de invloed van niet-lineariteiten in de mondiale koolstofcyclus.

De analyse laat zien dat naar mate de historische emissies vanaf een vroeger tijdstip worden meegenomen de bijdrage van Annex-I regio's aan totale klimaatverandering in 2000 hoger wordt. Als het eindjaar verder in de toekomst wordt gekozen, dan neemt de bijdrage van niet-Annex-I landen toe, vanwege sterk groeiende emissies in de 21^{ste} eeuw. Door het evaluatiejaar te kiezen later dan het eindjaar van de emissies worden ook de vertraagde klimaateffecten van emissies meegenomen. Hoe groter het gat tussen eindjaar en evaluatiejaar, hoe meer de bijdrage van niet-Annex-I landen afneemt, met name door het relatief grote aandeel van methaan in de totale emissies, met een korte verblijftijd in de atmosfeer.

Om rekening te kunnen houden met niet-lineaire processen in de koolstofcyclus, wordt in dit rapport een nieuwe transparante methode voorgesteld om de bijdrage van landen aan de totale verhoogde CO₂ concentratie te berekenen. Bij gebruik van deze methode wordt de bijdrage van Annex-I landen kleiner. Het effect is groter dan het effect van niet-lineaire stralingsforcering door CO₂ (verzadiging), met tegengesteld teken. Aangezien het verzadigingseffect toeneemt in de tijd, heffen de twee effecten elkaar op tegen het eind van de 21^{ste} eeuw.

Voor de IPCC regio's heeft de keuze van emissiebronnen die worden meegenomen in de analyse (alleen fossiel CO₂, alle CO₂ of alle Kyoto gassen) de grootste invloed of de bijdrage per regio aan mondiale klimaatverandering in 2000. Daarnaast hebben ook de tijdschik en keuze van indicator voor klimaatverandering (CO₂ concentratie, stralingsforcering, temperatuurstijging, of zeespiegelstijging) een grote invloed. Niet-lineariteiten in de koolstofcyclus hebben een kleinere invloed, terwijl niet-lineariteit in stralingsforcering nog onbelangrijk is. Bij het berekenen van bijdragen in 2050 spelen niet-lineariteiten wel een rol. Voor alle onderzochte onderwerpen geldt dat er aanzienlijke heterogeniteit bestaat binnen geaggregeerde IPCC groepen. Daardoor gelden algemene conclusies met betrekking tot groepen als geheel niet voor elke kleinere emissie-eenheid (land) daarbinnen.

Introduction

During the negotiations of the Kyoto Protocol, the delegation of Brazil presented an approach for distributing the burden of emissions reductions among Annex I Parties based on the effect of their cumulative historical emissions, from 1840 onwards, on the global-average surface temperature (UNFCCC, 1997). Although the proposal was initially developed to help discussions on differentiation of future commitments among Annex I countries, it can also be used as a framework for discussions between Annex I and non-Annex I countries on future participation of all countries in emission reductions. During the Kyoto negotiations the Brazilian Proposal was not adopted, but did receive support, especially from developing countries. The Third Conference of the Parties (COP-3) requested the Subsidiary Body on Scientific and Technical Advice (SBSTA) of the United Nations Framework Convention on Climate Change (UNFCCC) to further study the methodological and scientific aspects of the proposal.

As a starting point, the Brazilian proposal concentrates on contributions of emissions to global mean surface-air temperature increase (henceforth known simply as 'temperature increase'). During the initial discussion at the SBSTA-8 meeting in February 1998, some participants suggested considering the contribution of emissions to the rate of temperature increase and sea level rise as well. At COP-4 in Buenos Aires in November 1998, SBSTA-9 noted the information provided by Brazil on recent scientific activities, including a revision of the methodology (Filho and Miguez, 1998). Since COP-3 several groups in various countries, including China, Canada, France, the United States of America, Australia and the Netherlands, have assessed the Brazilian proposal and its analysis, and found similar deficiencies both in the original proposal and its analysis (e.g. Enting, 1998; Berk and Den Elzen, 1998). Further research concluded that in the revised Brazilian methodology (Filho and Miguez, 1998) most of these deficiencies were adequately addressed (e.g., Den Elzen et al., 1999; Den Elzen and Schaeffer, (2002)). During a first expert meeting at COP-4 it was concluded that the scientific and technical basis for putting the Brazilian proposal into operation would be sufficient (UNFCCC, 1999). During the second expert meeting in 2001, organised by the UNFCCC secretariat, the SBSTA encouraged Parties to pursue and support the research effort on the scientific and methodological aspects of the Brazilian proposal (UNFCCC, 2001) and to communicate such activities to the secretariat. The SBSTA requested the secretariat to continue to co-ordinate the review of this proposal, to organise the third expert meeting to review the scientific and methodological aspects of the proposal by Brazil, to broaden participation in emission reduction regimes and to build scientific understanding of this subject before its seventeenth session (November 2002).

To this end, the secretariat encourages research institutions active in the field of climate change modelling to participate in a co-ordinated modelling exercise (UNFCCC, 2002). Primary objective of this exercise is to generate new and comparable results that could be discussed at an expert meeting in September 2002. The results of this UNFCCC project entitled 'Assessment of Contributions to Climate Change' (ACCC) will be discussed at the third expert meeting. The UNFCCC secretariat will provide a summary of the workshop for consideration at SBSTA-17. Details of this exercise are described in a Terms of Reference (UNFCCC, 2002) (ACCC-TOR, included in Appendix B).

In this paper, the Dutch RIVM contribution to ACCC, we will focus on two issues. Firstly, a new interesting element, compared to the original Brazilian proposal, is the timeframe of the attribution calculations. Variations are possible in the length of the period over which historical emissions are taken into account. In addition, contributions can be calculated for an evaluation date some time after the emissions end date, so that future, or

delayed, effects are included, as well as the different atmospheric decay rates of the various greenhouse gases. In this way, the climate indicator is ‘backward looking’ (takes into account historical emissions), ‘backward discounting’ (early emissions weigh less depending on the decay in the atmosphere) and ‘forward looking’ (future effects of the emissions are considered). Note that the latter two offer a parallel to using GWPs for calculating the relative (future) effect of emissions (see section 3). The time-frame parameters are illustrated in figure 1.

The second issue assessed in this paper is the sensitivity of attribution calculations to non-linearities at various points in the cause-and-effect chain of the climate change. We will assess the influence on the attribution calculations when including or excluding two non-linearities. Our evaluation analyses the influence of non-linear radiative forcing in the attribution, as put forward by (Enting, 1998), see also (Den Elzen and Schaeffer, 2002). In addition, we will present a new methodology of calculating the contribution of emission regions to total atmospheric CO₂ concentration. The alternative method provides a way of attributing (non-linear) global removal processes of CO₂ from the atmosphere to emission regions. In contrast, for the ACCC default, removal rates are based on carbon cycle calculations for each region in isolation. Emissions from other regions, or changes in atmospheric residence time of CO₂ (non-linearities) resulting from global emissions have no influence. The alternative attribution method also allows for the use of a different (non-linear) carbon-cycle model, which includes projections of the (increasing) domination of the land biosphere by anthropogenic influences (land use, deforestation, reforestation, afforestation).

This paper is built up as follows. Section 1 describes the aim, methodology and modelling approach of the analysis. Section 2 presents an analysis of contributions for various groups of countries for the different indicators, like emissions, concentrations, temperature change and sea level rise. Section 3 analyses the impact of time frame and non-linearities on the attribution projections, using temperature change as indicator. Section 4 concludes our evaluation.

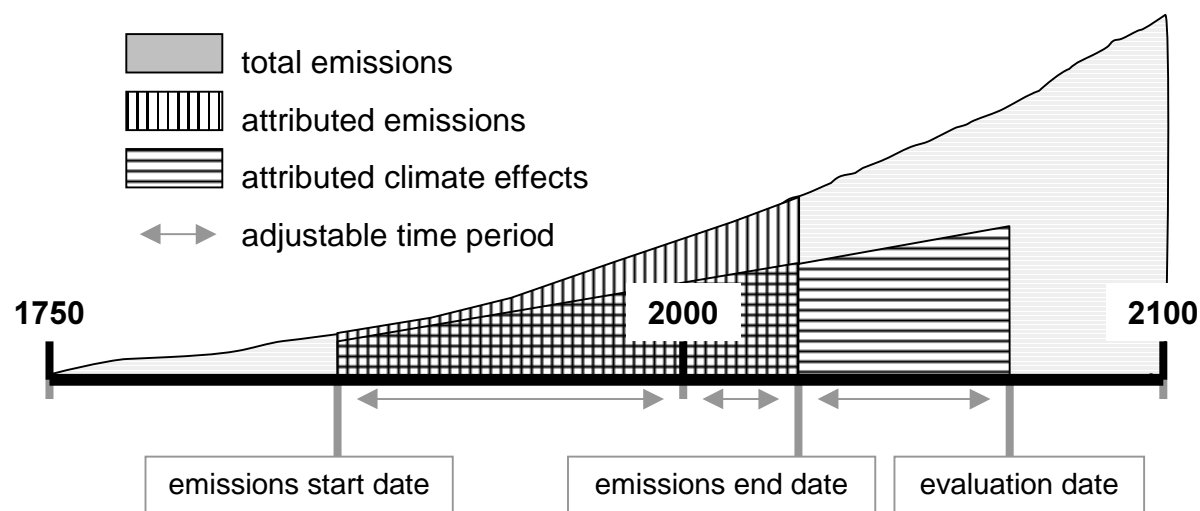


Figure 1. Illustration of time-frame parameters.

1. Attributing anthropogenic climate change

1.1. Aim and methodology of the analysis

Details of the ACCC project are described in a Terms of Reference (UNFCCC, 2002) (ACCC-TOR, included in Appendix B) and cover the issues of historical emissions data, future emissions scenarios, timeframe of calculations, regions, model parameters for the carbon cycle and climate models, and indicators of climate change. The project consists of two phases. In phase 1, the participating groups* should demonstrate the ability of their simple models to reproduce the global mean results of more complex carbon cycle, atmospheric chemistry and climate models. To this end, concentrations of greenhouse gases, radiative forcing, temperature increase should be calculated, using an agreed set of parameters, for historical emissions and the A2 future emission scenario from the Intergovernmental Panel on Climate Change (IPCC) Special Report on Emission Scenarios (SRES, (Nakicenovic et al., 2000)). Data on global mean indicators from our ACCC default model implementation have been provided as the Dutch RIVM contribution to Phase 1 of the ACCC exercise and are included in Appendix E.

In phase 2, the results should be presented in terms of the contribution made by four country groups (OECD90, Eastern Europe and Former Soviet Union, Asia, and Africa, Latin America and the Middle East) and the sensitivity of simple model results to changes in model parameters should be analysed. All participants were required to undertake one run with the default model configuration. The methodology of calculations for phase 2 as described in ACCC-TOR differs from the original Proposal with respect to the inclusion of historical anthropogenic non-CO₂ greenhouse gas emissions and CO₂ emissions from land use changes, future emissions scenarios, non-Annex I regions, other climate indicators besides global temperature increase as well as an improved methodology.

In a previous analysis, Den Elzen and Schaeffer (2002) assessed in detail the sensitivity of attribution calculations to a range of scientific uncertainties (see Text Box). Rather than repeating such analysis for ACCC phase 2, we focus here on calculations using different indicators (section 2) and on the following two sensitivity experiments. Firstly (section 3.1), we will assess the sensitivity of choosing various emissions start, end and evaluation dates, as defined in the introduction. In this timeframe analysis, we will also pay some attention to the impact of various historical emissions databases, including the update of the EDGAR-HYDE 1.4 historical emissions database (Olivier and Berdowski, 2001; Van Aardenne et al., 2001), and future emission scenarios of the IPCC SRES (Nakicenovic et al., 2000). Secondly (section 3.2), we will assess the sensitivity of the attribution calculations to including or excluding non-linearities in calculating CO₂ concentrations and radiative forcing, as explained in the introduction.

For the calculations, our IMAGE 2.2 Atmosphere Oceanic System (IMAGE-AOS) submodels are used, i.e. the oceanic carbon cycle, atmospheric chemistry and climate models (Eickhout et al., 2002), supplemented with a 'attribution' model to calculate the regional contributions. For the default calculations we have included the ACCC-TOR impuls response functions for the global carbon cycle and surface-air temperature response. For easier comparison with results of other modelling groups, we have decided to present our results by

* Participating Institutes as of July 2002: Battelle, USA; CICERO, Norway; CRG (UIUC) USA; Climatic Research Unit (CRU), UK; CSIRO, Australia; DEA (DEA-CCAT), Denmark; Fabian International Energy Studies Group (LBNL), USA; Federal University of Rio de Janeiro, Brazil; Hadley Centre, UK; EPA, USA; Institute of Applied Energy (IAE), Japan; Klima und Umwelt Physik, Switzerland; Ministry of Science and Technology, Brazil; National Institute for Public Health and Environment (RIVM), The Netherlands; NIWA, New Zealand; Research Institute of Innovative Technology for the Earth (RITE), Japan; UCL-ASTR, Belgium; UIUC, USA.

default only for the model configuration as defined in ACCC-TOR. Because the principle conclusions of the analysis also hold for IMAGE-AOS, we refer to the tables in Appendix F for results of this model. When we compare the effects of different carbon-cycle models in section 3.2, we will also present IMAGE-AOS results. The overall set of climate models forms the climate assessment model, as integral part of the overall FAIR 1.1 model (Framework to Assess International Regimes for differentiation of future commitments). The FAIR 1.1 model was developed to explore options for international differentiation of future commitments, including the Brazilian approach (Den Elzen et al., 1999; Den Elzen et al., 2001; Den Elzen, 2002).

1.2. Modelling approach

In this section, we will briefly discuss the modelling approach of IMAGE-AOS (also meta-IMAGE 2.2) in FAIR and the ‘default model’ as defined in ACCC-TOR (from here on referred to simply as ‘ACCC’, Appendix B). Details of both models, equations and parameter settings, can be found in Appendix C. Equations used for the calculations of contributions of emission regions to global concentrations, radiative forcing, temperature change and sea level rise are included in Appendix D.

Meta-IMAGE 2.1 was discussed in detail in (Den Elzen and Schaeffer, 2002). Some important changes have been made, forming an update to meta-IMAGE 2.2, or IMAGE-AOS. Basically, the oceanic carbon cycle, atmospheric chemistry and climate model are replaced by the corresponding AOS components of IMAGE 2.2 (Eickhout et al., (2002). The atmospheric chemistry model uses single fixed lifetimes for the atmospheric decay of non-CO₂ gases, except for CH₄, HCFCs and HFCs, for which dependencies on the concentration of the OH radical are included (based on the IPCC-TAR (Third Assessment Report) methodology of (Prather et al., 2001)). The default climate model is the Upwelling-Diffusion Climate Model (UDCM) based on the MAGICC-model (Wigley and Schlesinger, 1985; Hulme et al., 2000; Raper et al., 2001). The global carbon cycle is modelled using a mass balance equation, with a carbon flux between atmosphere and with natural vegetation (NEP, Net Ecosystem Productivity) as exogenous input, using data from scenario runs with IMAGE 2.2 (IMAGE-team, 2001). This includes changes in terrestrial uptake resulting from global warming and changes in ambient CO₂ concentration, as well as anthropogenic land use and land cover changes. The oceanic uptake is calculated with the oceanic carbon model of IMAGE 2.2 (Eickhout et al., 2002), i.e. the box-diffusion type model of Joos et al. (Joos et al., 1996; 1999). IMAGE-AOS forms the core of the climate assessment module in FAIR 1.1, with the possibility of using alternative modules.

One alternative model configuration is as specified in ACCC-TOR. Here, Impulse Response Functions (IRFs) are used in convolution integrals for concentrations, temperature change and sea level rise. For CO₂, four independent carbon pools are defined with fixed lifetimes, whereas single-fixed lifetimes are defined for non-CO₂ gases. For both temperature change and sea level rise, two-term IRFs were fit to data from a 900 years long experiment using the HadCM3 Coupled General Circulation climate Model (CGCM).

Contributions of emission regions to climate change indicators like greenhouse gas concentration, radiative forcing, temperature change and sea level rise are calculated for ACCC by applying all equations defined at global level to the emissions of the individual emitting regions separately. Linearity of the equations ensures that global totals are correct. For example, the total global concentration ρ_{CO_2} of CO₂ for evaluation date t is a simple sum of concentration contributions from R regions at time t , plus a pre-industrial (‘background’) concentration ρ_{pi} :

$$\rho_{CO_2}^{global}(t) = \sum_{r=1}^R \rho_{CO_2}^r(t) + \rho_{CO_2,pi} = C_{CO_2} \sum_{r=1}^R \int_{t_0}^t IRF(t-t') \cdot E_{CO_2}^r(t') dt' + \rho_{CO_2,pi} \quad (1)$$

where C_{CO_2} is a conversion factor for emissions to concentrations and the impulse response function $IRF(t)$ is defined in Appendix C, with the integral starting at emissions start date t_0 .

Thus, in this approach, the global carbon cycle is divided into R hypothetical independent carbon pools, or isolated boxes, one for each emitting region, described by the same C-cycle model and parameters. The global total is simply the linear addition of contributions by all isolated region boxes. We will term this the 'linear approach' of concentration attribution. Concentrations and removal rates for region r in this approach only depend on (anthropogenic) emission (history) of this one region, not on emissions of other regions. In reality, there is only one global carbon cycle, of course. The following alternative calculation of regional attribution to global CO_2 concentrations appreciates this. For convenience the CO_2 subscript and the explicit time-dependency of concentrations and emissions is omitted in the notation, e.g. the time-varying CO_2 concentration $\rho_{CO_2}(t)$ is simply expressed as ρ below.

The change in global CO_2 concentrations (time derivative) is broken down into two factors

$$\dot{\rho}^{global} = \dot{\rho}_+^{global} - \dot{\rho}_-^{global} \quad (2)$$

The increase term $\dot{\rho}_+^{global}$ is a function of global emissions:

$$\dot{\rho}_+^{global} = C_{CO_2} E^{global} \quad (3)$$

The removal term $\dot{\rho}_-^{global}$ is given by the (non-linear) global carbon-cycle processes that remove CO_2 from the atmosphere. Combining (2) and (3) gives:

$$\dot{\rho}_-^{global} = \dot{\rho}_+^{global} - \dot{\rho}^{global} = C_{CO_2} E^{global} - \dot{\rho}^{global} \quad (4)$$

The change in concentration for region r is now also split into increase and decrease terms. The increase term $\dot{\rho}_+^r$ is now a function of the emissions of this region only, $\dot{\rho}_+^r = C_{CO_2} E^r$. The decrease term $\dot{\rho}_-^r$ is given by the global removal term $\dot{\rho}_-^{global}$ scaled by the contribution to global concentrations of region r :

$$\dot{\rho}_-^r = \frac{\rho^r}{\rho^{global}} \dot{\rho}_-^{global} \quad (5)$$

Thus $\dot{\rho}^r = \dot{\rho}_+^r - \dot{\rho}_-^r = C_{CO_2} E^r - \frac{\rho^r}{\rho^{global}} \dot{\rho}_-^{global}$ (6)

Combining (4) and (6) gives:

$$\dot{\rho}^r = C_{CO_2} E^r - \frac{\rho^r}{\rho^{global}} (C_{CO_2} E^{global} - \dot{\rho}^{global}) = C_{CO_2} E^r - \rho^r \frac{C_{CO_2} E^{global} - \dot{\rho}^{global}}{\rho^{global}} \quad (7)$$

We now define $\tau(t)^*$ as a time-depending global single 'effective' lifetime, or rather instantaneous turnover time, of the excess CO_2 mass in the atmosphere by:

$$\dot{\rho}^{global} = C_{CO_2} E^{global} - \rho^{global} / \tau(t) \Leftrightarrow \tau(t) = \frac{\rho^{global}}{C_{CO_2} E^{global} - \dot{\rho}^{global}} \quad (8)$$

Combining (7) and (8r) gives:

$$\dot{\rho}^r = C_{CO_2} E^r - \rho^r / \tau(t) \quad (9)$$

Thus this alternative approach of attributing the removal term of CO_2 in the global carbon cycle to the individual regions is equivalent to applying a single time-varying global turnover

* To stress the time dependence of effective global lifetime, its dependence on time (t) is made explicit in the notation.

time to all regions. Note that, like eq. (1), equations (2)-(9) define ‘anthropogenic concentrations’ as a perturbation of concentrations from pre-industrial levels.

Removal rate in each ‘region pool’ now depends on global carbon-cycle dynamics, including non-linearities induced by emissions of all regions. An advantage of this method is that global concentrations can be calculated using any (non-linear) carbon-cycle model, like the model in IMAGE-AOS. Calculations are not restricted to the ACCC impulse response functions (see eq. (B3b)) or other linearised models. Non-linearities in the carbon cycle are potentially important. For example, (Enting and Law, 2001) showed that atmospheric lifetime of CO₂ increases with higher CO₂ concentration, which can be accounted for using the alternative attribution approach. Here, we will use the IMAGE-AOS model, which, in contrast to the ACCC carbon cycle model, includes saturation of the CO₂-fertilisation effect over the whole historical plus scenario time period. It also includes scenario-dependant land use changes and therefore direct anthropogenic influence on the terrestrial carbon cycle, whereas the ACCC carbon cycle model in a sense represents the natural ‘undisturbed’ carbon cycle. The effects of using the alternative approach to attribute concentrations and the effect of using a carbon cycle including these non-linearities will be analysed in section 3.2

Because the main goal of the analyses below is to assess the relative contribution of groups of greenhouse-gas emitting countries to past and future global warming, the database of historical emissions is a key element. The historical emissions of the greenhouse gases CO₂, CH₄ and N₂O are based on the CDIAC-ORNL database (Andres et al., 1998; Marland et al., 1999) and EDGAR 1.4 (Emission Database for Global Atmospheric Research) database (Olivier and Berdowski, 2001; Van Aardenne et al., 2001). The CDIAC-ORNL database includes the CO₂ emissions from fossil fuel combustion and cement production for the period 1751-1995 on a country-level*, as well as the regional CO₂ emissions from land-use changes, based on (Houghton (1999)). The CDIAC database does not include regional historical emissions of the non-CO₂ greenhouse gas emissions. The EDGAR 1.4 database includes historical emissions of greenhouse gases CO₂, CH₄ and N₂O for the fossil fuel combustion, industrial and agricultural sources as well as from biomass burning and deforestation for the period 1890-1995. For the default ACCC calculations we use the emissions of CO₂ from CDIAC-ORNL and CH₄, N₂O and the considered halocarbons from EDGAR 1.4. For IMAGE-AOS, historical CO₂ land-use emissions are reconstructed as a residue; a function of observed concentrations, historical non-land-use emissions and modelled ocean uptake for the period 1765-1990. Global land-use emissions thus obtained are generally close to CDIAC (Eickhout et al., 2002). Regional land-use emissions are estimated by applying fractions of the global total from the CDIAC database. In Section 3.1 we analyse the impact of using either CDIAC, or EDGAR data in the attribution calculations.

The future emissions are based on the A2 (ACCC-TOR default), A1 and B1 emissions scenario from IPCC SRES (Nakicenovic et al., 2000). These IPCC SRES emissions scenarios are at the level of four aggregated IPCC SRES regions: (i) States that were members of the OECD in 1990 (OECD90), (ii) Eastern Europe and Former Soviet Union (EEUR&FSU, referred to as ‘countries undergoing economic reform’ (REF) in (Nakicenovic et al., 2000), (iii) Asia and (iv) Africa, Latin America and the Middle East (ALM). These aggregated countries/regions are used in the attribution calculations (as specified in ACCC-TOR). In addition, we have performed our analysis for the IMAGE 2.2 regional aggregation of seventeen world regions, i.e. Canada, USA, Central America, South America, North, West, East and Southern Africa, OECD Europe, Eastern Europe, Former USSR, Middle East, South Asia (incl. India), East Asia (incl. China), South East Asia, Oceania and Japan. To this end,

* The global bunker (international shipping and aviation) and feedstock emissions can be calculated from the difference between the global and total sum of regional CDIAC emissions allocated to the regional CO₂ emissions using the country contribution data of the EDGAR 1.4.

we have used the detailed regional information of our own IMAGE 2.2 implementation of the IPCC SRES emissions scenarios (IMAGE-team, 2001) for disaggregating the regional emissions of the IPCC SRES scenarios. For our alternative country group analyses presented below, we have selected 7 regions, representative for (current or future) 'major' UNFCCC parties: USA, OECD Europe, Former USSR, South Asia, East Asia, Southern Africa and Latin America.

2. Contributions to various climate-change indicators

In this section, we will present global mean calculations and contributions of emissions regions for various indicators of global warming. In figure 2, the results of the ACCC default model are expressed both in terms of absolute values and percentage contributions by the IPCC regions. These results were calculated for evaluation dates between 1765 and 2100, with (CDIAC) CO₂ regional emissions starting in 1765 and non-CO₂ (EDGAR) emissions from 1890 onwards. After 1990, the IPCC SRES A2 scenario is used. Note that, although calculated CO₂ concentrations are realistic (at about 351 ppmv in 1990, compared with the observed value of 354 ppmv in 1990 (Houghton et al., 2001)), the global total values for radiative forcing, temperature change and sea level rise are higher than observed. These values are also higher than simulated by the HadCM3 GCM and higher than the RIVM Phase 1 results, both given in Appendix E. In this and the following sections, aerosol and other forcings not attributed to individual emission regions are not included in the calculations. Only the gases included in the Kyoto protocol are considered. Because of the significant negative radiative forcing by sulphate aerosols, calculated totals for temperature increase and sea level rise are higher if aerosol forcing is excluded.

The crossing dates of contributions by different regions illustrate the time lags in the climate system when progressing through the cause-and-effect chain. OECD90 and Asia contributions cross around 1870 for CO₂ concentrations and around 1910 for sea level rise, then later again around 2060 and 2100, respectively. Expressed in percentages, Asia appears to make the major contribution before 1870 for CO₂ concentrations. In the CDIAC database, historical CO₂ emissions for Asia are larger than OECD90 emissions until 1840, though small compared to present-day values. OECD90 contributes most by the late 19th century until the second half of the 21st century, irrespective of the indicator considered. Following a rise in the 20th century, EEUR&FSU contributions start to decrease after 1990 and stay on a relatively low level until 2100, dropping below growing ALM contributions. Note that in absolute terms, the contribution to global warming of all regions increases in time.

In figure 3, the percentage contributions are re-calculated for emissions start date 1890 (as in the ACCC-TOR default). Evaluation dates 1970-2100 are shown for IPCC regions, as well as for the 7 selected IMAGE regions. USA contributions are much higher than those from OECD-Europe, but the evolution in time is comparable; a monotonic decrease relative to regions within Asia. Because emissions in South Asia start to increase relatively late, contributions drop initially, but start to increase and follow the increase in East-Asia contributions after the year 2000 (2020 for sea level rise). Contributions of South America and Southern Africa stay relatively low and constant, slowly decreasing and increasing, respectively. The rise in total ALM contributions is due to the increase in emissions of Central America, Southern Africa, Northern Africa and especially the Middle East (see table F.1).

To focus on the effect of the time lags in the system as we assess indicators further along the cause-and-effect chain of global warming, in figure 4 we show contributions for each region for evaluation dates 2000, 2050 and 2100. For Asia, the largest difference between contribution to radiative forcing and temperature increase occurs for evaluation date 2050. Here, the inertia of the climate system exerts its strongest influence, following the most rapid increase in concentrations attributed to this region within the time frame of this analysis.

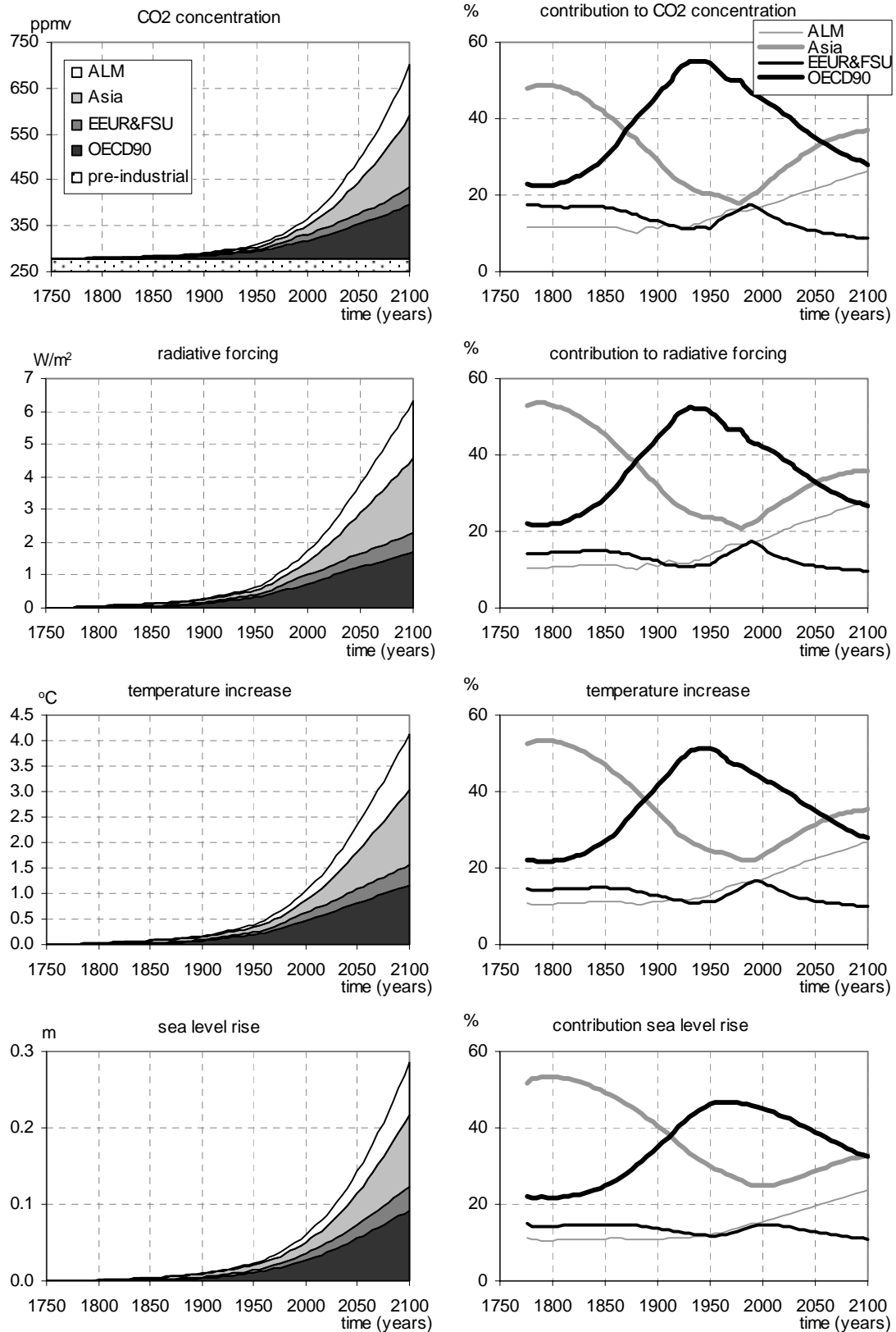


Figure 2. **Climate indicators** attributed to four IPCC regions for evaluation dates 1765-2100 for the IPCC SRES A2 scenario for the ACCC model.

Summarising, various inertia's in the climate system cause an increasing time lag in the change in contributions by individual regions when progressing along the climate change cause-and-effect chain of emissions to concentrations, to forcing, temperature change and, finally, sea level rise. The inertia in temperature response exerts its strongest influence on the attribution analysis following a time period of rapid increase in concentrations attributed to a certain region. This is most noticeable for Asia around 2050. The small, but dominant, historical emissions in Asia before 1840 cause its contributions to dominate until OECD90 contributions become larger in the second half of the 19th century. Up to the mid-21st century OECD90 contributions are dominant, thereafter being exceeded by Asia. Contributions by EEU&FSU and ALM are smaller, ALM contributions exceed EEU&FSU contributions by the year 2000. The latter decrease monotonically from 1990 onwards. Dominant contributors within each IPCC regions through the whole time period from 1970 to 2100 are USA (within OECD90), East Asia (Asia), Former Soviet Union (EEU&FSU) and South America (ALM), though in the latter case, the Middle East surpasses the contribution of South America by the end of the 21st century.

For early emitters, contributions are reduced by choosing an indicator which decreases the time lag between emission and impact as measured by the indicator. Thus, generally speaking, contributions of Annex-I countries are lower for concentrations, or forcing as an indicator, than for temperature increase, or sea level rise. In addition, taking into account CO₂ only reduces the contributions of non-Annex-I regions, compared to including all anthropogenic greenhouse gases (see (Den Elzen and Schaeffer, 2002) and text box). Depending on the evaluation year (2000, 2050, or 2100), individual IMAGE 2.2 regions form exceptions to these rules, see table F.1 for details. The exceptions are obviously formed by those regions showing deviant development in historical, or future emissions within their aggregated IPCC, or Annex-I/non-Annex-I groups. In the concluding section, we will provide a summarizing table indicating the increase, or decrease in the contribution of each individual region for the parameter and policy choices assessed in this paper.

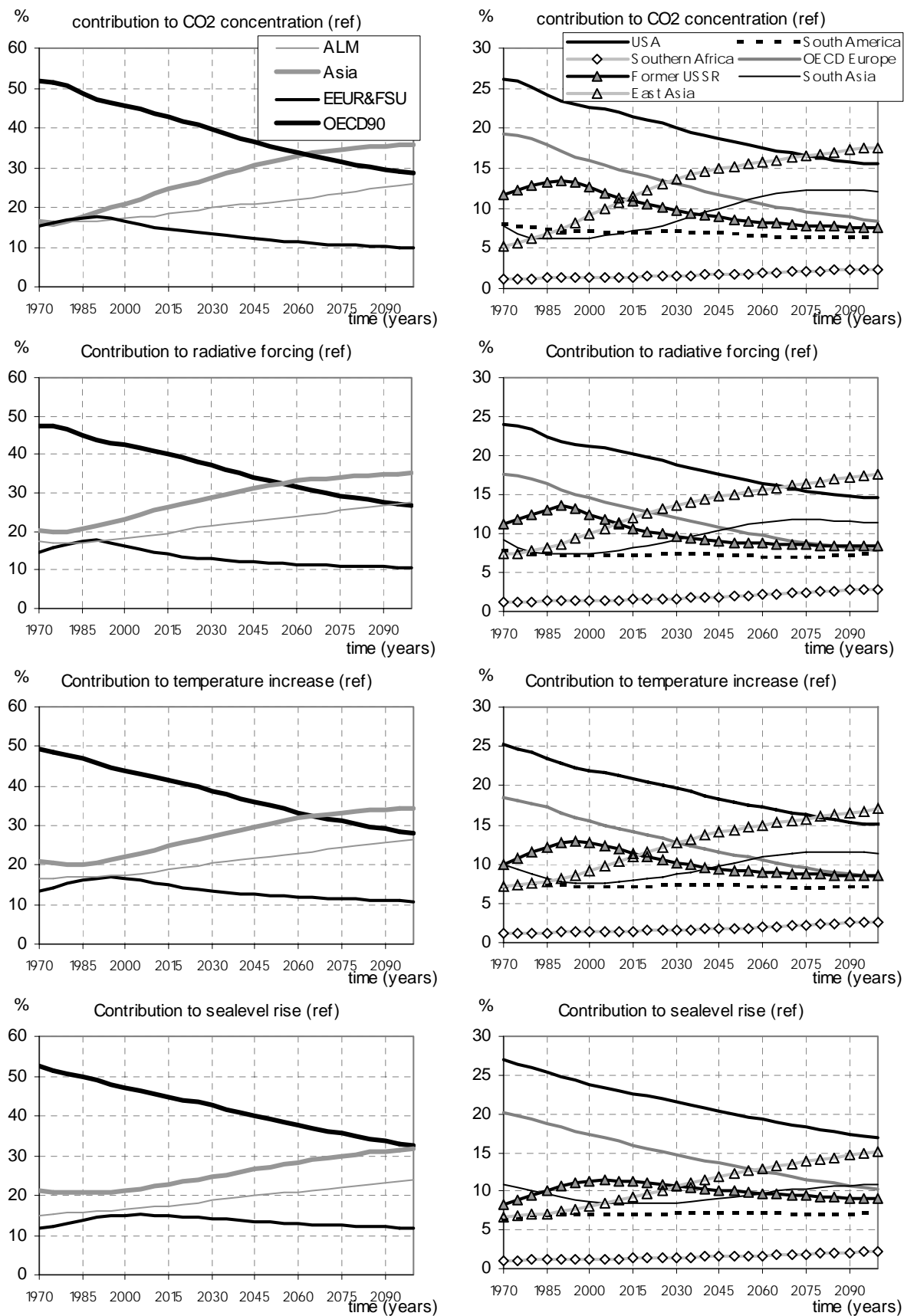


Figure 3. Regional contribution to **climate indicators** for the four IPCC regions (left) and seven selected regions (right) for evaluation dates 1970-2100 for the default calculations (start date 1890, end date 2100) for the ACCC model.

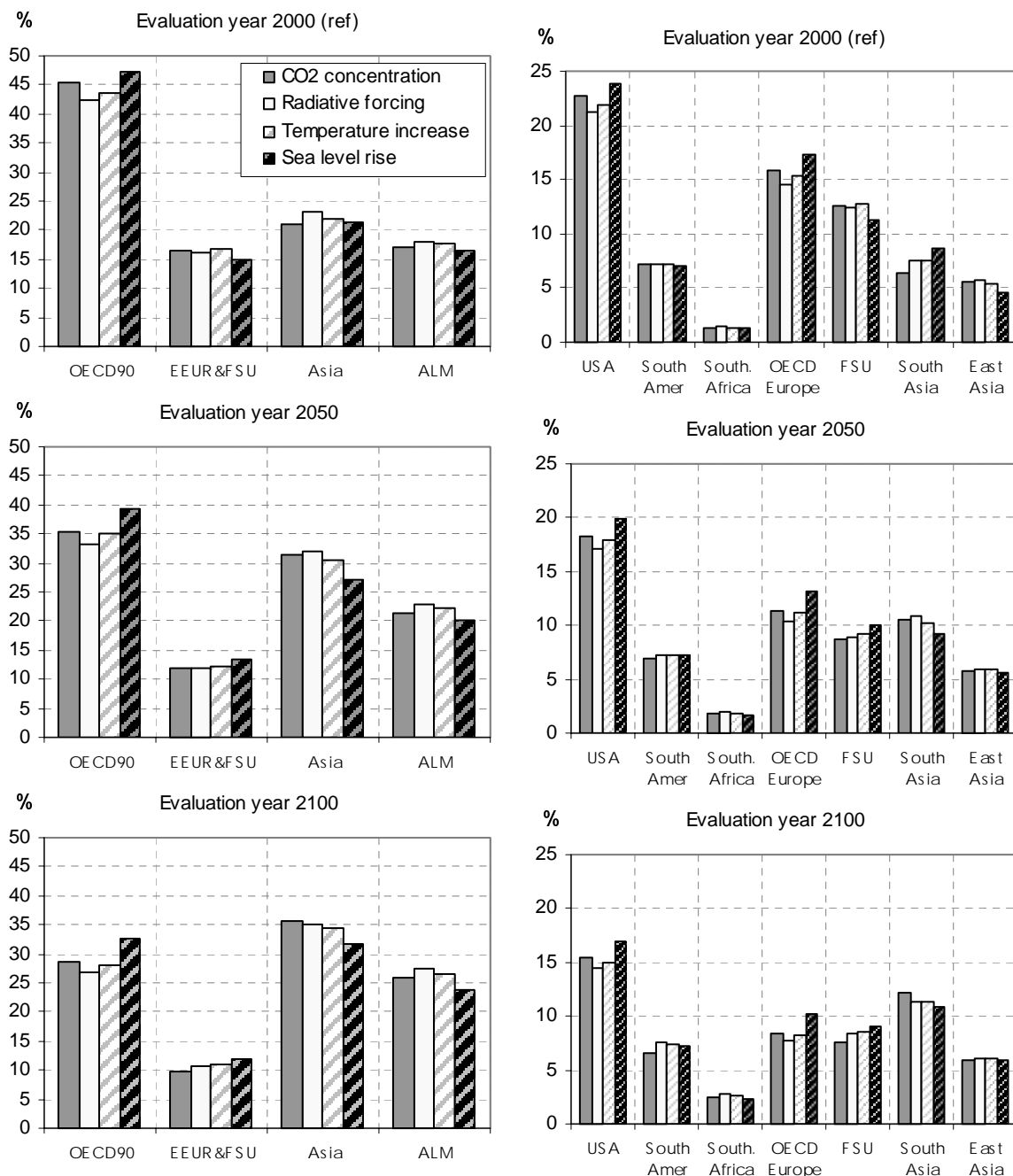


Figure 4. Regional contribution to *climate indicators* for the four IPCC regions (left panels) and seven selected regions (right panels) for evaluation dates 2000, 2050 and 2100 (start date 1890, end date 2100) for the ACCC model.

3. Sensitivity analysis of contributions to climate change

In Phase 2 of ACCC, participating institutions are requested to assess the sensitivity of the attribution calculations to changes in (model) parameters. We will focus on two issues, time frame of calculations (section 3.1) and non-linearities at different points in the cause-and-effect chain (section 3.2). Using meta-IMAGE 2.1 in (Den Elzen and Schaeffer, (2002), we have analysed the sensitivity of attribution calculations to a range of other scientific/model uncertainties and methodological choices. The main conclusions from this earlier analysis are also valid for IMAGE-AOS, ACCC and other models, and are summarised in the Text Box.

3.1. The timeframe of emissions

In the introduction, we have presented three key choices related to the time frame of calculating responsibility for climate change: (1) horizon of historical emissions ('backward looking'), or emissions start date, (2) horizon of future emissions ('forward looking'), or emission end date and (3) evaluation date of attribution calculations (see also figure 1). The impact of choosing different values for these dates on the attribution of temperature change will be analysed in the subsections below. First, we will illustrate the dynamics of the 'memory' of the system to provide a context for the analysis on time frame in the subsections below. Figure 5 shows the contribution of total anthropogenic CO₂ emissions from various historical (and scenario) time periods to the total atmospheric CO₂ concentration and temperature increase at a point in time further into the future. The total curve gives the global CO₂ concentration, respectively temperature increase, from historical emissions and from the IPCC-SRES A2 emission scenario. The lowest segment gives the amount of the concentration (temperature increase) that is due to the pre-1990 emissions, and each subsequent segment gives the additional contribution from the emissions over the next twenty-year period. For this IPCC-Bern TAR carbon-cycle model there is only a fraction of about 15% of the anthropogenic CO₂ emissions that remains in the atmosphere, and about 30% disappears very rapidly. By the year 2100, most of the deviation of atmospheric CO₂ from pre-industrial concentrations, and most of the temperature increase, is caused by the emissions after 1990. The remaining part from the pre-1990 emissions only forms about 10% of the CO₂ concentration deviation by this time.

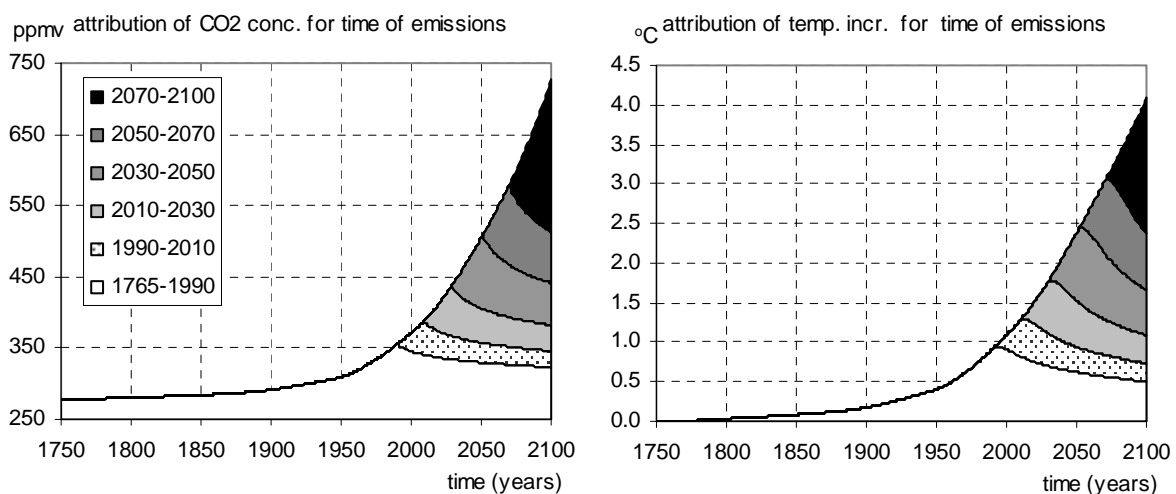


Figure 5. The attribution of CO₂ concentration and temperature increase according to the *time of emissions* for the ACCC model.

Text Box

Sensitivity of attribution calculations to other parameters and policy options

In this report, only a limited set of (new) parameters and policy options for attribution calculations is assessed. In an earlier paper, we have assessed a range of other model uncertainties and policy options (Den Elzen and Schaeffer, 2002). The influence on calculations of contributions was evaluated of (i) scientific and model uncertainties concerning the global carbon cycle and climate system dynamics, (ii) methodological choices related to choice of mixture of greenhouse gases included in the analysis, indicator and implementing non-linear radiative forcing, (iii) various future emission scenarios. In addition, (iv) the sensitivity of contribution calculations to these uncertainties was evaluated depending on the composition of the group of regions within which relative contributions are calculated. The main conclusions will be recaptured below.

(i) Global carbon cycle and climate system dynamics

- Over time, the influence of uncertainties in land-use CO₂ emissions quickly decreases, mainly due to the increasing dominating role of fossil fuel emissions.
- Uncertainty in climate sensitivity plays a dominant role in determining the range of absolute temperature increase, but has no influence on the projections of relative contributions. The latter are entirely determined by parameters characterizing the time scale of response of the climate system
- Uncertainty in the dynamic response of the climate system influences the contribution of regions in times of fast growing or decreasing emissions (South Asia and East Asia in the 21st century).

(ii) Methodological choices

- Taking into account not only fossil fuel CO₂ emissions, but emissions of all Kyoto gases sharply increases the contribution of non-Annex-I to temperature increase. However, the range in outcomes spanned by the cases 'only fossil CO₂' and 'all Kyoto gases' decreases in the future, because of the increasing dominating effect of fossil fuel emissions. Early 21st century this range is projected to equal the effect of model uncertainties under (i)

(iii) Scenarios

- Halfway through the 21st century, the range of contributions for various scenarios is comparable to the range resulting from model uncertainties (i) and methodological choices (ii).

(iv) Composition of participating emission regions

- The group of regions within which relative contributions to total (group) temperature change are calculated strongly determines the impact of the uncertainties above. If only regions from Annex-I are included, the uncertainties have a small effect, compared to calculations for all world regions

Summarizing, this earlier assessment showed the impact of different classes of uncertainty to be comparable, though the relative impact is different for different emission time periods.

Since the choice of mixture of greenhouse gases included in the analysis has a large impact on the calculated contributions, these were re-calculated using the ACCC default model and are presented in figures 6 and 7.

Text Box

Sensitivity of attribution calculations to other parameters and policy options

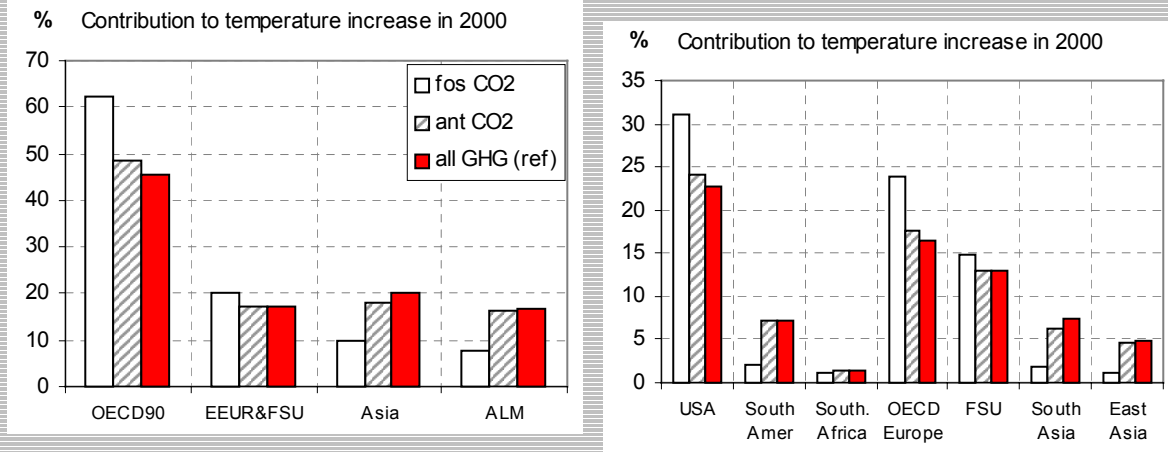


Figure 6. Regional contributions to the global-mean surface temperature increase for the *emissions source dataset cases* (start-date 1890, end-date 2100) for evaluation date 2000 for the IPCC SRES A2 scenario for the ACCC model.

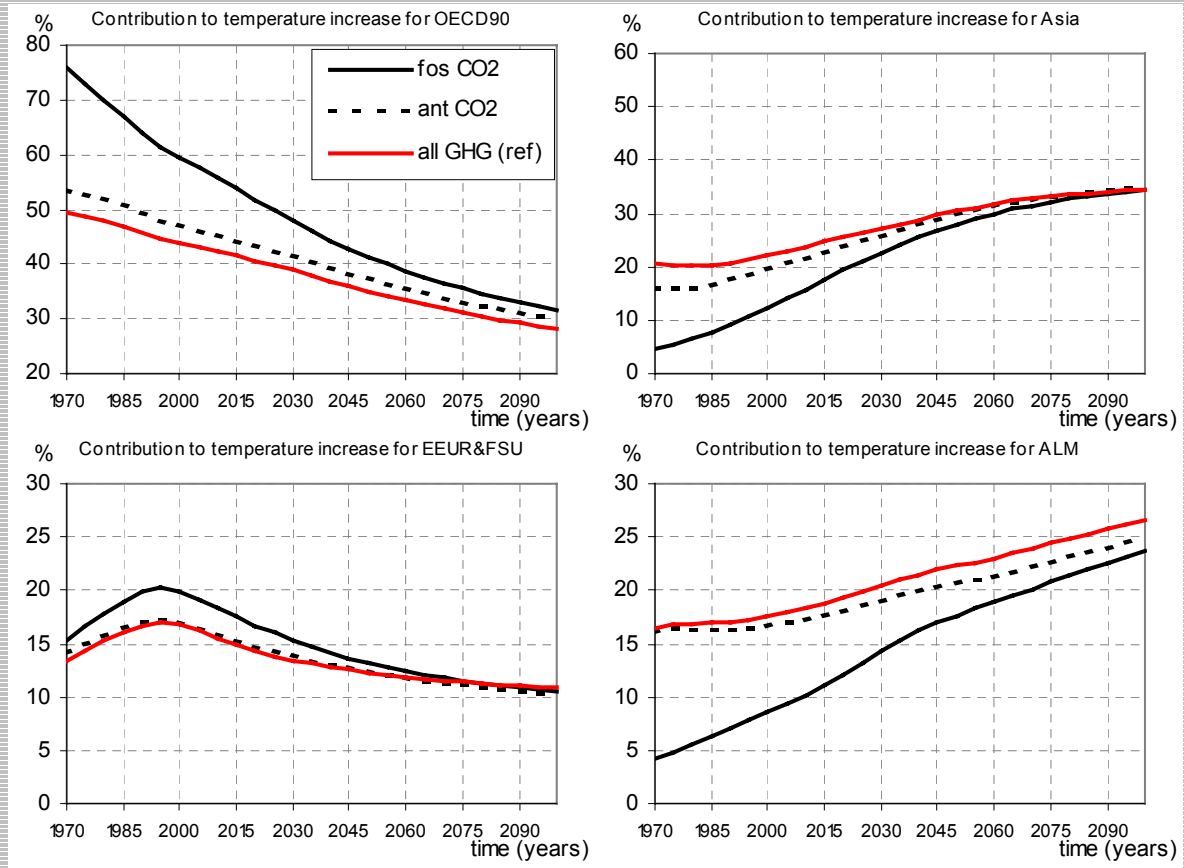


Figure 7. Regional contributions to the global-mean surface temperature increase for the *emissions source dataset cases* (start-date 1890, end-date 2100) for evaluation dates 1970-2100 for the IPCC SRES A2 scenario for the ACCC model.

3.1.1. The impact of time horizon historical emissions (start date)

The time horizon of the historical emissions is defined by the time period counting backwards to the emissions start date, taken between 1765 and 1995. The ACCC-TOR suggests the analysis of the following emissions start dates: 1765, 1890, 1950 and 1990 (default-value is underlined). For the analysis below we assume default values for the emissions end dates (2000). Western Europe emissions already start by 1765, whereas the emissions of other Annex-I regions start somewhat later (1800-1890) and at lower emission levels. The emissions of other non-Annex I regions become significant again later. For the IPCC region Asia, emissions start early at dominant levels, but these are low compared to 1990 levels and therefore of little influence for the evaluation date 2000. Therefore only Western Europe and South Asia (for the IPCC aggregated regions only Asia) show an increase in contribution to temperature increase when choosing a start date 1765 instead of 1890, whereas for all other regions contributions decrease for starting date 1765 instead of 1890 (figure 8). The largest shifts in the share in total emissions for the individual regions occurs after 1900, so that choosing a starting date 1900 or any earlier date has a relatively low impact on temperature increase contributions compared to choosing a date after 1900, like 1950 or 1990. In general choosing a later start date decreases the share of Annex-I regions, and increases that of non-Annex I regions. Because EEU&FSU emissions increase slowly compared to OECD90 from 1900-1950, as for non-Annex I regions, choosing start date 1950 raises the contribution of EEU&FSU. However, because emissions for EEU&FSU rise faster than for non-Annex I regions between 1945 and 1990, choosing start date 1990 lowers EEU&FSU contributions. As can be seen in figure 9, for evaluation dates further into the future choosing start date 1990 is by far optimal for minimising EEU&FSU contributions, while choosing later evaluation dates does not change the general conclusions on emission start date for the other regions.

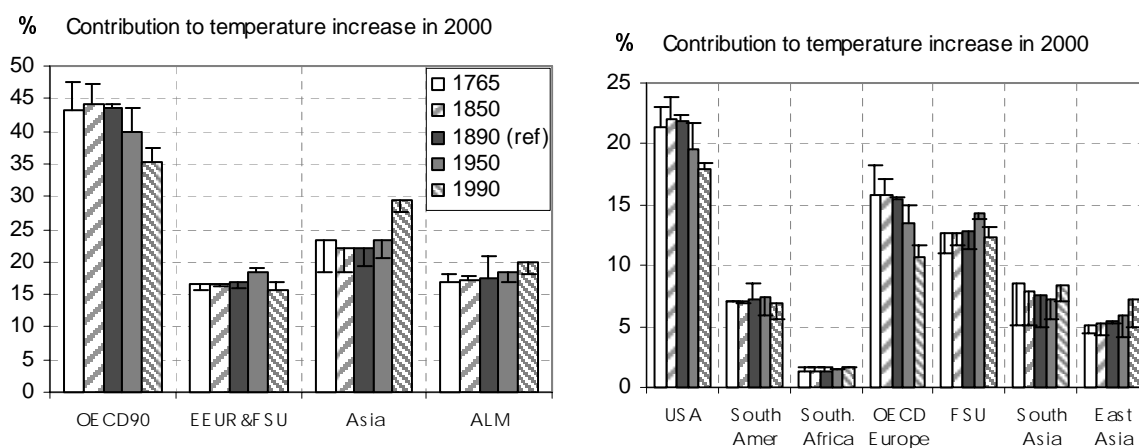


Figure 8. Regional contributions to the global-mean surface temperature increase for the **alternative start-date cases** (including the reference case 1890) for the evaluation date 2000 (end date 2000). The error bars represent the change in results when the historical emissions are based on the EDGAR dataset, instead of the CDIAC database.

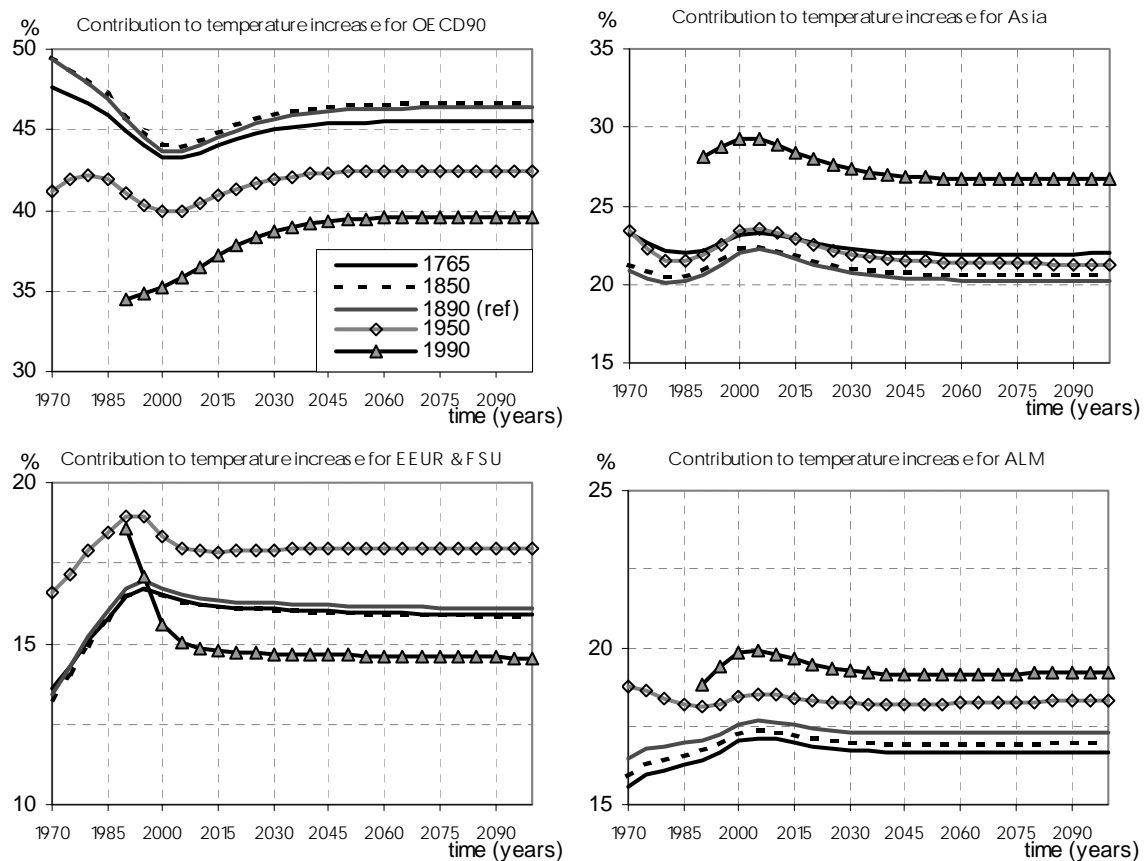


Figure 9. Regional contributions to the global-mean surface temperature increase for the **alternative start-date cases** (including the reference case 1890) for evaluation dates 1970-2100 (end date 2000).

Of course, this analysis is subject to uncertainties in historical emissions. In the default case, we have used CO₂ fossil fuel combustion and cement production emissions from the CDIAC-ORNL database. The error bars in figure 8 show results of the same analysis on emission start date as discussed above when using historical data from EDGAR 1.4 (Olivier and Berdowski, 2001; Van Aardenne et al., 2001) instead. For most regions, the general conclusions above hold, with some important exceptions. Taking EDGAR emissions instead of CDIAC reverses the effect of choosing an earlier/later emission start date for South America and the IPCC region Africa/Latin-America as a whole, although 1990 still gives lowest contributions. For the Former Soviet Union, 1990 significantly increases contributions. For more details see tables F.2 and F.3.

Concluding, the time horizon of the historical emissions has a strong impact on the contribution of the temperature increase of most regions. Choosing a shorter time horizon (e.g. 1950 or 1990 instead of 1890) minimises the contributions of the industrialised countries ('early emitters') to temperature increase. An exception is the Former Soviet Union, for which contributions increase for start date 1950. Choosing a longer time horizon (1765 instead of 1890) lowers contributions of most regions, the exceptions being Western Europe and South Asia, the dominant emitters in the period 1765-1890. These general conclusions above hold for most regions for both historical emissions datasets used here.

3.1.2. The impact of time horizon future emissions (end date)

The time horizon of future emissions is defined by the time period 1995 (emissions scenario starts) till the emissions end date. The ACCC-TOR suggests to assess the emission end dates 1990, 2000, 2050 and 2100 (default-value is underlined). We assume the default value for the emissions start date (1890), but for the calculation evaluation date we use 2100, since it should be at least after the emission end date. Figure 10 illustrates the contribution to global temperature increase of the selected regions for the various end dates. The contributions of most of the Annex I regions decline with emission end date further into the future, in particular Western Europe, Eastern Europe and the FSU, whereas the non-Annex I regions show an increase, in particular for African regions and South Asia.

Like the historical emissions in the emission start-date analysis, the emissions scenario might be of influence on the emission end-date analysis. Therefore, we have indicated by way of the error bars in figure 10 the range of outcomes when other IPCC SRES emission scenarios are used (A1, A2 (default), B1, or B2 (Nakicenovic et al., 2000)). The different baselines for future greenhouse gas emissions have a strong influence on a region's relative contribution to temperature change. The share of developing regions in the temperature increase will increase when high economic growth is combined with a diminishing economical gap between Annex-I and non-Annex-I regions (for data on individual scenarios, see tables F.5 and F.6). In spite of the large difference in results when using a different IPCC SRES greenhouse-gas emission scenario, the general conclusions of the analysis above on the relative influence of choosing alternative emission end dates still apply.

For the various end dates, figure 11 illustrates the contribution to global temperature increase for IPCC regions at evaluation dates between 1970 and 2100. The contributions of Annex-I regions follow the general downward trend until the emission end date (for EEUR&FSU only after the year 2000). The declining trend turns into a stabilisation for a period of five to ten years immediately following the emission end date. After this period, an opposite trend occurs for OECD90 towards increased contributions to global temperature increase, stabilising at a higher level than when evaluated immediately after the emission end date. We will further discuss this dynamic behaviour in section 3.1.3 on evaluation dates.

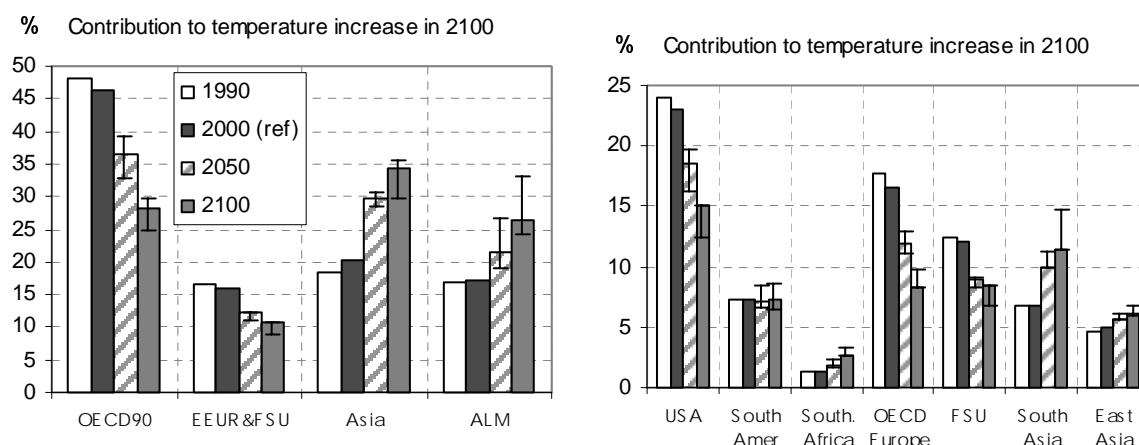


Figure 10. Regional contributions to the global-mean surface temperature increase for the **alternative end-date cases** (including the reference case 2000) evaluation date 2100 (start date 1890) for the IPCC SRES A2 scenario. The error bars represent the range in results when the future emissions are based on the IPCC SRES A1, A2, B1 and B2 scenario for the ACCC model.

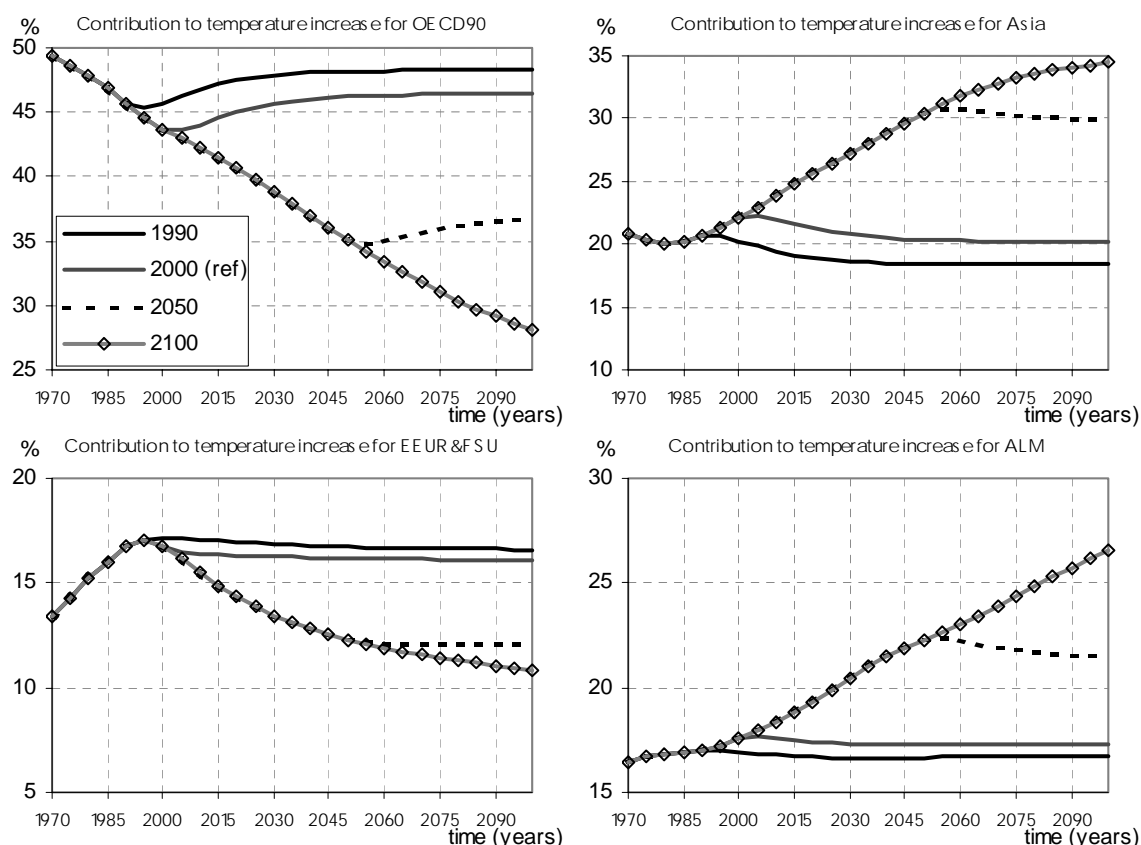


Figure 11. Regional contributions to the global-mean surface temperature increase for the **alternative end-date cases** (including the reference case 2000) for evaluation dates 1970-2100 (start date 1890) for the IPCC SRES A2 scenario.

Concluding, the time horizon of the future emissions (emissions end date) has a strong impact on the contribution of the temperature increase of most regions. Choosing a point in time further into the future lowers contributions of Annex-I regions and raises those of non-Annex-I regions, especially those with fast-growing emissions after 2000. Using a different IPCC SRES greenhouse-gas emission scenario does not fundamentally change these general observations regarding the impact of changing the emissions end date.

3.1.3. The impact of calculation evaluation date

The third time-frame choice is the calculation evaluation date, the year in which the attribution calculations are performed (default value 2000). Here we will assess the impact of various evaluation dates, 2000 and 2100 (ACCC-TOR), using the default values for the emissions start-date (1890) and emissions-end date (2000). Zero emissions are assumed for all regions after the end date.

Figure 12 presents the contribution to global temperature increase for the selected regions for the various evaluation dates. In general, with a fixed emissions end date, contributions will drop for non-Annex-I regions, for an evaluation date shifted further into the future. This was also shown in figure 11 showing the time-dependant behaviour of contributions when the evaluation date is chosen some period after the emission end date. For the IPCC regions, especially for OECD90, the contributions rise and those of Asia drop. One factor explaining this is the large OECD90 share in historical CO₂ emissions. For emissions from a time period long before the evaluation date (historical emissions), a large part of contribution to concentrations resides in carbon pools with a long residence time.

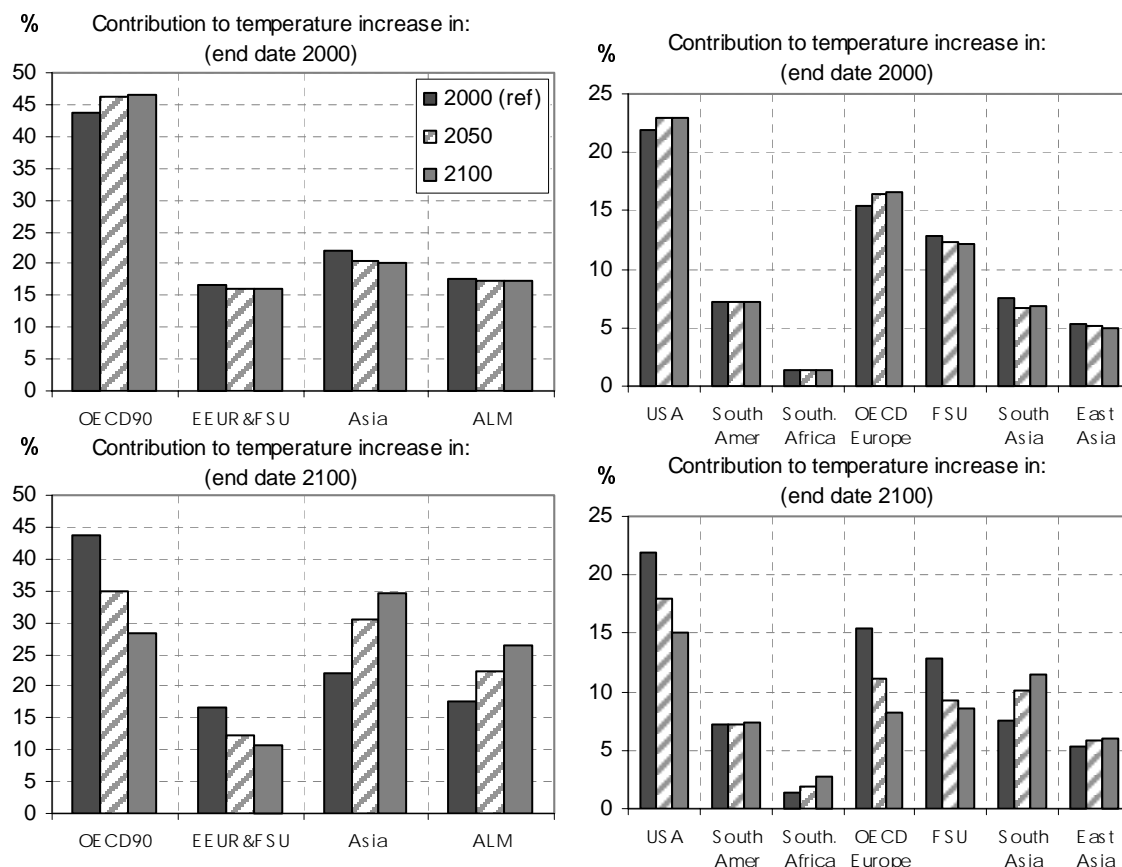


Figure 12. Regional contributions to the global-mean surface temperature increase for the **alternative evaluation-date cases** (including the reference case 2000) (start date 1890) for end dates 2000 (upper panels) and 2100 (lower panels).

Thus, the fraction of total contribution caused by emissions from this time period will fade away more slowly than the contribution from more recent emissions (see also figure 5 for contribution of various emission time periods to global concentrations). The contribution to total CO₂ concentrations of the relatively recent non-Annex-I emissions will fade away more quickly, because of the larger fraction that resides in the carbon pools with a shorter residence time. Therefore, the Annex-I contribution to the delayed global warming exceeds the non-Annex-I contribution of this delayed warming, the more so when the evaluation time shifts further into the future. Evidently non-Annex-I regions show an opposite pattern, an increase in their contribution to temperature increase turns, after the relaxation period, towards a declining trend, in particular for South Asia and South East Asia. For East Asia with a larger share in the historical emissions, this decline is much slower compared to the decline of South Asia and African regions.

Another part of the explanation is related to the relatively small share of CH₄ emissions of OECD90. Since CH₄ has a relatively short life time in the atmosphere, the large fraction of forcing resulting from CH₄ emissions of non-Annex-I regions just before the end date will dissipate quickly, lowering non-Annex-I (CH₄) contributions compared to Annex-I regions as the evaluation time is shifted further into the future. Note the analogy with Global Warming Potentials (GWPs). This familiar policy evaluation tool (Houghton et al., 2001) can be used to attach a relative value to emissions of different greenhouse gases, to estimate their relative future effect on climate change, which may play a role in assessments of the effectiveness of mitigation efforts. The GWP of a greenhouse gas also depends on the time horizon. Because CH₄ is removed from the atmosphere more quickly than CO₂ and other greenhouse gases, its

GWP decreases rapidly as the time horizon shifts from 20, to 50, to 100 years (Houghton et al., 2001). Thus, when GWPs are used to compare the future effect of Annex-I and non-Annex-I emissions, the relatively large portion of CH₄ with respect to total non-Annex-I emissions means that GWP-weighted non-Annex-I total emissions become smaller if a longer GWP time horizon is used, as compared to GWP-weighted Annex-I emissions.

To assess to which extend these two explanations above contribute to the rise in OECD90 contributions and the drop in Asia contributions following the emission end date, figure 13 shows contribution to CO₂ concentrations and radiative forcing for these two regions, for the same end dates as for temperature change in figure 11. In the CO₂ concentrations, the OECD90 rise and Asia drop are visible immediately after the emission end date, showing the influence of the larger fraction of early emissions of OECD90 now residing in long-turnover time carbon pools. However, the OECD90 rise and Asia drop are much more pronounced for radiative forcing, showing the added effect of the different fractions of CH₄ in total emissions for OECD90 and Asia. Compared to temperature change, the change in time in radiative forcing following the emission end date is more abrupt, which illustrates the time lag in temperature response. Note that temperature contributions for Asia slightly rise immediately after the emission end date, instead of drop, which is caused by the lag in temperature response to the relatively fast-growing Asia emissions just before the emission end date. This causes the stabilisation of contributions in the 5 to 10 years following the emission end date that was noted in section 3.1.2.

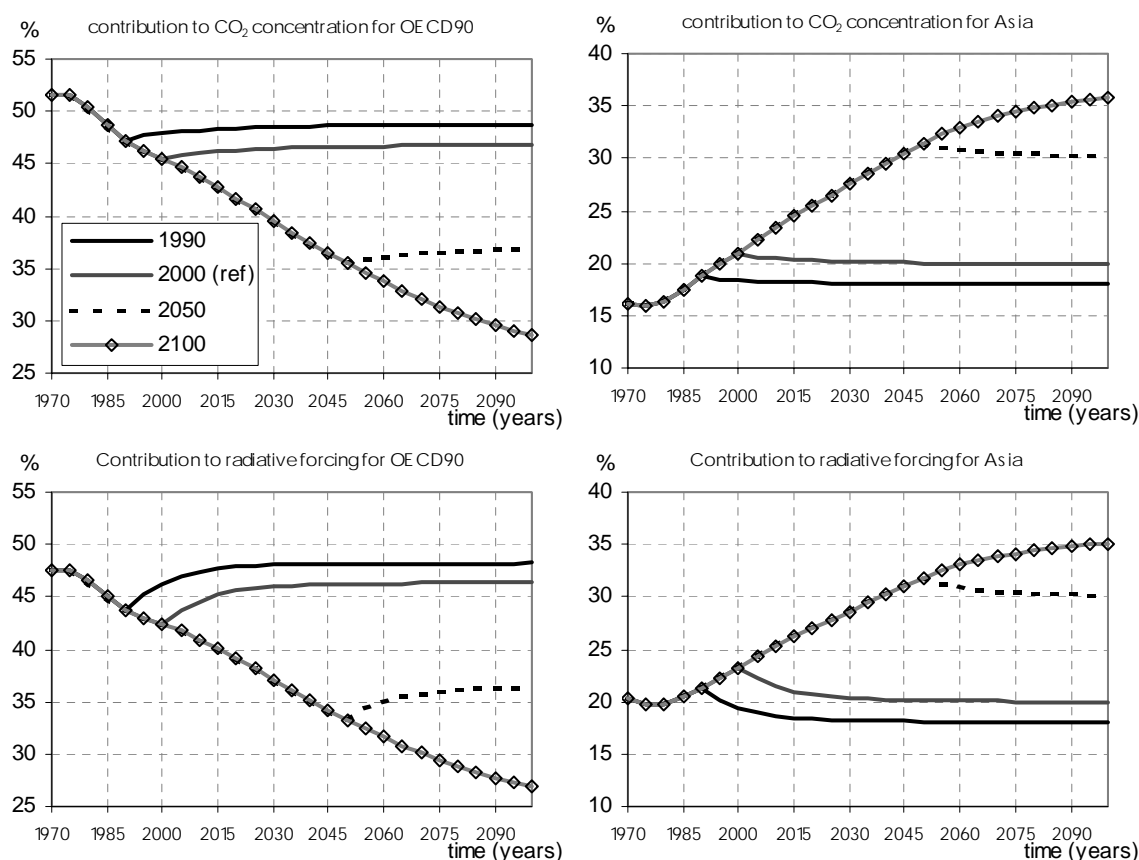


Figure 13. Regional contributions to CO₂ concentration (upper panels) and radiative forcing (lower panels) for the **alternative end-date cases** (including the reference case 2000) for evaluation dates 1970-2100 (start date 1890) for the IPCC SRES A2 scenario.

Concluding, if the evaluation date is chosen some period after the emission end date, the contributions for Annex-I regions rise and non-Annex-I regions drop. This is caused by the variation between the regions regarding early, or late emission and the fraction of different Kyoto gases in total radiative forcing. Contributions stabilise for evaluation dates 50 years or more after the emission end date. Annex-I contributions are minimised with a calculation evaluation date chosen at a point soon after the emissions ends, whereas for the non-Annex I regions a date further into the future lowers contributions.

3.2. Non-linearities in the climate change cause-and-effect chain

A disadvantage of the default ACCC model framework is the inability to capture potentially important non-linear effects. Here, we define a linear approach as a method that calculates contributions by emission regions or greenhouse gases in isolated boxes, one for each region/gas. Subsequently, the changes in these isolated boxes are added to determine global totals. Changes in functioning of the global climate system as a result of contributions of all regions/gases are thus not taken into account. If non-linearities are to be taken into account, this affects the way the climate system is modelled, as well as the attribution calculations.

With respect to climate modelling, the coupled biosphere/atmosphere/hydrosphere/cryosphere system shows sensitivities to external forcing, which depend on the system's state. For example, the removal rate of atmospheric CO₂ as part of the global carbon cycle might decrease as CO₂ fertilisation saturates (Prentice et al., 2001), one element in the functioning of the global terrestrial biosphere as a carbon sink. A sudden shift of the terrestrial carbon cycle from a net sink to source (Cox et al., 2000) can be classified as a so-called 'singular phenomenon'. A singular phenomenon in this context refers to a sudden change in the climate system's state, with possibly profound impacts, as an expression of strong feedbacks or non-linearity, whereby a return to the previous condition often occurs over a much longer time scale and via a different route ('hysteresis'). Other examples are a sudden shutdown of the thermohaline circulation or a collapse of the West Antarctic ice sheet. To describe such phenomena, a more complex, process-based model is needed, or the relevant processes have to be represented somehow in the parameters of the simpler model (Den Elzen and Schaeffer, 2002). Another example of non-linearity is the saturation of radiative forcing. This can be modelled fairly simple (Harvey et al., 1997), as is indeed included in the ACCC default. A final example is the potential time-dependency of climate sensitivity, resulting from its dependency on the climate system's state (Senior and Mitchell, 2000). Although non-linearity of radiative forcing can be modelled fairly simple, a special functional form for the attribution calculations is needed to account for this (see Appendix D and (Enting, 1998)). Likewise, to account for non-linearities in the carbon cycle, concentrations can be attributed following an alternative approach, as presented in section 1.

In this section, we assess the sensitivity of attribution calculations when the alternative attribution method for concentrations is used, as well as when, instead of the ACCC default, the IMAGE-AOS carbon-cycle model is used, which includes non-linearities in the global carbon cycle (see section 1, Appendix C, (Alcamo et al., 1998); (IMAGE-team, 2001)). For comparison, we will also assess the influence of non-linearity in radiative forcing, which was assessed earlier by (Enting, 1998) and (Den Elzen and Schaeffer, 2002). We have also assessed the influence of non-linearity in CH₄ lifetime (parameterisation of OH chemistry as in IPCC TAR). Although the choice between fixed and calculated CH₄ lifetime, has a strong impact on absolute CH₄ concentration, we found that it has negligible consequences for the calculated contributions, because (1) contribution of CO₂ to total radiative forcing is dominant and increasing in time in the IPCC SRES scenarios and (2) calculated life times are not very different from fixed life times and equal for all regions at a certain point in time.

This conclusion is comparable to the limited effect of changes in global residence time of carbon as a result from non-linearities in the carbon cycle as presented in section 3.2.1.

3.2.1. The impact of the non-linear approach to attributing CO₂ concentrations

The central non-linearity issue in this paper is non-linearity in calculating (attribution of) CO₂ concentrations from the emissions of each region. In figure 14, we show the effect on attributions when the alternative attribution method is applied to the ACCC default model (compare ACCC-single with the default ACCC-ref). To put this in the perspective of other uncertainties, the error bars indicate the range given by the results using the various Bern-SAR carbon-cycle model parameterisations (Appendix C), which include different (fixed) strengths of CO₂ fertilisation. For evaluation year 2000, the alternative non-linear attribution the share of historical early emitters like USA, OECD-Europe and South Asia, while contributions of East Asia, and regions within EEUR&FSU and ALM increase. However, the difference is of comparable magnitude or smaller than the parameterization uncertainty range. For evaluation year 2100 the alternative attribution method increases the share of most non-Annex-I regions and decreases those of all Annex-I regions. The difference between the methods is larger than that between the various carbon-cycle parameterisations. South America, with relatively stable emissions, forms an exception within the non-Annex-I group. The difference between the two approaches increases in time (figure 15).

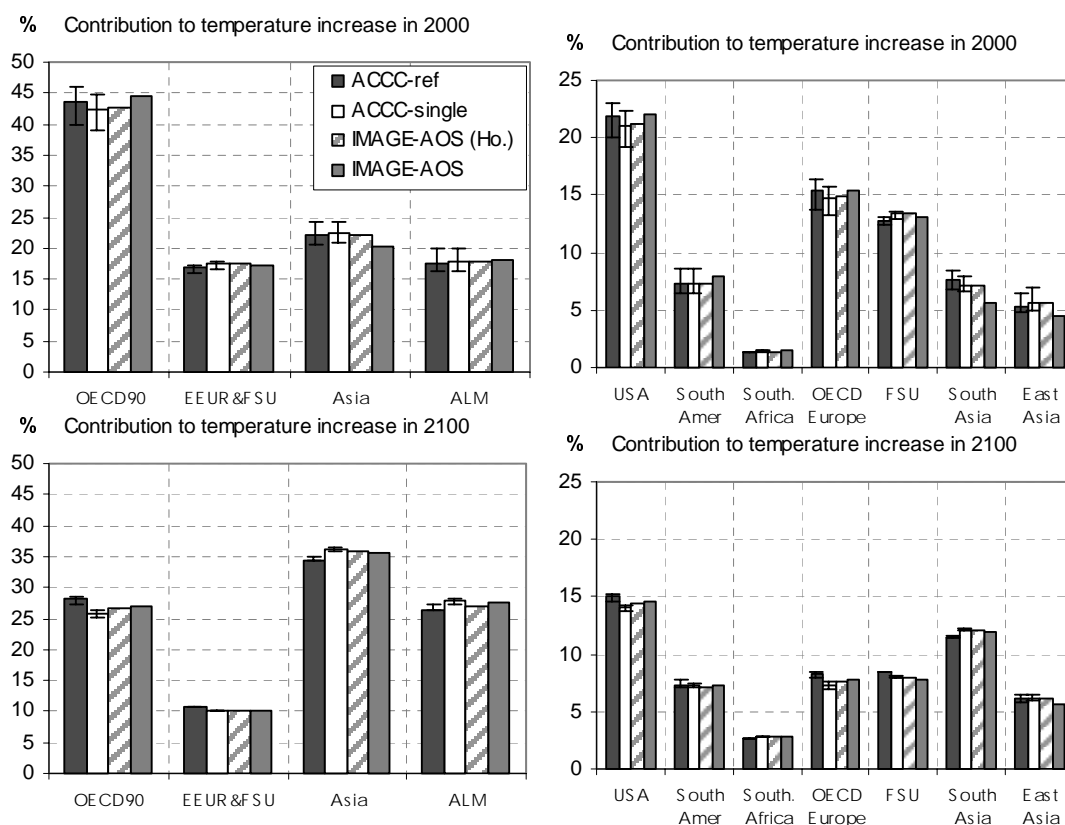


Figure 14. Regional contributions to the global-mean surface temperature increase for the non-linearities in attributing CO₂ concentration cases (start-date 1890) for the view- & end-dates 2000 (upper panels) and 2100 (lower panels). The error bars give the results for the Bern Low and Bern High carbon cycle models.

Explanation: ACCC-ref is ACCC-TOR model, i.e. Bern-TAR 4-exponential function, ACCC-single is Bern-TAR single turnover time formulation, IMAGE-AOS (Ho.) is single turnover time using Houghton historical land use emissions and IMAGE-AOS is single turnover time using IMAGE 2.2 historical land use emissions

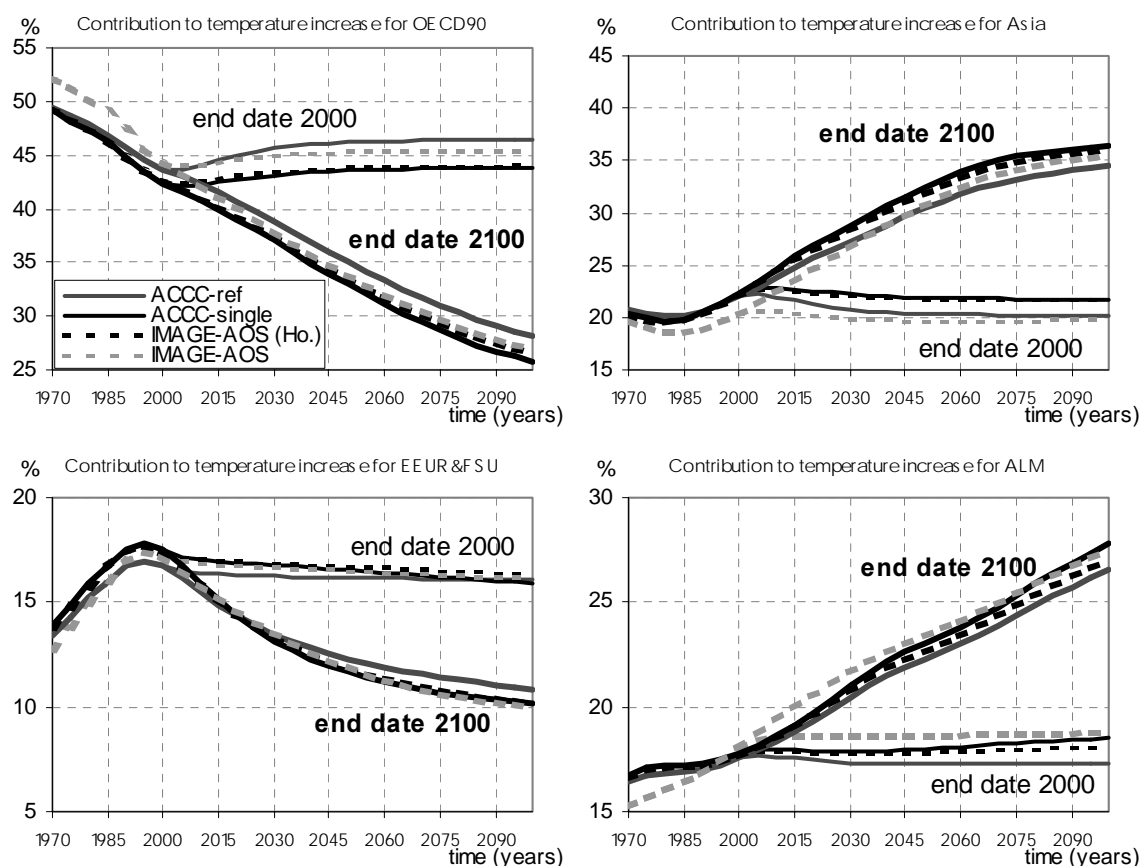


Figure 15. Regional contributions to the global-mean surface temperature increase for the **non-linearities in attributing CO₂ concentration cases** (start-date 1890, end-dates 2000 and 2100) for evaluation dates 1970-2100.

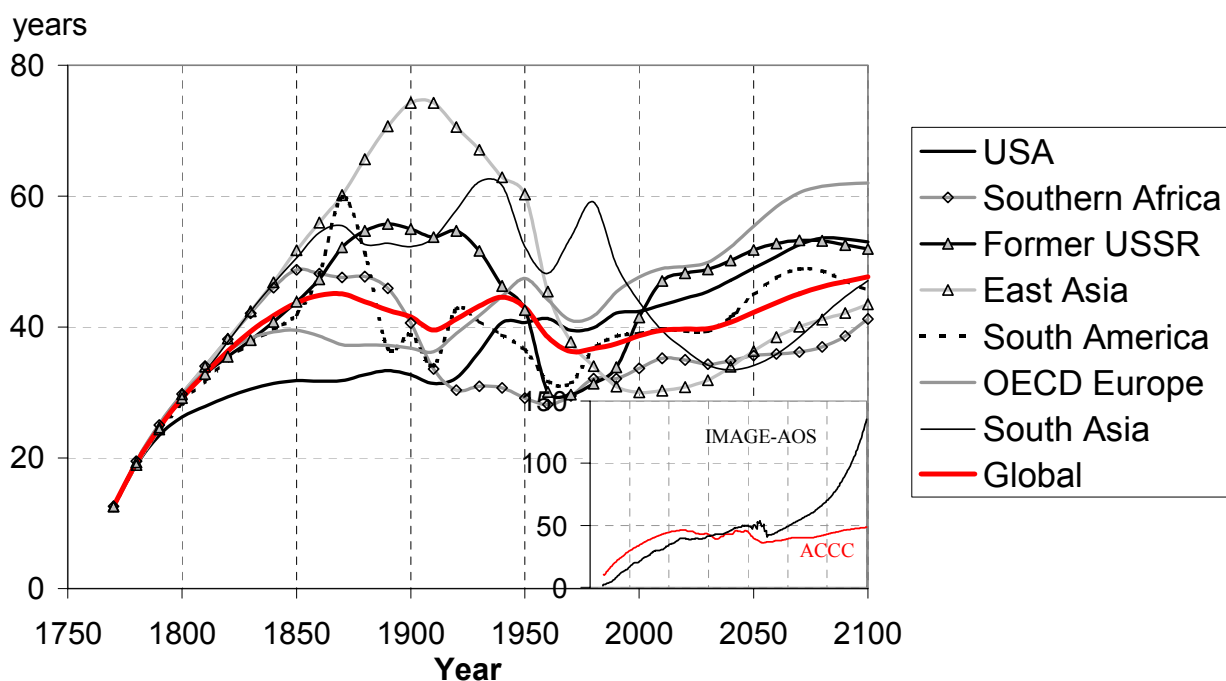
Explanation: ACCC-ref is ACCC-TOR model, i.e. Bern-TAR 4-exponential function, ACCC-single is Bern-TAR single turnover time formulation, IMAGE-AOS (Ho.) is single turnover time using Houghton historical land use emissions and IMAGE-AOS is single turnover time using IMAGE 2.2 historical land use emissions

To explain the observations above, we show in figure 16 the effective single global turnover time of perturbed atmospheric CO₂, as diagnosed from output of the ACCC-default carbon-cycle model. After a relatively fast increase, the global value stabilises. The effective CO₂ turnover time increases proportionally to concentrations and inversely to emissions. Thus, turnover time is high in periods of relatively high concentrations, combined with relatively low emissions. For the individual regions, turnover times calculated from ACCC are long in the 21st century for emitters with relatively high historical emissions (see figure 16). The reason is that, compared to the global carbon pools, a relatively large part of concentrations resides in the mathematical terms with a long turnover time in the ACCC model. In periods of strong emission growth, turnover time will be short. This can be seen by comparing the effective life times in the isolated regional boxes in the upper panel of figure 16 with the emission growth in the lower panel, for periods of higher and lower growth than the global mean. Thus, in figure 16, turnover time is relatively short for USA and OECD Europe in the historical period, while it increases relative to the global mean after 1950. At the end of the 21st century, regions with relatively high emission growth rates in the 21st century (East Asia, South Asia, Southern Africa) experience a low region-specific turnover time, while regions with a relatively low growth rate (USA, OECD Europe, FSU) experience long turnover times. Thus contributions from the latter three (Annex-I) regions are lowered in the alternative approach, while they are raised for the first three (non-Annex-I).

As explained above, IMAGE-AOS includes some non-linearities not represented in ACCC. In the inset of the upper panel of figure 16, we compare the single time-varying global turnover time as diagnosed from output of the carbon-cycle models ACCC-default (also shown in the main upper panel of figure 16) and of IMAGE-AOS. Turnover times are close for both models in the historical period. The effective turnover time increases for the historical period to about 50 years in the second half of the 20th century. However, effective turnover times for the two models diverge after 2000, when saturation of CO₂ fertilisation and the influence of climate change on land cover (and thus on the terrestrial carbon cycle) in IMAGE-AOS become significant. The result is that for the IPCC SRES-A2 emission scenario the CO₂ concentration reaches a level of about 860 ppmv in 2100 for IMAGE-AOS (not shown), as opposed to 700 ppmv for ACCC. Whether a region's contribution will decrease from a short, or long global turnover time depends on the balance between the region's relative contribution to total emissions and contribution to global concentrations. This can be made clear by noting that a long global turnover time is equivalent to a long 'memory' of the system. A long memory (turnover time) is in the interest of regions with (1) low contributions to concentrations, or (2) medium concentration contributions, combined with medium to high emissions. A shorter memory lowers the share of regions with (1) high concentrations, or (2) medium concentrations, combined with low to medium emissions. Of course, strong emission growth, or decrease, and a time-varying turnover time complicate this simple picture. For example, the contribution of a region exhibiting medium-low concentration contributions and emissions growing from medium-low to high, would decrease for a shorter turnover time in the beginning and a longer turnover time later on (e.g. South Asia). On the other hand, contributions of a region with medium concentrations and emissions decreasing from medium-high to low, would be reduced for a long turnover time at the start, followed by a shorter turnover time (e.g. USA). In this case, a growing turnover time as in figure 16 would thus raise contributions. We see this in figure 14, comparing the second (ACCC-single) and third (IMAGE-AOS (Ho.)) column bar for each region. Obviously, for view year 2000, there is no difference between the models as turnover times are very close up to the year 2000. For view year 2100, the increasing turnover time of CO₂ in IMAGE-AOS raises contributions from USA and OECD Europe, the difference extends the error bars. However, as life times of the two models only begin to diverge in the course of the 21st century, the full potential impact is not yet seen at the end of this century. The effect of increasing global life time is generally smaller than the impact of using the alternative attribution approach and of opposite sign. The fourth column bar in figure 14 represents the IMAGE-AOS results. The difference with IMAGE-AOS (Ho.) is that in the latter case historical land use emissions equal to those in ACCC are used, more easily compared with ACCC-single, while IMAGE-AOS uses its own calibration (see section 1).

Summarising, the calculation of contributions of emission regions to global warming is sensitive to the method of attributing concentrations. The linear approach of calculating contributions of regions in isolated carbon-cycle boxes lowers contributions of regions in periods of, or following, high emission growth with respect to the global mean. In the 21st century, applying the non-linear approach raises contributions of non-Annex-I regions, lowering those of Annex-I regions. The non-linear effect of increasing global residence time of CO₂ in the atmosphere is smaller and has opposite sign. A longer residence time extends the 'memory' of the system, thereby increasing contributions of early emitters.

Effective single CO₂ turnover time calculated per region



Regional growth of CO₂ emissions (15-year running mean)

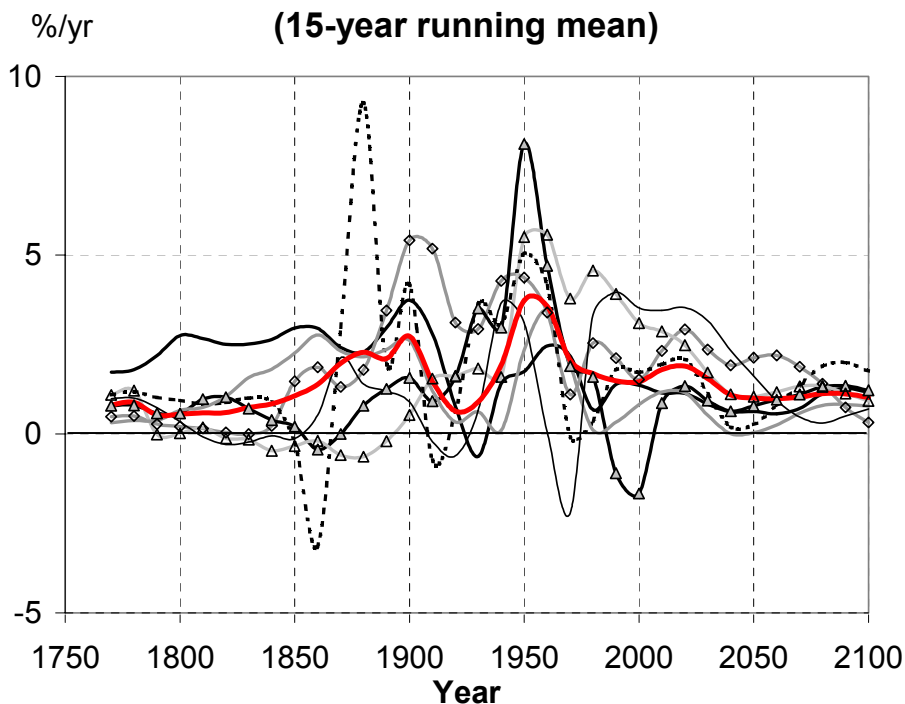


Figure 16. Upper panel: Effective single atmospheric turnover time for CO₂ mass in excess of pre-industrial levels, resulting from emissions and concentrations for each regional 'box model' in isolation using the ACCC default carbon cycle model Bern-TAR. Inset upper panel: global effective life time (red) compared to single turnover time calculated from IMAGE-AOS output (black) for the same time period 1750-2100. Lower panel: 15-year running mean of emission growth per region.

3.2.2. The impact of the non-linear approach to attributing radiative forcing

The second non-linearity assessed here is attribution of radiative forcing. In figures 17 and 18, we compare the linear and non-linear attribution approaches. As saturation of radiative forcing only becomes significant in the course of the 21st century (figure 18), we only show in figure 17 the column graph for evaluation date 2100. The non-linear approach lowers the share of late emitters (non-Annex-I regions). The difference between the approaches increases in time (figure 18) and, by the end of the 21st century is comparable to, or slightly smaller than the difference between the two approaches of attributing concentrations.

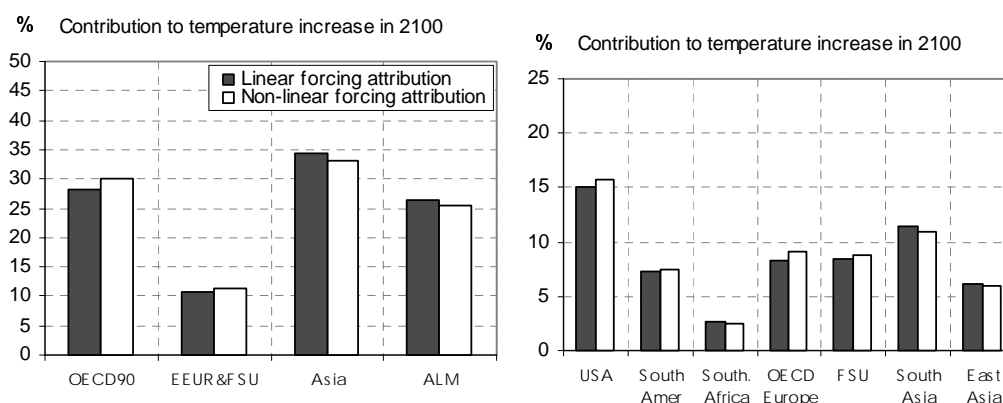


Figure 17. Regional contributions to the global-mean surface temperature increase for the non-linear radiative forcing cases (start date 1890, end date 2100) for evaluation date 2100.

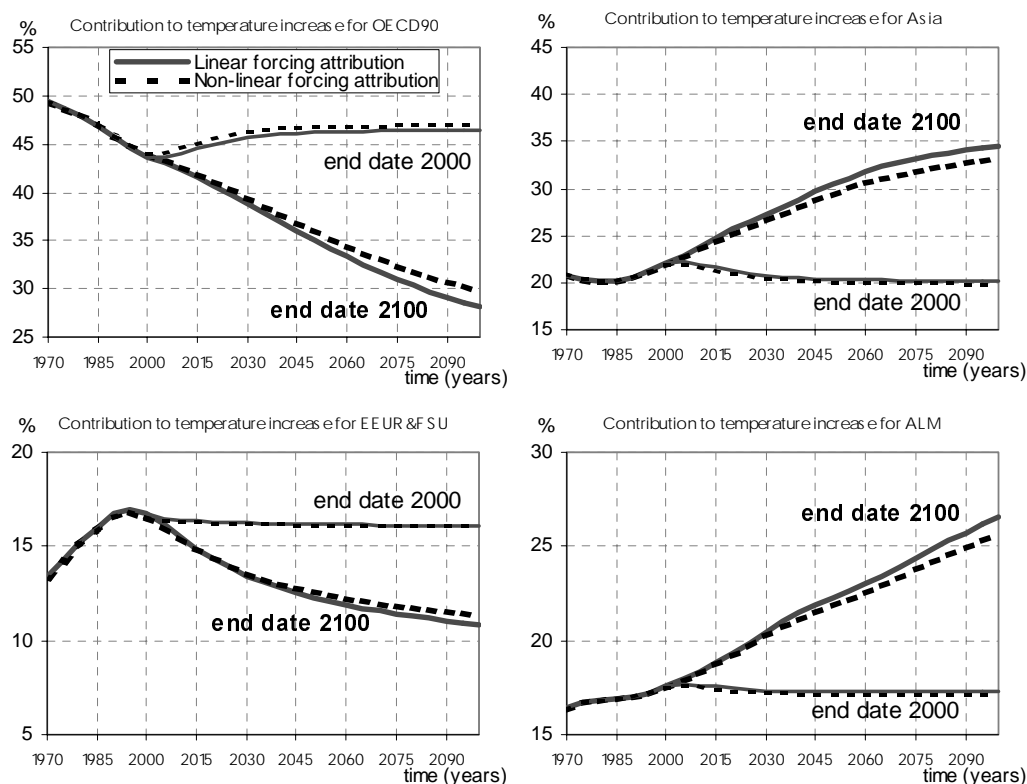


Figure 18. Regional contributions to the global-mean surface temperature increase for the non-linear radiative forcing cases (start-date 1890, end dates 2000 and 2100) for evaluation dates 1970-2100.

3.2.3. Combining alternatives for calculating contribution to radiative forcing and CO₂ concentration

The effect of the non-linear approach of attributing radiative forcing has been assessed earlier. In section 3.2.1 we have analysed a new element, the non-linear attribution of CO₂ concentration. The sign of the effects of implementing these two non-linear approaches is opposite and figure 19 shows that for late emission end dates the two effects almost cancel out when implemented both.

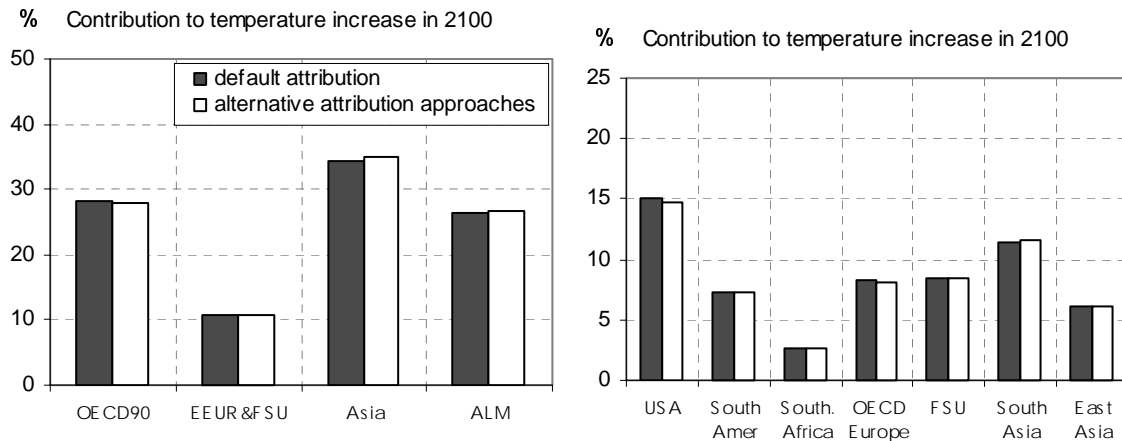


Figure 19. Regional contributions to the global-mean surface temperature increase for the reference and **combined non-linear attribution case** (start-date 1890, end date 2100).

4. Conclusions

For convenience, we have summarised the results of our analyses in table 1, for emissions end date 2000, and table 2, for 2050. In these tables, we show the change in contributions for each region when different options are implemented regarding time horizons, parameter settings, model approaches, etc. The tables are sorted in such a way from left to right, that options lowering total non-Annex-I contributions can be found in columns more to the left, while options lowering Annex-I contributions are found more to the right. The numerical values indicate change in percentage contribution per region when an alternative option is implemented. In addition, the colour of cells indicate the change in relative terms, with respect to the region's contribution as calculated by the default model configuration and parameters settings. For example, the absolute change in contribution (value) of Canada when only fossil CO₂ emissions are taken into account is much lower than of USA, but for both this option falls into the same relative impact class (colour).

Combining various options not necessarily leads to the total linearly added change in contributions as read from tables 1 and 2. For example, combining the three options that individually most strongly decrease the contributions of OECD Europe (start date 1950, non-linear attribution of CO₂ concentrations and using radiative forcing as indicator) lowers contribution in the year 2000 by 2.4%. Linearly adding the impact of these three options from table 1 results in a reduction of 3.4%. The cause of the difference is that choosing 1950 as a start date strongly reduces the impact of the non-linear CO₂ concentration attribution and taking radiative forcing as indicator.

Some combinations of options that change contributions for a specific region might be impossible or meaningless. For example, for East Asia choosing CO₂ concentrations as indicator obviously precludes opting for the 'decrease option' of forcing as indicator and makes the non-linear radiative forcing option meaningless. Presuming all Kyoto gases are included, the option most strongly decreasing East-Asia contributions for emissions end date 2050 would be to combine non-linear radiative forcing with using sea level rise as indicator and historical emissions from the EDGAR database, which results in contributions reduced by 3.3%, while linear addition of options in table 2 gives -3.1%. In this case the difference is caused by the strong influence of historical emissions on contributions to the slowly responding sea level rise. Thus the impact of using the EDGAR database (decreasing contributions) is amplified, if combined with sea level rise as indicator. In table 2, choosing evaluation date 2100 is also marked as an option lowering East-Asia contributions. However, because of the large time lag of sea level rise, the effect of taking 2100 as evaluation date is reversed, if contributions to sea level rise are considered, instead of temperature change. Evaluation date 2100 is only lowers the share of non-Annex-I regions when other indicators than sea level rise are used.

For the IPCC aggregated regions, the strongest influence on contributions for emissions end date 2000 is exerted by the choice of emission sources in- or excluded (fossil CO₂ only, all anthropogenic CO₂, or default: all Kyoto gases), which are found on the extreme left of right of table 1. Next, the time horizons (start date and gap between end and evaluation date) and choice of indicator (CO₂ concentrations, radiative forcing, temperature increase (default), or sea level rise) have a large impact. Non-linear attribution of CO₂ concentrations and the alternative (EDGAR) historical emissions database also have considerable impact, while non-linear attribution of radiative forcing is less important. For emissions end date 2050, non-linearities are much more important, while the impact of historical emissions is reduced. The future emissions scenario now emerges as an influential choice.

Some regions form exceptions within the larger IPCC, or Annex-I/non-Annex-I aggregations. If the colour of a cell near the middle of tables 1 and 2 is dark, or if the colour is light for a cell at the extreme left or right, the corresponding option has a very different effect for a particular region than for the aggregated group. Canada, Eastern Europe and Former USSR (within Annex-I), and Central America, South America and South Africa (within non-Annex-I) are relatively insensitive if the option of only accounting for CO₂ emissions is implemented. Contributions of Central America, Northern Africa, Southern Africa, South Asia and Japan are relatively sensitive to the choice of historical emissions database.

Table 1. Summarising table of sensitivity analysis for evaluation date 2000.

Explanation: In the first column, the percentage contribution is given for each region. In the other columns, the change in percentage contribution is indicated for the alternative cases. The columns are sorted from left to right with increasing contribution for non-Annex-I. The colour of the cells is a function of the relative change of a region's contribution with respect to the region's own default contribution (see legend). The AOS C-Cycle case is an exception in that change with respect to the non-linear concentration attribution case is taken.

	default	only fossil CO ₂ emissions	only CO ₂ emissions	indicator SLR	evaluation date 2050	indicator CO ₂ concentrations	AOS C-cycle (w.r.t. NonLinConc)	non-lin. forcing	EDGAR	non-lin. CO ₂ concentration	indicator forcing	start date 1950
Canada	1.7	0.5	0.0	-0.1	0.0	0.0	0.3	0.0	0.1	0.0	0.0	0.0
USA	21.9	7.7	1.6	1.9	1.4	0.8	0.8	0.2	0.4	-0.8	-0.6	-2.3
Central America	3.0	-1.5	-0.1	0.2	0.0	-0.3	-0.8	0.0	1.5	-0.1	-0.1	-0.1
South America	7.2	-4.9	0.0	-0.2	-0.1	-0.1	0.2	0.0	1.3	0.0	0.0	0.2
Northern Africa	0.9	-0.2	-0.1	0.0	0.0	-0.1	0.0	0.0	0.3	0.0	0.1	0.0
Western Africa	1.7	-1.4	-0.3	-0.2	-0.2	-0.2	-0.1	0.0	0.0	0.0	0.1	0.2
Eastern Africa	1.1	-1.0	-0.2	-0.1	-0.1	-0.1	0.0	0.0	-0.1	0.0	0.1	0.1
Southern Africa	1.4	-0.1	0.0	-0.1	-0.1	0.0	-0.1	0.0	0.3	0.0	0.1	0.1
OECD Europe	15.4	6.8	1.5	1.9	1.4	0.5	0.7	0.2	0.3	-0.7	-0.9	-1.8
Eastern Europe	3.9	1.3	0.1	-0.2	-0.1	0.0	0.1	0.0	0.5	0.1	-0.2	0.1
Former USSR	12.8	1.8	0.1	-1.5	-1.0	-0.2	-0.5	-0.1	-1.4	0.7	-0.3	1.5
Middle East	2.3	0.2	-0.1	-0.5	-0.2	0.4	0.1	-0.1	-0.1	0.2	0.4	0.3
South Asia	7.6	-5.1	-1.2	1.1	0.1	-1.3	-0.9	0.1	-2.6	-0.4	-0.1	-0.4
East Asia	9.1	-0.7	-1.1	-1.1	-0.7	0.0	-0.1	-0.2	-0.1	0.4	0.9	1.1
South East Asia	5.4	-4.0	-0.3	-0.8	-0.4	0.2	0.4	-0.1	-0.1	0.3	0.4	0.6
Oceania	1.3	-0.1	-0.2	-0.1	-0.1	-0.2	0.3	0.0	0.0	0.0	0.0	0.1
Japan	3.4	0.8	0.5	-0.3	0.0	0.6	-0.4	0.0	-0.4	0.2	0.1	0.2
OECD90	43.7	15.7	3.4	3.4	2.8	1.7	1.7	0.4	0.4	-1.3	-1.3	-3.8
EEUR & FSU	16.7	3.1	0.2	-1.6	-1.1	-0.2	-0.3	-0.1	-0.8	0.8	-0.5	1.6
Asia	22.0	-9.8	-2.6	-0.8	-1.0	-1.1	-0.5	-0.2	-2.8	0.3	1.2	1.3
Africa & Lam	17.6	-9.0	-0.9	-1.0	-0.6	-0.4	-0.8	-0.1	3.2	0.2	0.6	0.9
Annex-I	60.4	18.8	3.5	1.8	1.7	1.5	1.3	0.2	-0.4	-0.5	-1.8	-2.2
non-Annex I	39.6	-18.8	-3.5	-1.8	-1.7	-1.5	-1.3	-0.2	0.4	0.5	1.8	2.2

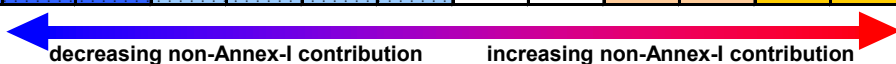


decrease relative to default contribution > 20%			increase relative to default contribution > 20%
decrease > 10%			increase > 10%
decrease > 5%			increase > 5%
decrease > 1%			increase > 1%

Table 2. Summarising table of sensitivity analysis for evaluation date 2050.

Explanation: In the first column, the percentage contribution is given for each region. In the other columns, the change in percentage contribution is indicated for the alternative cases. The columns are sorted from left to right with increasing contribution for non-Annex-I. The colour of the cells is a function of the relative change of a region's contribution with respect to the region's own default contribution (see legend). The AOS C-Cycle case is an exception in that change with respect to the non-linear concentration attribution case is taken.

	default	only fossil CO ₂ emissions	indicator SLR	only CO ₂ emissions	evaluation date 2100	non-lin. forcing	AOS C-cycle (w.r.t. NonLinConc)	indicator CO ₂ concentrations	EDGAR	start date 1950	indicator forcing	non-lin. CO ₂ concentration	Alb scenario
Canada	1.6	4.8	3.0	-4.3	-3.0	1.2	0.4	-7.4	3.5	-0.6	-2.9	-2.1	-16.0
USA	17.9	17.2	11.3	6.4	3.8	2.8	1.7	1.6	-1.0	-5.2	-4.4	-5.7	-14.8
Central America	2.9	-24.0	1.3	-9.5	-4.8	1.0	-1.0	-10.7	20.9	-0.7	-1.0	-2.2	10.9
South America	7.3	-34.0	-0.7	-4.3	-2.1	0.4	-0.2	-6.1	1.3	1.0	-1.2	-0.6	11.3
Northern Africa	1.7	-0.7	-21.0	-7.4	-3.6	-5.1	-3.2	4.0	1.2	3.9	10.9	9.5	25.4
Western Africa	2.1	-57.5	-7.0	-29.1	-11.1	0.0	-2.6	-28.2	-7.6	3.8	2.0	0.2	9.4
Eastern Africa	1.0	-73.7	0.7	-24.5	-11.6	1.4	-1.4	-26.0	-16.1	3.0	-0.6	-2.3	2.6
Southern Africa	1.8	-7.2	-12.1	-8.2	-3.9	-2.2	-1.8	-3.0	4.3	3.5	6.4	4.1	32.8
OECD Europe	11.2	22.1	18.1	8.6	6.6	4.4	2.6	1.0	2.1	-7.5	-6.9	-9.0	-7.3
Eastern Europe	3.1	20.5	8.2	6.6	3.4	1.9	1.9	2.3	8.5	-0.7	-3.9	-3.5	-8.3
Former USSR	9.2	3.1	8.5	-1.1	-2.8	2.9	1.8	-6.2	-6.4	1.8	-3.5	-5.5	-8.9
Middle East	5.4	11.7	-23.8	1.2	-1.2	-6.0	-2.2	11.1	-1.6	5.5	9.4	11.9	20.7
South Asia	10.1	-13.8	-8.6	-4.7	-2.5	-3.2	-2.6	4.1	-19.1	0.7	6.7	5.4	13.8
East Asia	14.4	9.0	-14.7	0.3	-0.6	-4.3	-1.4	6.1	16.4	4.9	5.0	8.9	-1.6
South East Asia	5.9	-39.9	-4.7	-5.7	-4.4	-1.0	-0.2	-3.7	-9.1	3.6	1.2	2.3	8.6
Oceania	1.2	0.6	1.3	-6.6	2.6	-0.3	-0.4	-6.7	3.3	2.4	-1.3	1.6	-12.1
Japan	3.1	17.6	4.2	11.8	6.4	1.3	2.6	7.2	-3.1	1.1	-4.2	-1.8	-7.9
OECD90	35.1	17.6	12.1	6.6	4.6	3.0	2.0	1.2	0.1	-4.9	-5.0	-6.0	-11.8
EEUR & FSU	12.3	7.4	8.4	0.8	-1.3	2.7	1.8	-4.1	-2.7	1.2	-3.6	-5.0	-8.7
Asia	30.4	-8.1	-10.7	-2.5	-2.0	-3.3	-1.6	3.5	-0.4	3.2	4.8	6.4	5.5
Africa & Lam	22.3	-20.8	-9.1	-7.4	-3.8	-1.7	-1.5	-4.5	1.8	2.7	3.3	3.4	15.8
Annex-I	47.3	15.0	11.2	5.1	3.0	2.9	1.9	-0.2	-0.6	-3.3	-4.7	-5.7	-11.0
non-Annex I	52.7	-13.5	-10.0	-4.6	-2.7	-2.6	-1.5	0.1	0.5	3.0	4.2	5.2	9.9



decrease relative to default contribution > 20%		increase relative to default contribution > 20%	
decrease > 10%		increase > 10%	
decrease > 5%		increase > 5%	
decrease > 1%		increase > 1%	

Concluding, in this paper we have assessed different approaches to calculating contributions of emission regions to global warming. Firstly, we have analysed the impact of choosing indicators for global warming on the calculated contributions. The contributions of early emitters are reduced for a choice of indicator, which minimises the time lag between emission and effect (e.g. longer time lag for sea level rise than for CO₂ concentration). Thus, generally speaking, the share of Annex-I countries would be lower for concentrations or forcing as an indicator, compared to temperature, or sea level rise.

Secondly, we have shown that the back- and forward-looking time horizons of the analysis have a large impact on the contributions. The parameters in question are the emission start date (backward-looking horizon: earlier emission are not taken into account), emission end date (later emission are not taken into account) and evaluation date (date at which contributions to global warming are calculated, equal to, or later than emission end date). The latter two define the forward-looking horizon. In general, an early emission start date raises contributions of Annex-I regions. A late emission end date increases non-Annex-I contributions, while a time gap between emission end and evaluation dates again raises Annex-I contributions. This time gap enables one to account for delayed, but inevitable global warming, which is in a sense equivalent to the approach using Global Warming Potentials (GWPs) with varying time horizon.

The third focus in our analysis is the issue of non-linearities. The issue of non-linearity in radiative forcing was assessed earlier. Applying the non-linear approach raises contributions of early emitters, due to saturation of radiative forcing as concentrations rise. In this paper, we bring forward a new method of calculating contributions to CO₂ concentrations. In this alternative method, the residence time of CO₂ in the atmosphere, which is attributed to a certain region, depends on global carbon cycle processes and total emissions. In contrast, the default method assesses concentration contributions for each region in isolation, then adding contributions linearly to calculate the global total. Using the alternative, non-linear approach has a large impact on a region during periods of strong emission growth or decrease. High emission growth as compared to the global mean results in lower contributions when using the alternative method. Although the mechanism is thus different from that of non-linear forcing, the two effectively cancel out for late emission end and evaluation dates.

We found considerable heterogeneity within aggregated Annex-I/non-Annex-I, or IPCC groups among smaller region aggregates. Therefore, the general conclusions above, drawn for groups as a whole, not always hold for all regions within the groups.

References

- Alcamo, J., Ed.: 1994, *IMAGE 2.0. Integrated modeling of global climate change*. Kluwer Academic Publishers.
- Alcamo, J., R. Leemans, and E. Kreileman, Eds.: 1998, *Global change scenarios of the 21st century. Results from the IMAGE 2.1 model*. Pergamon & Elseviers Science, 296 pp.
- Alcamo, J., E. Kreileman, M. Krol, R. Leemans, J. Bollen, J. van Minnen, M. Schaeffer, S. Toet, and B. de Vries: 1998, 'Global Modeling of Environmental Change: An overview of IMAGE 2.1', *Elsevier*.
- Andres, R. J., D. J. Fielding, G. Marland, and T. A. Boden: 1998, 'Carbon dioxide emissions from fossil-fuel use, 1751-1950', *Tellus (submitted)*.
- Berk, M. M. and M. G. J. Den Elzen: 1998, 'The Brazilian Proposal evaluated', *CHANGE*, **44**, 19-23.
- Cox, P. M., R. A. Betts, C. D. Jones, S. A. Spall, and I. J. Totterdell: 2000, 'Acceleration of global warming due to carbon-cycle feedbacks in a coupled climate model', *Nature*, **408**, 184-187.
- Den Elzen, M. G. J.: 2002, 'Exploring post-Kyoto climate regimes for differentiation of future commitments to stabilise greenhouse gas concentrations', RIVM Report RIVM-report 728001020.
- Den Elzen, M. G. J. and M. Schaeffer: 2002, 'Responsibility for past and future global warming: uncertainties in attributing anthropogenic climate change', *Climatic change*, **54**, 29-73.
- Den Elzen, M. G. J. and M. Schaeffer: 2002, 'Responsibility for past and future global warming', *Environmental Science and Policy (in preparation)*.
- Den Elzen, M. G. J., M. Berk, S. Both, A. Faber, and R. Oostenrijk: 2001, 'FAIR 1.0 (Framework to assess international regimes for differentiation of commitments): a decision-support model to explore options for differentiation of future commitments in international climate policy making.' RIVM report 728001013.
- Den Elzen, M. G. J., M. M. Berk, M. Schaeffer, J. G. J. Olivier, C. Hendriks, and B. Metz: 1999, 'The Brazilian proposal and other options for international burden sharing: an evaluation of methodological and policy aspects using the FAIR model.', RIVM report 728001011.
- Eickhout, B., M. G. J. den Elzen, and G. J. J. Kreileman: 2002, 'The atmosphere-ocean system in IMAGE 2.2', RIVM report 481508017 (in preparation).
- Enting, I. G.: 1998, 'Attribution of greenhouse gas emissions, concentrations and radiative forcing', Technical Paper 363.738740994.
- Enting, I. G. and R. M. Law: 2001, 'Characterising historical responsibility for the greenhouse effect', Technical Paper Draft Report.
- Filho, M. L. G. and M. Miguez: 1998, 'Time dependent relationship between emissions of greenhouse gases and climate change.
- Harvey, D., G. Gregory, M. Hoffert, A. Jain, M. Lal, R. Leemans, S. Raper, T. M. L. Wigley, and J. de Wolde: 1997, 'An introduction to simple climate model used in the IPCC Second Assessment report', in: Cambridge University Press.
- Hasselmann, K., R. Sausen, E. Maier-Reimer, and R. Voss: 1993, 'On the cold start problem in transient simulations with coupled atmosphere-ocean models', *Climate Dynamics*, **9**, 53-61.
- Haywood, J. M., D. L. Roberts, A. Slingo, J. M. Edwards, and K. P. Shine: 1997, 'General circulation model calculations of the direct radiative forcing by anthropogenic sulfate and fossil-fuel soot aerosol', *Journal of Climate*, **10**, 1562-1577.

- Houghton, J. T., Y. Ding, D. J. Griggs, M. Noguer, P. J. v. d. Linden, X. Dai, K. Maskell, and C. A. Johnson, Eds.: 2001, *Climate Change 2001. The Scientific Basis. Contribution of Working Group I to the Third Assessment Report of the Intergovernmental Panel on Climate Change*. Cambridge university press.
- Houghton, R. A.: 1999, 'The annual net flux of carbon to the atmosphere from changes in land use 1850-1990', *Tellus*, **51B**, 298-313.
- Hulme, M., T. Wigley, E. Barrow, S. Raper, A. Centella, S. Smith, and A. Chipanski: 2000, 'Using a climate scenario generator for vulnerability and adaptation assessments: MAGICC and SCENGEN version 2.4 workbook, 52 pp. pp.
- IMAGE-team: 2001, 'The IMAGE 2.2 implementation of the SRES scenarios. A comprehensive analysis of emissions, climate change and impacts in the 21st century. RIVM CD-ROM publication 481508018.
- Joos, F., G.-K. Plattner, T. F. Stocker, O. Marchal, and A. Schmittner: 1999, 'Global warming and marine carbon cycle feedbacks on future atmospheric CO₂', *Science*, **284**, 464-467.
- Joos, F., M. Bruno, R. Fink, U. Siegenthaler, T. F. Stocker, C. L. Quéré, and J. L. Sarmiento: 1996, 'An efficient and accurate representation of complex oceanic and biospheric models of anthropogenic carbon uptake', *Tellus*, **48B**, 397-417.
- Klein Goldewijk, C. G. M., J. G. van Minnen, G. J. J. Kreileman, M. Vloedveld, and R. Leemans: 1994, 'Simulating the carbon flux between the terrestrial environment and the atmosphere', *Journal of Water Air Soil Pollution*, **76**, 199-230.
- Manabe, S. and R. J. Stouffer: 1994, 'Multiple-century response of a coupled ocean-atmosphere model to an increase of atmospheric carbon dioxide', *Journal of Climate*, **7**, 5-23.
- Marland, G., T. A. Boden, R. J. Andres, A. L. Brenkert, and J. C.A.: 1999, *Global, regional, and national fossil fuel CO₂ emissions, In: Trends: A Compendium of Data on Global Change, Carbon Dioxide Information Analysis Center (CDIAC), Oak Ridge National Laboratory (ORNL)*.
- Nakicenovic, N., J. Alcamo, G. Davis, B. de Vries, J. Fenhann, S. Gaffin, K. Gregory, A. Grübler, T. Y. Jung, T. Kram, E. Emilio la Rovere, L. Michaelis, S. Mori, T. Morita, W. Pepper, H. Pitcher, L. Price, K. Riahi, A. Roehrl, H. Rogner, A. Sankovski, M. Schlesinger, P. Shukla, S. Smith, R. Swart, S. van Rooyen, N. Victor, and Z. Dadi: 2000, *Special Report on emissions scenarios. IPCC Special Reports*, Cambridge University Press, 599 pp.
- Olivier, J. G. J. and J. J. M. Berdowski: 2001, 'Global emissions sources and sinks', in: J. Berdowski, R. Guicherit, and B. J. Heij, Eds., *The Climate System*, A.A. Balkema Publishers/Swets & Zeitlinger Publishers, Lisse, The Netherlands. ISBN 90 5809 255 0, 33-78.
- Prather, M., D. Ehhalt, F. J. Dentener, R. Derwent, E. Dlugokencky, E. Holland, I. Isaksen, J. Katima, V. Kirchhoff, P. Matson, P. Midgley, and M. Wang: 2001, 'Atmospheric chemistry and Greenhouse Gases', in: J. T. Houghton, Y. Ding, D. J. Groggs, M. Nogour, P. J. van der Linden, X. Dai, K. Maskell, and C. A. Johnson, Eds., *IPCC Third Assessment - Climate Change 2001, The Scientific Basis*, Cambridge University Press.
- Prather, M. J.: 1994, 'Lifetimes and eigenstates in atmospheric chemistry', *Geophysical Research Letters*, **21(9)**, 801-804.
- Prather, M. J.: 1996, 'Time scales in atmospheric chemistry: Theory, GWPs for CH₄ and CO, and runaway growth', *Geophysical Research Letters*, **23**, 2597-2600.
- Prentice, I. C., G. D. Farquhar, M. J. R. Fasham, M. L. Goulden, M. Heimann, V. J. Jaramillo, H. S. Khashgi, C. Le Quéré, R. J. Scholer, and D. W. R. Wallace: 2001, '

- The carbon cycle and atmospheric carbon dioxide', in: J. T. Houghton, Y. Ding, D. J. Griggs, M. Noguer, P. J. van der Lindern, X. Dai, K. Maskell, and C. A. Johnson, Eds., *Climate change 2001: The scientific basis*, Cambridge University Press, 183-237.
- Ramaswamy, V., O. Boucher, J. Haigh, D. Hauglustaine, J. Haywood, G. Myhre, T. Nakajima, G. Y. Shi, and S. Solomon: 2001, 'Atmospheric chemistry and Greenhouse Gases', in: J. T. Houghton, Y. Ding, D. J. Groggs, M. Nogour, P. J. van der Linden, X. Dai, K. Maskell, and C. A. Johnson, Eds., *IPCC Third Assessment - Climate Change 2001, The Scientific Basis*, Cambridge University Press.
- Raper, S. C. B., J. M. Gregory, and T. J. Osborn: 2001, 'Use of an upwelling-diffusion energy balance climate model to simulate and diagnose A/OGCM results', *Climate Dynamics*, **17**, 601-613.
- Senior, C. A. and J. F. B. Mitchell: 2000, 'The Time-Dependence of Climate Sensitivity', *Geophysical Research Letters*, **27**, 2685-2688.
- UNFCCC: 1997, 'The Kyoto Protocol to the Convention on Climate Change', Climate Change Secretariat.
- UNFCCC: 1999, 'Report on the Expert Meeting on the Brazilian Proposal: scientific aspects and data availability', <http://unfccc.int/sessions/workshop/010528/mrep1999.pdf>.
- UNFCCC: 2001, 'Scientific and methodological aspects of the Proposal by Brazil, Progress report on the review of the scientific and methodological aspects of the proposal by Brazil, FCCC/SBSTA/2001/INF.2 (<http://www.unfccc.int>).'
- UNFCCC: 2002, 'Assessment of contributions to climate change, Terms of Reference (<http://unfccc.int/issues/cc.html>).'
- Van Aardenne, J. A., F. J. Dentener, J. G. J. Olivier, C. G. M. Klein Goldewijk, and J. Lelieveld: 2001, 'A 1 x 1 degree resolution dataset of historical anthropogenic trace gas emissions for the period 1890-1990 (<http://www.rivm.nl/env/int/coredata/edgar/>)', *Global Biogeochemical Cycles*, **15(4)**, 909-928.
- Voss, R., R. Sausen, and U. Cubasch: 1998, 'Periodically Synchronously Coupled Integrations with the Atmosphere-Ocean General Circulation Model ECHAM3/LSG', *Climate Dynamics*, **14**, 249-266.
- Watterson, I. G.: 2000, 'Interpretation of simulated global warming using a simple model', *Journal of Climate*, **13**, 202-215.
- Wigley, T. M. L. and M. E. Schlesinger: 1985, 'Analytical solution for the effect on increasing CO₂ on global mean temperature', *Nature*, **315**, 649-652.
- Wigley, T. M. L. and S. C. B. Raper: 1993, 'Future changes in global mean temperature and sea level', in: R. A. Warrick, E. M. Barrow, and T. M. L. Wigley, Eds., *Climate and sea level change: observations, projections and implications*, Cambridge University Press.
- Wigley, T. M. L. and S. C. B. Raper: 1995, 'An heuristic model for sea level rise due to the melting of small glaciers', *Geophysical Research Letters*, **22**, 2749-2752.

Appendix A Mailing list

VROM

1. B. Borst
2. M. Goote
3. R. Brieskorn
4. R. Ch. Hernaus
5. M. Hildebrand
6. L. de Jonge
7. E. Koekkoek
8. J. Lenstra
9. E. Mulders
10. H. Nieuwenhuis
11. P. Ruysenaars
12. E. Trines

EZ

13. O.G. Aardenne
14. M. Blanson Henkemans
15. W. Monna

V&W

16. W. Fransen
17. K. Verbeek

BZ

18. J. Frederiks
19. M. van Giezen
20. R. Lefeber
21. H. van der Molen
22. M. Oosterman
23. J. Rooimans

LNV

24. H. Haanstra
25. F. Hoogveld

Novem

26. D. Both
27. H. Wittenhorst

28. C. Artusio, Dept. of State, USA
29. R. Ball, Dept. of Energy, USA
30. I. Enting, CSIRO Atmospheric Research, Australia
31. C.E. Ereño, University of Buenos Aires, Argentina
32. J. Gundermann, Danish Environmental Protection Agency, Denmark
33. W. Hare, Greenpeace International, Amsterdam

34. H. Hengeveld, Environment Canada, Canada
35. N. Höhne, ECOFYS, Germany
36. Y. Igarashi, Min. of Foreign Affairs, Japan
37. A. Keil, Meteorological Office, UK
38. A. Kurosawa, Institute of Applied Energy, Japan
39. L.G. Meira Filho, Brazilian Space Agency, Brazil
40. J.D.G. Miquez, MTU, Brazil
41. W. Ogana, University of Nairobi, Kenya
42. N. Paciornik, MTU, Brazil
43. A. Paul, TERI, India
44. C. Philibert, International Energy Agency, France
45. R. Prince, Dept. of Energy, USA
46. B. Romstad, Cicero, Norway
47. C.A. Senior, Hadley Centre for Climate Prediction and Research, U.K. Met Office., UK
48. T.L. Stratton, Dept. of Foreign Affairs and International Trade, Canada
49. D. Tirpak, UNFCCC, Germany
50. S. Towprayoon, King Mongkut's University of Technology Thonburi, Thailand
51. D. Warrilow, Dept. of Environment, Food and Rural Affairs, UK
52. M. Weiß, Federal Environmental Agency, Germany
53. N. Ying, China Meteorological Administration, China
54. Depot Nederlandse Publikaties en Nederlandse Bibliografie
RIVM
55. H. Pont
56. N.D. van Egmond
57. F. Langeweg
58. R. Maas
59. A. van der Giessen
60. J. Hoekstra
61. D. van Lith
62. B. Metz
63. O.J. van Gerwen
64. J. Oude Lohuis
65. R. van den Wijngaart
- 65-80. afdeling MNVi
81. J. Olivier
82. J. Peters
- 83-125. Auteurs
126. SBD/Voorlichting & Public Relations RIVM
127. Bureau Rapportenregistratie RIVM
128. Bibliotheek RIVM
- 129-138. Bureau Rapportenbeheer RIVM

Appendix B UNFCCC-ACCC Terms of Reference

Assessment of Contributions to Climate Change - TERMS OF REFERENCE

Phase 1 - Initial check

In a first phase, all groups that wish to participate should assess whether their simple models can represent the results of more complex carbon cycle and climate models. To this end, groups should calculate the increase in global-average surface temperature for historical emissions and the SRES A2 future emissions scenario. The results of this initial check will then be compared between the models and changes can be made to the models, if necessary.

RIVM in the Netherlands and the Met Office's Hadley Centre in the United Kingdom have provided a set of parameters that can be used to tune simple carbon cycle and simple climate models or to complete those models if they do not include all aspects that are included in the complex models used for the SRES scenarios. Those data are available at the project web site

<http://unfccc.int/issues/cc.html>

Timeframe

1760 to 2100

Historical emissions data

CDIAC database (<http://cdiac.esd.ornl.gov/trends/trends.htm>) for

- Carbon Dioxide Emissions from Fossil-Fuel Consumption
- Carbon Flux from Land-Cover Change

Future emission scenarios

Future emissions scenarios A2 from the IPCC Special report on emission scenarios.

(<http://www.grida.no/climate/ipcc/emission/index.htm>)

Countries/regions

Global (No regional groups)

Model parameters

Emissions to concentrations:

- Carbon cycle parameters, representing the Bern carbon cycle model (see project web site)
- Single (IPCC TAR) lifetimes should be used for other greenhouse gases, the OH chemical feedback effects will be neglected.

Concentrations to radiative forcing:

- The saturation of the absorption bands for CO₂ should be included as a logarithmic relationship, as in the IPCC TAR.
- The N₂O-CH₄ band overlap should be included as in the IPCC TAR.
- Global mean aerosol particle forcing as provided by the Hadley Centre (see project web site).

Radiative forcing to temperature increase:

- Climate response parameters obtained from the HadCM3 climate model (see project web site).

Climate output indicators

- Output indicators should include
- Cumulative emissions
- Concentration
- Radiative forcing
- Global-average surface air temperature change

Output requirements

To satisfy the project output requirements participating institutions will need to produce both graphical results and simple ASCII files of their outputs. The results must be submitted to the project web site.

Submission of results

The results of this phase should be submitted to Dr. Sarah Raper (unfccc_assessment@uea.ac.uk) by **1 June 2002** and will be placed on the web (<http://unfccc.int/issues/cc.html>) as to enable the modelling groups to adjust their models if necessary. The results will be compiled for the expert meeting in September 2002.

Phase 2 - Sensitivity study

As a second step, the modelling groups should present their results in terms of the contributions made by four country groups (specified below). This will be referred to in this document as an attribution calculation. Group should also analyse the influence of changes in the model parameters. To ensure that all institutions undertake a few similar model runs that can be compared, a default parameter is underlined>. All participants are required to undertake one run with the default parameters. Only one parameter should be varied at the time when assessing the sensitivity to of the parameters listed below. Participants are free to undertake any number of additional sensitivity runs for other parameters than those specified below.

Timeframe

- Emissions start dates: 1890, 1950 and 1990
- Emission end dates: 1990, 2000, 2050 and 2100
- The time for which the attribution calculations will be performed: 2000, 2050, 2100, 2500

Clearly not all combinations of start and end date are meaningful. Start dates must always be before the end date. Attribution calculations made for a point in time before the emissions end dates will not include the effect of emissions beyond the date of the attribution calculation. Attribution calculation made for a point in time after the emissions end date assumes zero emissions after the end date.

Historical emissions data

- CDIAC database (<http://cdiac.esd.ornl.gov/trends/trends.htm>) and
- EDGAR database (<http://www.rivm.nl/env/int/coredata/edgar/>)

Bunker emissions should be treated as a separate country/group.

Future emission scenarios

Future emissions scenarios should comprise the B1, A2 and A1FI emission scenario from the IPCC Special report on emission scenarios.

<http://www.grida.no/climate/ipcc/emission/index.htm>

Countries/regions

The groups of countries considered should include at least the groups used in the IPCC Special report on emission scenarios, which consist of

- States that were members of the OECD in 1990 (OECD90)
- Eastern Europe and former Soviet Union (REF)
- Asia (ASIA)
- Africa and Latin America (ALM)

Model parameters

Emissions to concentrations:

- A range of carbon cycle parameters from the Bern CC model with a low, reference and high CO₂ case (see project web site) or other own carbon cycle representation.
- Single (IPCC TAR) lifetimes should be used for other greenhouse gases, the OH chemical feedback effects will be neglected.

Concentrations to radiative forcing:

- The saturation of the absorption bands for CO₂ should be included as a logarithmic relationship, as in the IPCC TAR.
- The N₂O-CH₄ band overlap should be included as in the IPCC TAR.
- Global mean aerosol particle forcing as provided by the Hadley Centre (see project web site). These forcings can be used in the calculation of global mean climate change, but not in the attribution of responsibility calculations.

Radiative forcing to temperature increase:

- A range of climate response parameters, representing several different GCM models (see project web site for the default values) or own climate response, default is the HadCM3 climate model used also in phase I. Non-linearities in the carbon cycle, radiative forcing and climate model may be investigated, but feedback between temperature and chemistry will not be included at this stage.

Climate output indicators

- Cumulative emissions
- Concentration
- Radiative forcing
- Global-average temperature change
- Rate of change of temperature
- Global-average sea level rise (only the thermal expansion component of sea level rise)

A damage function is optional at this stage.

Socio-economic indicators

In addition to the basic attribution calculations, groups may wish to present results using also socio-economic factors, such as GDP or population. This is at the discretion of the modelling groups.

Output requirements

To satisfy the project output requirements groups will need to produce both graphical results and simple ASCII files of their outputs. The results must be submitted to the project web site.

Submission of results

The results of this phase should be submitted to Dr. Sarah Raper (unfccc_assessment@uea.ac.uk) by **1 August 2002** and will be placed on the web (<http://unfccc.int/issues/ccc.html>). The results will be compiled for an expert meeting in September 2002.

For some literature on the Brazilian proposal please refer to <http://unfccc.int/sessions/workshop/010528/index.html>.

Appendix C Model description of IMAGE-AOS and ACCC

Equations and parameters used in IMAGE-AOS ('IMAGE-AOS') and the default configuration for ACCC-TOR ('ACCC').

Emissions to Concentrations

Concentration (ρ , in ppmv) is defined as perturbation from a pre-industrial ('background') concentration (ρ_{pi}) caused by anthropogenic emissions. ρ is calculated from the integral of $\dot{\rho}$ (change of ρ in time)

$$\rho(t) = \int_{t_0}^t \dot{\rho}(t') dt', \text{ with } t_0 \text{ emission start date and } t \text{ evaluation date.} \quad (C1)$$

$$\text{The total global concentration including 'background' is defined as } \rho_{total}(t) = \rho(t) + \rho_{pi} \quad (C2)$$

1) CO_2

$$\rho_{pi} = 278 \text{ ppmv.}$$

$$C_{CO_2} = 0.471 \text{ ppmv/GtC (conversion factor for emissions to concentrations)}$$

IMAGE-AOS

For global mean C-cycle calculations in IMAGE-AOS a mass conservation equation can be used, reflecting the global carbon balance:

$$\dot{\rho}(t) = C_{CO_2} [E_{CO_2}(t) - (S_{oc}(t) + E_{for}(t) + NEP(t))] \quad (C3c)$$

where $E_{CO_2}(t)$ is the total anthropogenic emissions, S_{oc} is the CO_2 uptake by the oceans, E_{for} the CO_2 uptake through forest regrowth and NEP is CO_2 uptake by the full-grown vegetation (all components in gigatons of carbon content per year = GtC/yr). In IMAGE-AOS, $E_{for}(t)$ and $NEP(t)$ is exogenous input, taken from scenario runs of IMAGE 2.2. The latter calculates the terrestrial uptake from the atmosphere as altered by atmospheric CO_2 concentrations, climate change and different land cover conversions. The spatial resolution of the calculations is horizontally 0.5 degree latitude by 0.5 degree longitude. In addition, carbon storage and removal is calculated for 7 carbon pools (living biomass: leaves, stems, branches and roots, and dead biomass: litter, soil humus and charcoal)(Klein-Goldewijk et al., (1994); Alcamo et al., (1998); (IMAGE-team, 2001)). The oceanic uptake S_{oc} is calculated with the oceanic carbon model of IMAGE 2.2, i.e. the box-diffusion type oceanic carbon model of Joos et al. (Joos et al., 1996; 1999). The model is based on a mixed-layer-pulse-response function, which allows for describing time-dependent non-linear effects of seawater chemistry resulting from changes in the atmospheric CO_2 concentration. The analytical representation (impulse response function, or known as a convolution integral) of the mixed layer response function of the Princeton 3-D model (Joos et al., 1996; 1999) is used. This model includes a positive temperature feedback on chemical CO_2 buffering system, leading to reduced transport to the deeper oceanic layers at higher temperatures.

ACCC

$\dot{\rho}$ is defined as a summation of the time derivative of carbon content in $S+1$ independent carbon pools:

$$\dot{\rho}(t) = \sum_{s=0}^S \dot{\rho}_s(t), \text{ with } \dot{\rho}_0(t) = f_0 \cdot C_{CO_2} \cdot E_{CO_2}(t) \text{ and } \dot{\rho}_s(t) = f_s \cdot C_{CO_2} \cdot E_{CO_2}(t) - \rho_s(t)/\tau_s \quad (C3a)$$

where $E_{CO_2}(t)$ the total anthropogenic emissions (emissions from fossil fuel combustion, industrial sources and land use changes) (GtC).

Combining eq. (C1) and (C3a) gives the alternative expression of ρ by the convolution integral

$$\rho(t) = C_{CO_2} \int_{t_0}^t R(t-t') \cdot E(t') dt', \text{ with } R(t) = f_0 + \sum_{s=1}^3 f_s e^{-t/\tau_s} \quad (C3b)$$

Table C.1. The coefficients f_s (-) and τ_s (years) as calculated by fitting the impulse response function with different Bern C-cycle models, as used in the ACCC. The ACCC default is Bern C-cycle of (Joos et al., 1996; 1999)], as used in the carbon cycle model calculations in the IPCC Second and Third Assessment Report (Bern SAR and TAR).

coefficients	Bern SAR (S=5)			Bern TAR (S=3)
	standard	low	high	default
f_0	0.1369	0.1253	0.1504	0.152
f_1	0.1298	0.0909	0.1787	0.253
f_2	0.1938	0.1839	0.1798	0.279
f_3	0.2502	0.2674	0.2201	0.316
f_4	0.2086	0.2380	0.1725	
f_5	0.0807	0.0865	0.0975	
τ_1	371.6	407.2	330.8	171.0
τ_2	55.70	50.86	67.03	18.0
τ_3	17.01	15.19	21.72	2.57
τ_4	4.16	3.73	5.61	
τ_5	1.33	1.42	1.51	

2) non-CO₂

IMAGE-AOS and ACCC

For both models, the change in concentration in time of non-CO₂ gas g (CH₄, N₂O, HFCs, PFCs, or SF₆) is defined by a single-lifetime expression:

$$\dot{\rho}_g(t) = C_g \cdot E_g(t) - \rho_g(t)/\tau_g \quad (C4a)$$

ρ_g and E_g are the concentration and emissions expressed in ppbv and MtCH₄ for CH₄, in ppbv and MtN for N₂O and in pptv and Mt for the other gases, and τ_g is the atmospheric lifetime.

Table C.2. Parameter values for different greenhouse gases used in equations (B2-B10), as used in the ACCC model.

g	$\rho_{g,pi}^*$	τ_g^* (years)	C_g^{**}	α_g^* (10 ⁻³ Wm ⁻² /pptv)
CH ₄	700 ppbv	8.4	0.353 ppbv/MtCH ₄	
N ₂ O	270 ppbv	120	0.202 ppbv/MtN	
HFC-23	0 pptv	260	0.086 pptv/Mt	0.16
HFC-32	0 pptv	5	0.116 pptv/Mt	0.09
HFC-43-10mee	0 pptv	15	0.07442 pptv/Mt	0.40
HFC-125	0 pptv	29	0.05211 pptv/Mt	0.23
HFC-134a	0 pptv	13.8	0.07442 pptv/Mt	0.15
HFC-143a	0 pptv	52	0.07142 pptv/Mt	0.13
HFC-152a	0 pptv	1.4	0.09469 pptv/Mt	0.09
HFC-227ea	0 pptv	33	0.035 pptv/Mt	0.30
HFC-236fa	0 pptv	220	0.0394 pptv/Mt	0.28
HFC-245ca	0 pptv	5.9	0.0448 pptv/Mt	0.23
CF ₄	44 pptv	50000	0.068 pptv/Mt	0.08
C ₂ F ₆	0 pptv	10000	0.0508 pptv/Mt	0.26
SF ₆	0 pptv	3200	0.041 pptv/Mt	0.52

* (Houghton et al., 2001), (Ramaswamy et al., 2001)

** (Alcamo, 1994)

IMAGE-AOS

For CH₄, HCFCs and HFCs, fixed lifetimes are used in the ACCC model. However, by default in IMAGE-AOS, lifetimes for these gases depend on OH abundance, because of the reactivity of these gases with the OH radical (Eickhout et al., (2002)). τ_g for these gases is calculated based on the IPCC-TAR methodology (Prather et al., 2001) as follows:

$$\frac{1}{\tau_g(t)} = \frac{1}{\tau_{chemical}(t)} + \frac{1}{\tau_{stratospheric}} + \frac{1}{\tau_{soil-loss}} \quad (C5)$$

where $\tau_{chemical}(t)$ is the time-dependant chemical lifetime, $\tau_{stratospheric}$ the lifetime due to loss to stratosphere and $\tau_{soil-loss}$ the lifetime due to loss to biosphere (only methane is absorbed by soils, with a specific time constant of 150 years (Harvey et al., 1997)). $\tau_{chemical}$ is determined by the reaction rate for the oxidation by OH radicals: $1/(k_{g+OH} \cdot \rho[OH])$, with k_{g+OH} is the reaction rate (cm³/years) and $\rho[OH]$ the OH concentration (molecules per cm³). The OH concentration will depend on the

emissions of CH₄ and the ozone precursors CO, NO_x and NMVOC, and determines the lifetimes of these compounds. In the IPCC-TAR, this dependency is represented by the linear interpolation mentioned in Table 4.11 in the TAR (Prather et al., 2001), with the use of sensitivity coefficients for the reaction of OH with CH₄, and the CO, NO_x and NMVOC. The chemical removal rate and atmospheric lifetime of methane also depend on the concentration of CH₄ itself. This important OH-feedback, the so-called chemical feedback is defined as $1/(1 + FF)$, in which the sensitivity FF represents the relative change (%) in the globally averaged CH₄ loss frequency for a +1% increase in CH₄ concentration above 1700 ppbv (1990-concentration) (Prather, 1994; Prather, 1996). The central IPCC-TAR value for RR is 1.45 (FF : -0.32%) (Prather et al., 2001). This means that tropospheric OH concentration declines by 0.32% for every 1% increase in CH₄. The change in concentration of the gases influenced by OH chemistry is now expressed by combining eq. (C4a) and (C5):

$$\dot{\rho}_g(t) = C_g \cdot E_g(t) - \rho_g(t)/\tau_g(t) \quad (C4b)$$

Concentrations to Radiative Forcing

IMAGE-AOS and ACCC

In both models global radiative forcing $F_{total}(t)$ (Wm⁻²) is calculated as the linear sum of forcing $F_g(t)$ (Wm⁻²) by all gases g plus a contribution by aerosol forcing. The contribution to global radiative forcing by each greenhouse gas g is calculated using the following functional dependencies (Ramaswamy et al., 2001):

$$F_{CO_2}(t) = 5.325 \log(\rho_{total}(t)/\rho_{pi}) \quad (C6)$$

$$F_{CH_4}(t) = 0.036 \left[\sqrt{\rho_{CH_4, total}(t)} - \sqrt{\rho_{CH_4, pi}} \right] - f(\rho_{CH_4, total}(t), \rho_{N_2O, pi}) + f(\rho_{CH_4, pi}, \rho_{N_2O, pi}) \quad (C7)$$

$$F_{N_2O}(t) = 0.12 \left[\sqrt{\rho_{N_2O, total}(t)} - \sqrt{\rho_{N_2O, pi}} \right] - f(\rho_{CH_4, pi}, \rho_{N_2O, total}(t)) + f(\rho_{CH_4, pi}, \rho_{N_2O, pi}) \quad (C8)$$

with the overlap forcing of CH₄ and N₂O defined by

$$f(\rho_{CH_4}, \rho_{N_2O}) = 0.47 \ln \left[1 + 2.01 \cdot 10^{-5} (\rho_{CH_4} \rho_{N_2O})^{0.75} + 5.31 \cdot 10^{-15} \rho_{CH_4} (\rho_{CH_4} \rho_{N_2O})^{.72} \right] \quad (C9)$$

For the other gases radiative forcing is given by

$$F_g(t) = \alpha_g (\rho_{g, total}(t) - \rho_{g, pi}) = \alpha_g \rho_g(t) \quad (C10)$$

See table C.2 for values of α_g .

The forcings of aerosols and of chlorinated and brominated halocarbons are used in the calculation of global radiative forcing, and thus global mean temperature increase, but not in the attribution of responsibility calculations.

IMAGE-AOS

The radiative forcing of tropospheric and stratospheric ozone and stratospheric water vapour is based on IPCC-TAR and Harvey (Harvey et al., 1997). The direct and indirect forcing from sulphate aerosols are calculated according to (Harvey et al., 1997). Hence, the direct effect is scaled linearly with the emissions of SO₂ and the indirect effect varies with the logarithm of SO₂ emissions. The forcing of the fossil and biomass burning organic and black-carbon aerosol is based on the forcing functions, as described in (Eickhout et al., 2002).

ACCC

A time series for total forcing by sulphate aerosols (direct + indirect) from the HadCM3 GCM is taken for both the historical period. After 1990, data is taken from the appropriate HadCM3 IPCC SRES scenario experiment.

Temperature Change and Sea Level Rise

IRFs

Both global mean surface-air temperature (T) and sea-level rise (SLR) are calculated by impulse response functions of radiative forcing, mathematically equivalent to a model consisting of two independent (parallel) box models:

$$\dot{T}(t) = \sum_{s=1}^2 \dot{T}_s(t) = \sum_{s=1}^2 \left[\frac{T_{eq}}{F_{eq}} \frac{a_s^T}{\tau_s^T} F_{total}(t) - T_s(t) / \tau_s^T \right] \quad (C11)$$

$$T(t) = \int_{t_0}^t \dot{T}(t') dt', \text{ which, with (C11), is equivalent to } T(t) = \frac{T_{eq}}{F_{eq}} \int_{t_0}^t R^T(t-t') F_{total}(t') dt' \quad (C12)$$

$$\text{with } R^T(t) = \sum_{s=1}^2 \frac{a_s^T}{\tau_s^T} e^{-t/\tau_s^T} \quad (C13)$$

$$S\dot{L}R(t) = \sum_{s=1}^2 S\dot{L}R_s(t) = \sum_{s=1}^2 \left[\frac{SLR_{eq}}{F_{eq}} \frac{a_s^{SLR}}{\tau_s^{SLR}} F_{total}(t) - SLR_s(t) / \tau_s^{SLR} \right] \quad (C14)$$

$$SLR(t) = \int_{t_0}^t S\dot{L}R(t') dt', \text{ which, with (C14), is equivalent to } SLR(t) = \frac{SLR_{eq}}{F_{eq}} \int_{t_0}^t R^{SLR}(t-t') F_{total}(t') dt' \quad (C15)$$

$$\text{with } R^{SLR}(t) = \sum_{s=1}^2 \frac{a_s^{SLR}}{\tau_s^{SLR}} e^{-t/\tau_s^{SLR}} \quad (\text{C16})$$

Table C.3. Parameters for for temperature change Impulse Response Functions derived from a range of GCM experiments, as described in (den Elzen and Schaeffer, (2002).

Climate model (aliases used in this article)	Reference	T_{eq} (°C)	τ_1^T (years)	a_1^T	τ_2^T (years)
ECHAM1/LSG	(Hasselmann et al., 1993)	1.58	2.86	0.685	41.67
ECHAM3/LSG	(Voss et al., 1998)	2.5	14.4	0.761	393
GFDL '90	(Hasselmann et al., 1993)	1.85	1.2	0.473	23.5
GFDL '93 2×	(Manabe and Stouffer, 1994)	3.5	6.5	0.671	388
GFDL '93 4×	(Manabe and Stouffer, 1994)	3.5	8.5	0.665	233
GFDL '97	(Haywood et al., 1997)	3.7	12.6	0.613	145
HadCM2	(Senior and Mitchell, 2000)	3.0	7.4	0.527	199
CSIRO	(Watterson, 2000)	3.6	12.7	0.605	432
IMAGE 2.2	(den Elzen and Schaeffer, 2002)	2.37	2.19	0.654	76
Brazilian revised	(Filho and Miguez, 1998)	3.06	20	0.634	990

IMAGE-AOS

The IRF calculations above can be used in the climate assessment module in FAIR 1.1. However, by default IMAGE-AOS is used, which includes the Upwelling-Diffusion Climate Model (UDCM) of IMAGE 2.2 (Eickhout et al., (2002)) is used to derive global-mean surface-air temperature changes and temperature changes in the ocean from radiative forcings. UDCM is based on the MAGICC-model of Climate Research Unit (CRU) (Wigley and Schlesinger, (1985); (Hulme et al., 2000); Raper et al., (2001)). The model consists of an atmosphere box, two land and two ocean boxes (representing the Northern and Southern Hemisphere). The two ocean boxes are divided into 40 layers each, with a mixed layer on top that absorbs the energy of solar radiation. It is assumed that no energy is adsorbed above land. The energy balance of the climate system can be described as follows: $F = \lambda T + F_{oc}$, where F_{oc} is the net global-mean heat flux into the ocean. The term λT is the change in the rate of heat loss to space from the climate system. The feedback parameter λ is the inverse of the climate sensitivity. Hence, the radiative forcing is partitioned between increased heat loss to space and additional uptake of heat by the climate system (Raper et al., 2001). The absorbed heat is exchanged between the four boxes (determined by k_{LO} and k_{NS} ; the land-ocean and northern-southern hemisphere exchange coefficient respectively). On time scales relevant to climate change, the atmosphere may be assumed to be in equilibrium with the underlying oceanic mixed layer. The absorbed heat is transported within each ocean box by diffusion and upwelling. The upwelling decreases at increasing temperatures of the ocean to simulate the slowing down of the thermohaline circulation of the ocean (Raper et al., 2001). Sea level rise calculations are based calculations in UDCM. Thermal expansion is a non-linear function of the temperature in each oceanic layer (determined by UDCM). The influence by small glaciers is determined by the global mean surface temperature change, a minimum temperature at which the glacier would eventually disappear, an initial ice volume, the equilibrium ice volume and the glacier response time (Wigley and Raper, 1995). To take regional variations into account, a set of minimum temperatures and response times is applied. The influence by the Greenland and Antarctica ice sheets is calculated with two factors (Wigley and Raper, 1993): one that represents the gain or loss of ice due to the initial state of the ice sheet (in 1880) plus a factor to describe the influence of temperature change on the ice sheets. The West Antarctic Ice Sheet contains enough ice to raise the sea level by 6 metres and has attracted special attention because it may result in rapid ice discharge due to weak surrounding ice shelves. However, it was concluded that this was very unlikely to happen in the 21st century (IPCC, 2001).

ACCC

The default parameters for using eq. (C11)-(C16) in ACCC are given in table C.4.

Table C.4. Parameter values for temperature calculations (leftcolumn) and for sea level rise (right column) calculations and the in ACCC. These parameters were taken from a fit to a HadCM3 experiment, with $F_{eq} = 7.0 \text{ Wm}^{-2}$.

T	SLR
$T = 7.3583 \text{ K}$	$SLR_{eq} = 4.7395 \text{ m}$
$\tau_1 = 8.4007 \text{ years}$	$\tau_1^{SLR} = 1700.2 \text{ years}$
$a_1 = 0.59557$	$a_1^{SLR} = 0.96677$
$\tau_2 = 409.54 \text{ years}$	$\tau_2^{SLR} = 33.788 \text{ years}$
$a_2 = 0.40443$	$a_2^{SLR} = 0.03323$

Appendix D Calculation of contributions of emission regions

Concentrations

Calculations of concentration changes resulting from emissions are performed according to the equations in Appendix C for each emitting region separately. For example, the change in CO₂ concentration for ACCC for region r is expressed as in eq. (C3a):

$$\dot{\rho}^r(t) = \sum_{s=0}^3 \dot{\rho}_s^r(t) \quad (D1)$$

with $\dot{\rho}_0^r(t) = f_0 \cdot C_{CO_2} \cdot E_{CO_2}^r(t)$ and

$$\dot{\rho}_s^r(t) = f_s \cdot C_{CO_2} \cdot E_{CO_2}^r(t) - \rho_s^r(t)/\tau_s \quad (D2a)$$

with $E_{CO_2}^r(t)$ the time series of anthropogenic emissions (PgC) for region r .

The total global CO₂ concentration is then calculated for a total of R regions as

$$\rho^{total}(t) = \sum_{r=1}^R \sum_{s=0}^S \rho_s^r(t) + \rho_{pi} = \sum_{r=1}^R \sum_{s=0}^S \int_{t_0}^t \dot{\rho}_s^r(t') dt' + \rho_{pi} \quad (D3)$$

which equals $\rho(t)$ as calculated using eqs. (C2) and (C3b)

Thus, in this approach, the global carbon cycle is divided into R hypothetical independent pools, one for each emitting region, described with the same C-cycle model and parameters. Concentrations and removal rates for region r therefore only depend on emissions of this one region, not on emissions of other regions. In fact there is only one global carbon cycle, of course, which further shows distinct non-linearities. The following alternative calculation of regional attribution of CO₂ concentrations appreciates this. A time-dependent single effective global mean turnover time $\tau(t)$ is defined by the global carbon balance:

$$\dot{\rho}(t) = C_{CO_2} E_{CO_2}(t) - \rho(t)/\tau(t) \quad (D4)$$

$\tau(t)$ can thus be calculated from global total emission and concentration (perurbations from pre-industrial):

$$\tau(t) = \frac{\rho(t)}{C_{CO_2} E_{CO_2}(t) - \dot{\rho}(t)} = \frac{\rho^{total}(t) - \rho_{pi}}{C_{CO_2} E_{CO_2}(t) - \dot{\rho}(t)} \quad (D5)$$

The single turnover time $\tau(t)$ is applied to each region at each time step, so that residence time of carbon in the 'region pools' is equal for all regions at each point in time:

$$\dot{\rho}^r(t) = C_{CO_2} \cdot E_{CO_2}^r(t) - \rho^r(t)/\tau(t), \text{ so that} \quad (D2b)$$

$$\dot{\rho}(t) = \sum_{r=1}^R \dot{\rho}^r(t) = \sum_{r=1}^R C_{CO_2} \cdot E_{CO_2}^r(t) - \sum_{r=1}^R \rho^r(t)/\tau(t) = C_{CO_2} \cdot E_{CO_2}(t) - \rho(t)/\tau(t)$$

Removal rate in each 'region pool' thus depends on global carbon-cycle dynamics, including non-linearities and emissions by all other regions. An advantage of this method is that global concentrations can be calculated from emissions using any C-cycle model, like the model described by eq. (C3c). Attribution calculations are not restricted to a linearized model like the impulse response functions in eq. (C3b).

The formulation (D2b), applying a single time-varying global turnover time to each emission region, is equivalent to splitting the change in global concentrations into an increase (emission) term and a decrease (removal) term:

$$\dot{\rho}(t) = \dot{\rho}_+(t) - \dot{\rho}_-(t) \Rightarrow \dot{\rho}_-(t) = \dot{\rho}_+(t) - \dot{\rho}(t) = C_{CO_2} E(t) - \dot{\rho}(t) \quad (D6)$$

The global removal term is then applied to each region scaled by the contribution of that region to global concentrations:

$$\dot{\rho}_-^r(t) = \frac{\rho^r(t)}{\rho(t)} \dot{\rho}_-(t) \quad (D7)$$

The total change in concentrations for region r is then (using (D6) and (D7)):

$$\begin{aligned} \dot{\rho}^r(t) &= \dot{\rho}_+^r(t) - \dot{\rho}_-^r(t) = C_{CO_2} E^r(t) - \frac{\rho^r(t)}{\rho(t)} \dot{\rho}_-(t) = C_{CO_2} E^r(t) - \frac{\rho^r(t)}{\rho(t)} (C_{CO_2} E(t) - \dot{\rho}(t)) = \\ &= C_{CO_2} E^r(t) - \rho^r \frac{C_{CO_2} E(t) - \dot{\rho}(t)}{\rho(t)} = C_{CO_2} E^r(t) - \rho^r(t)/\tau(t) \end{aligned}$$

Forcing

In the default case, non-linearities in radiative forcing are not accounted for. The contribution of region r to total global forcing is calculated as:

$$F^r(t) = \sum_{g=1}^G F_g^{total}(t) \frac{\rho_g^r(t)}{\rho_g(t)} \quad (D8a)$$

The summation is performed over all G greenhouse gases.

For the case of non-linearities, most importantly resulting from the saturation effect in CO₂ forcing, Enting (1998) proposed the following solution:

$$\dot{F}_g^r(t) = \frac{\partial F_g}{\partial \rho_g} \dot{\rho}_g^r \Rightarrow F^r(t) = \sum_{g=1}^G \int_{t_0}^t \frac{\partial F_g}{\partial \rho_g}(t') \cdot \dot{\rho}_g^r(t') dt' \quad (D8b)$$

Temperature Change and Sea Level Rise

As for concentrations, the same equations as applied globally in Appendix C are applied for each region individually, with global forcing replaced by attributed forcing from eq. (D8a) or (D8b). For example, (C11) will become:

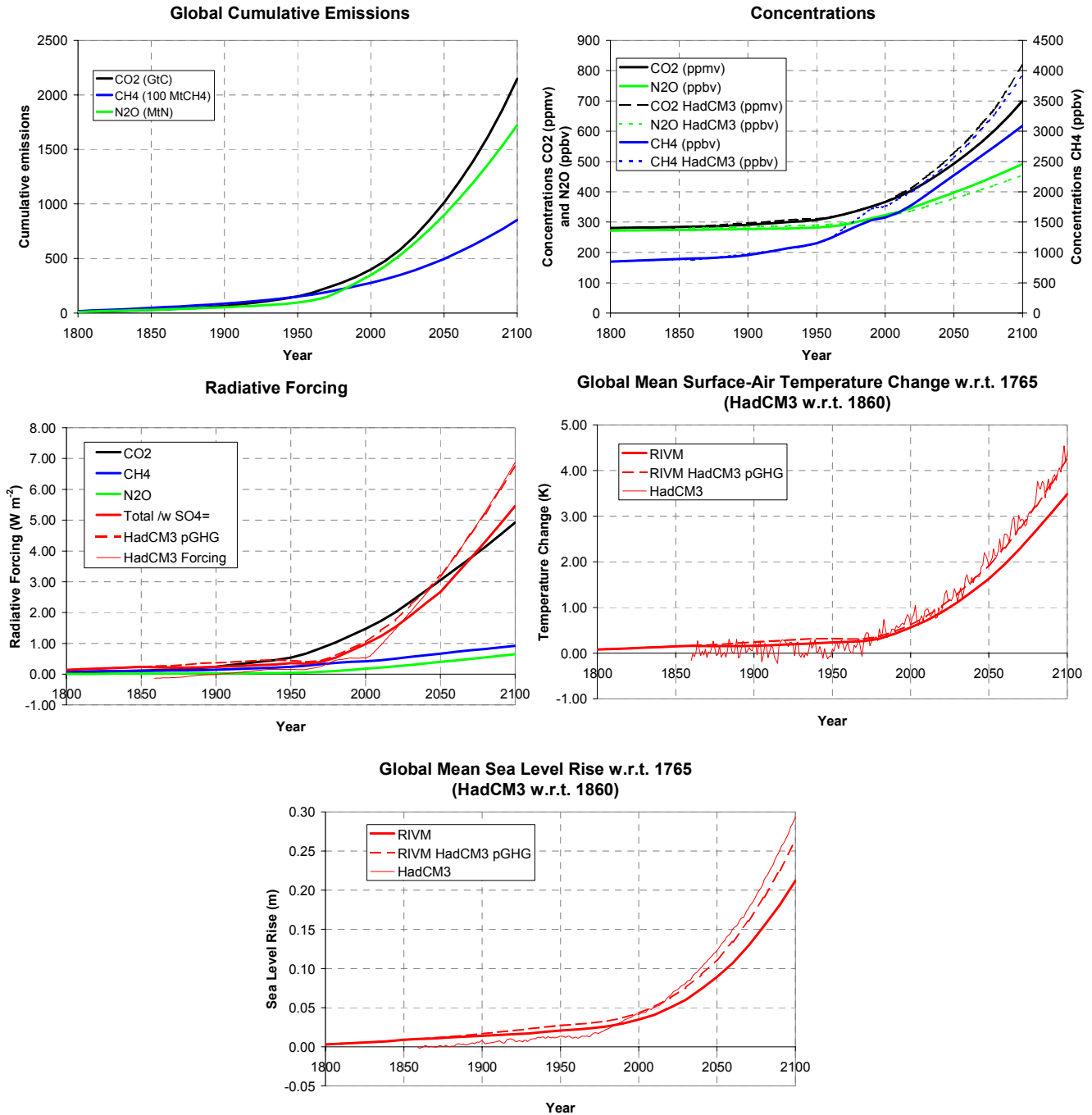
$$\dot{T}^r(t) = \sum_{s=1}^2 \dot{T}_s^r(t) = \sum_{s=1}^2 \left[\frac{T_{eq}}{F_{eq}} \frac{a_s^T}{\tau_s^T} F^r(t) - T_s^r(t) / \tau_s^T \right] \quad (D9)$$

and the convolution integral in (B12):

$$T^r(t) = \frac{T_{eq}}{F_{eq}} \int_{t_0}^t R^T(t-t') F^r(t') dt' \quad (D10)$$

Appendix E RIVM results Phase 1 of UNFCCC-ACCC

In the graphs below, RIVM results for UNFCCC-ACCC phase 1 are presented. For reference, concentrations as used in the HadCM3 experiment are also given, as well as climate impacts of these. Because concentrations used in the HadCM3 experiment deviate somewhat from calculations using the ACCC default model, calculations of radiative forcing, temperature change and sea level rise were also performed with the ACCC default model using the same concentrations as in the HadCM3 experiment.



Appendix F Numerical data

Table F.1 Regional contributions (%) to various *climate indicators*, i.e. cumulative emissions (cum. emis.), CO₂ concentration (CO₂ conc.), radiative forcing (rad.forc.), temperature increase (temp. incr.) and sea level rise (SLR) for evaluation dates: 2000, 2050 and 2100 (start-date: 1890 and **end-date: 2100**) for the IPCC SRES A2 scenario for the ACCC (upper table) and IMAGE-AOS model (lower table).

ACCC model climate Indicators	Evaluation-date 2000				Evaluation-date 2050				Evaluation-date 2100			
	CO ₂ conc	Rad. Forc.	Temp. incr.	SLR	CO ₂ conc	Rad. Forc	Temp. incr.	SLR	CO ₂ conc	Rad. Forc	Temp. incr.	SLR
Canada	1.7	1.7	1.7	1.6	1.5	1.6	1.6	1.7	1.3	1.4	1.5	1.5
USA	22.7	21.2	21.9	23.8	18.2	17.1	17.9	20.0	15.5	14.5	15.0	16.9
Central America	2.7	2.9	3.0	3.1	2.6	2.9	2.9	3.0	3.3	3.5	3.3	3.1
South America	7.1	7.2	7.2	7.0	6.8	7.2	7.3	7.2	6.6	7.6	7.4	7.2
Northern Africa	0.8	0.9	0.9	0.8	1.8	1.9	1.7	1.4	2.9	2.8	2.6	2.1
Western Africa	1.5	1.8	1.7	1.6	1.5	2.1	2.1	1.9	1.7	2.3	2.3	2.2
Eastern Africa	1.0	1.1	1.1	1.0	0.7	1.0	1.0	1.0	0.8	1.0	1.0	1.0
Southern Africa	1.4	1.4	1.4	1.2	1.8	1.9	1.8	1.6	2.4	2.8	2.7	2.2
OECD Europe	15.9	14.5	15.4	17.3	11.3	10.4	11.2	13.2	8.4	7.7	8.3	10.2
Eastern Europe	3.9	3.8	3.9	3.8	3.1	2.9	3.1	3.3	2.3	2.2	2.4	2.8
Former USSR	12.6	12.5	12.8	11.3	8.6	8.9	9.2	10.0	7.5	8.4	8.5	9.0
Middle East	2.6	2.7	2.3	1.8	6.0	5.9	5.4	4.1	8.1	7.4	7.2	6.1
South Asia	6.3	7.5	7.6	8.7	10.6	10.8	10.1	9.3	12.2	11.4	11.4	10.8
East Asia	9.1	10.0	9.1	8.0	15.2	15.1	14.4	12.3	17.6	17.6	17.0	15.1
South East Asia	5.6	5.8	5.4	4.6	5.7	6.0	5.9	5.6	6.0	6.1	6.1	5.9
Oceania	1.1	1.3	1.3	1.2	1.1	1.2	1.2	1.2	1.0	1.2	1.2	1.2
Japan	4.0	3.6	3.4	3.1	3.3	3.0	3.1	3.2	2.3	2.0	2.2	2.6
OECD90	45.4	42.4	43.7	47.1	35.5	33.3	35.1	39.3	28.6	26.9	28.2	32.5
EEUR & FSU	16.5	16.3	16.7	15.1	11.8	11.8	12.3	13.3	9.8	10.6	10.8	11.8
Asia	21.0	23.2	22.0	21.3	31.5	31.9	30.4	27.1	35.7	35.1	34.5	31.8
Africa & Lam	17.1	18.1	17.5	16.5	21.3	23.0	22.3	20.23	25.8	27.4	26.5	23.9
Annex-I	61.9	58.6	60.4	62.2	47.3	45.1	47.3	52.6	38.5	37.5	39.0	44.3
non-Annex I	38.1	41.4	39.6	37.8	52.7	54.9	52.7	47.4	61.5	62.5	61.0	55.7

IMAGE-AOS climate Indicators	Evaluation-date 2000				Evaluation-date 2050				Evaluation-date 2100			
	CO ₂ conc	Rad. Forc.	Temp. incr.	SLR	CO ₂ conc	Rad. Forc	Temp. incr.	SLR	CO ₂ conc	Rad. Forc	Temp. incr.	SLR
Canada	1.7	1.7	1.7	1.6	1.5	1.6	1.6	1.7	1.3	1.4	1.5	1.5
USA	22.7	21.2	21.9	23.8	18.2	17.1	17.9	20.0	15.5	14.5	15.0	16.9
Central America	2.7	2.9	3.0	3.1	2.6	2.9	2.9	3.0	3.3	3.5	3.3	3.1
South America	7.1	7.2	7.2	7.0	6.8	7.2	7.3	7.2	6.6	7.6	7.4	7.2
Northern Africa	0.8	0.9	0.9	0.8	1.8	1.9	1.7	1.4	2.9	2.8	2.6	2.1
Western Africa	1.5	1.8	1.7	1.6	1.5	2.1	2.1	1.9	1.7	2.3	2.3	2.2
Eastern Africa	1.0	1.1	1.1	1.0	0.7	1.0	1.0	1.0	0.8	1.0	1.0	1.0
Southern Africa	1.4	1.4	1.4	1.2	1.8	1.9	1.8	1.6	2.4	2.8	2.7	2.2
OECD Europe	15.9	14.5	15.4	17.3	11.3	10.4	11.2	13.2	8.4	7.7	8.3	10.2
Eastern Europe	3.9	3.8	3.9	3.8	3.1	2.9	3.1	3.3	2.3	2.2	2.4	2.8
Former USSR	12.6	12.5	12.8	11.3	8.6	8.9	9.2	10.0	7.5	8.4	8.5	9.0
Middle East	2.6	2.7	2.3	1.8	6.0	5.9	5.4	4.1	8.1	7.4	7.2	6.1
South Asia	6.3	7.5	7.6	8.7	10.6	10.8	10.1	9.3	12.2	11.4	11.4	10.8
East Asia	9.1	10.0	9.1	8.0	15.2	15.1	14.4	12.3	17.6	17.6	17.0	15.1
South East Asia	5.6	5.8	5.4	4.6	5.7	6.0	5.9	5.6	6.0	6.1	6.1	5.9
Oceania	1.1	1.3	1.3	1.2	1.1	1.2	1.2	1.2	1.0	1.2	1.2	1.2
Japan	4.0	3.6	3.4	3.1	3.3	3.0	3.1	3.2	2.3	2.0	2.2	2.6
OECD90	45.4	42.4	43.7	47.1	35.5	33.3	35.1	39.3	28.6	26.9	28.2	32.5
EEUR & FSU	16.5	16.3	16.7	15.1	11.8	11.8	12.3	13.3	9.8	10.6	10.8	11.8
Asia	21.0	23.2	22.0	21.3	31.5	31.9	30.4	27.1	35.7	35.1	34.5	31.8
Africa & Lam	17.1	18.1	17.6	16.5	21.3	23.0	22.3	20.2	25.8	27.4	26.5	23.9
Annex-I	61.9	58.6	60.4	62.2	47.3	45.1	47.3	52.6	38.5	37.5	39.0	44.3
non-Annex I	38.1	41.4	39.6	37.8	52.7	54.9	52.7	47.4	61.5	62.5	61.0	55.7

Table F.2 Regional contributions (%) to the global-mean surface temperature increase (as percentages of total temperature increase) for the **alternative start-date cases** (including the reference case (REF)) for the evaluation dates: 2000 and 2050 (end-date: 2000) for the IPCC SRES A2 scenario for the ACCC (upper table) and IMAGE-AOS model (lower table).

ACCC-model Start-date-case	Evaluation-date 2000					Evaluation-date 2050				
	1765	1850	1890	1950	1990	1765	1850	1890	1950	1990
	(REF)									
Canada	1.7	1.7	1.7	1.7	1.7	1.7	1.7	1.7	1.7	1.8
USA	21.4	22.0	21.9	19.6	17.9	22.3	23.0	23.0	20.6	19.6
Central America	3.0	3.0	3.0	2.9	2.6	3.0	2.9	2.9	2.8	2.3
South America	7.0	7.1	7.2	7.5	7.0	7.0	7.1	7.2	7.5	6.9
Northern Africa	0.9	0.9	0.9	0.9	1.2	0.8	0.8	0.8	0.8	1.1
Western Africa	1.7	1.7	1.7	1.9	2.3	1.5	1.6	1.6	1.8	2.0
Eastern Africa	1.0	1.0	1.1	1.2	1.4	0.9	1.0	1.0	1.1	1.2
Southern Africa	1.3	1.3	1.4	1.5	1.6	1.3	1.3	1.4	1.5	1.6
OECD Europe	15.8	15.8	15.4	13.6	10.6	16.9	16.9	16.5	14.6	12.3
Eastern Europe	3.9	3.9	3.9	4.1	3.3	3.8	3.9	3.9	4.1	3.3
Former USSR	12.6	12.6	12.8	14.3	12.3	12.1	12.1	12.3	13.9	11.3
Middle East	2.2	2.2	2.3	2.6	3.7	2.2	2.3	2.4	2.7	4.1
South Asia	8.6	7.9	7.6	7.2	8.4	8.1	7.2	6.8	6.0	6.6
East Asia	9.5	9.1	9.1	10.2	13.6	9.0	8.5	8.5	9.7	13.2
South East Asia	5.1	5.2	5.4	6.0	7.3	4.9	5.0	5.1	5.8	7.0
Oceania	1.2	1.2	1.3	1.4	1.5	1.1	1.2	1.2	1.3	1.4
Japan	3.2	3.3	3.4	3.6	3.4	3.5	3.6	3.8	4.1	4.3
OECD90	43.3	44.0	43.7	39.9	35.2	45.4	46.5	46.2	42.4	39.4
EEUR & FSU	16.5	16.5	16.7	18.3	15.6	16.0	15.9	16.2	18.0	14.6
Asia	23.2	22.2	22.0	23.3	29.3	22.0	20.7	20.3	21.4	26.8
Africa & Lam	17.0	17.3	17.6	18.4	19.9	16.6	16.9	17.3	18.2	19.1
Annex-I	59.8	60.5	60.4	58.2	50.8	61.4	62.4	62.4	60.3	54.1
non-Annex I	40.2	39.5	39.6	41.8	49.2	38.6	37.6	37.6	39.7	45.9

IMAGE-AOS Start-date-case	Evaluation-date 2000					Evaluation-date 2050				
	1765	1850	1890	1950	1990	1765	1850	1890	1950	1990
	(REF)									
Canada	2.2	2.2	2.1	1.9	1.7	2.3	2.2	2.1	1.9	1.8
USA	21.9	21.9	22.0	20.8	18.2	22.0	22.1	22.2	21.2	19.7
Central America	2.2	2.2	2.2	2.4	2.9	2.2	2.2	2.2	2.4	2.7
South America	8.0	8.0	8.0	7.8	7.4	8.0	7.9	7.9	7.8	7.4
Northern Africa	0.9	0.9	0.9	0.9	1.2	0.9	0.9	0.9	0.9	1.1
Western Africa	1.8	1.8	1.8	2.0	2.7	1.9	1.9	1.9	2.1	2.6
Eastern Africa	1.2	1.2	1.2	1.2	1.8	1.2	1.2	1.2	1.3	1.8
Southern Africa	1.4	1.4	1.5	1.6	1.9	1.5	1.5	1.5	1.7	1.9
OECD Europe	15.5	15.5	15.4	14.4	11.0	15.7	15.7	15.6	14.8	12.4
Eastern Europe	4.2	4.2	4.2	4.4	3.4	4.0	4.1	4.1	4.3	3.4
Former USSR	12.9	12.9	13.0	14.0	12.3	12.3	12.3	12.4	13.2	11.2
Middle East	2.5	2.5	2.5	2.7	3.8	2.8	2.8	2.8	3.1	4.2
South Asia	5.8	5.7	5.6	5.4	7.1	5.3	5.1	4.9	4.5	5.5
East Asia	10.3	10.2	10.3	11.2	13.9	10.5	10.4	10.4	11.3	13.7
South East Asia	4.6	4.5	4.4	4.2	5.5	4.5	4.4	4.3	4.0	4.9
Oceania	1.8	1.8	1.8	1.7	1.5	1.7	1.8	1.8	1.7	1.4
Japan	3.1	3.1	3.2	3.5	3.6	3.4	3.4	3.5	3.9	4.3
OECD90	44.4	44.5	44.5	42.3	36.0	45.0	45.2	45.2	43.5	39.6
EEUR & FSU	17.1	17.1	17.2	18.4	15.7	16.4	16.4	16.5	17.5	14.6
Asia	20.7	20.5	20.3	20.7	26.5	20.3	19.9	19.6	19.8	24.1
Africa & Lam	17.8	17.9	18.0	18.6	21.7	18.4	18.5	18.6	19.2	21.7
Annex-I	61.4	61.6	61.7	60.7	51.8	61.4	61.6	61.7	61.0	54.1
non-Annex I	38.6	38.4	38.3	39.3	48.2	38.6	38.4	38.3	39.0	45.9

Table F.3 Regional contributions (%) to the global-mean surface temperature increase for the alternative start-date cases for the CDIAC and EDGAR datasets for the evaluation dates: 2000 and 2050 (start-date: 1890 and end-date: 2000) for the IPCC SRES A2 scenario for the ACCC (upper table) and IMAGE-AOS model (lower table).

ACCC-model historical dataset	Evaluation-date 2000					Evaluation-date 2000				
	CDIAC fossil & land use CO2					EDGAR fossil & land use CO2				
	EDGAR non-CO2					EDGAR non-CO2				
	Start-date-case	1765	1850	1890	1950	1990	1765	1850	1890	1950
			(REF)							
Canada	1.7	1.7	1.7	1.7	1.7	1.8	1.8	1.8	1.9	1.9
USA	21.4	22.0	21.9	19.6	17.9	23.1	23.8	22.3	21.7	18.5
Central America	3.0	3.0	3.0	2.9	2.6	3.9	3.7	4.5	3.2	3.0
South America	7.0	7.1	7.2	7.5	7.0	7.0	6.9	8.5	6.0	5.5
Northern Africa	0.9	0.9	0.9	0.9	1.2	1.0	1.0	1.2	1.1	1.3
Western Africa	1.7	1.7	1.7	1.9	2.3	1.6	1.5	1.7	1.5	1.8
Eastern Africa	1.0	1.0	1.1	1.2	1.4	0.8	0.8	1.0	0.8	0.9
Southern Africa	1.3	1.3	1.4	1.5	1.6	1.7	1.6	1.7	1.6	1.6
OECD Europe	15.8	15.8	15.4	13.6	10.6	18.3	17.1	15.7	14.9	11.7
Eastern Europe	3.9	3.9	3.9	4.1	3.3	4.7	4.7	4.5	5.0	3.7
Former USSR	12.6	12.6	12.8	14.3	12.3	11.0	11.7	11.4	13.9	13.2
Middle East	2.2	2.2	2.3	2.6	3.7	2.1	2.2	2.2	2.7	3.9
South Asia	8.6	7.9	7.6	7.2	8.4	5.0	5.0	5.0	5.5	7.1
East Asia	9.5	9.1	9.1	10.2	13.6	9.1	9.2	9.0	10.9	15.7
South East Asia	5.1	5.2	5.4	6.0	7.3	4.4	4.3	5.3	4.2	5.0
Oceania	1.2	1.2	1.3	1.4	1.5	1.3	1.3	1.3	1.4	1.6
Japan	3.2	3.3	3.4	3.6	3.4	3.2	3.2	3.1	3.6	3.7
OECD90	43.3	44.0	43.7	39.9	35.2	47.6	47.3	44.1	43.6	37.4
EEUR & FSU	16.5	16.5	16.7	18.3	15.6	15.7	16.4	15.9	18.9	16.9
Asia	23.2	22.2	22.0	23.3	29.3	18.5	18.5	19.3	20.6	27.7
Africa & Lam	17.0	17.3	17.6	18.4	19.9	18.1	17.8	20.7	16.9	18.0
Annex-I	59.8	60.5	60.4	58.2	50.8	63.3	63.7	60.0	62.5	54.2
non-Annex I	40.2	39.5	39.6	41.8	49.2	36.7	36.3	40.0	37.5	45.8

Meta-IMAGE2.2 historical dataset	Evaluation-date 2000					Evaluation-date 2000				
	CDIAC fossil & land use CO2					EDGAR fossil & land use CO2				
	EDGAR non-CO2					EDGAR non-CO2				
	Start-date-case	1765	1850	1890	1950	1990	1765	1850	1890	1950
			(REF)							
Canada	2.2	2.2	2.1	1.9	1.7	2.2	2.2	2.2	2.0	1.8
USA	21.9	21.9	22.0	20.8	18.2	22.1	22.3	21.5	20.9	18.7
Central America	2.2	2.2	2.2	2.4	2.9	2.1	2.2	2.2	2.4	2.7
South America	8.0	8.0	8.0	7.8	7.4	7.4	7.4	8.0	7.4	7.3
Northern Africa	0.9	0.9	0.9	0.9	1.2	0.8	0.8	0.8	0.8	1.0
Western Africa	1.8	1.8	1.8	2.0	2.7	1.8	1.8	1.9	2.0	2.5
Eastern Africa	1.2	1.2	1.2	1.2	1.8	1.2	1.2	1.2	1.3	1.7
Southern Africa	1.4	1.4	1.5	1.6	1.9	1.5	1.5	1.6	1.6	1.8
OECD Europe	15.5	15.5	15.4	14.4	11.0	15.9	15.7	15.1	14.8	12.5
Eastern Europe	4.2	4.2	4.2	4.4	3.4	4.4	4.5	4.4	4.7	3.5
Former USSR	12.9	12.9	13.0	14.0	12.3	11.9	11.9	11.9	12.8	11.1
Middle East	2.5	2.5	2.5	2.7	3.8	2.8	2.8	2.9	3.1	4.1
South Asia	5.8	5.7	5.6	5.4	7.1	5.4	5.2	5.4	4.8	4.9
East Asia	10.3	10.2	10.3	11.2	13.9	11.1	11.1	11.3	12.2	15.7
South East Asia	4.6	4.5	4.4	4.2	5.5	4.1	4.0	4.2	3.7	4.7
Oceania	1.8	1.8	1.8	1.7	1.5	1.7	1.7	1.8	1.6	1.4
Japan	3.1	3.1	3.2	3.5	3.6	3.5	3.6	3.6	4.0	4.3
OECD90	44.4	44.5	44.5	42.3	36.0	45.5	45.5	44.1	43.3	38.8
EEUR & FSU	17.1	17.1	17.2	18.4	15.7	16.3	16.4	16.3	17.5	14.6
Asia	20.7	20.5	20.3	20.7	26.5	20.6	20.4	20.9	20.7	25.4
Africa & Lam	17.8	17.9	18.0	18.6	21.7	17.6	17.8	18.7	18.6	21.2
Annex-I	61.4	61.6	61.7	60.7	51.8	61.8	61.9	60.4	60.8	53.4
non-Annex I	38.6	38.4	38.3	39.3	48.2	38.2	38.1	39.6	39.2	46.6

Table F.4 Regional contributions (%) to the global-mean surface temperature increase for the alternative end-date cases for the evaluation dates: 2050 and 2100 (start-date: 1890) for the IPCC SRES A2 scenario for the ACCC (upper table) and IMAGE-AOS model (lower table).

ACCC-model End-date-case	Evaluation-date 2050				Evaluation-date 2100			
	1990	2000	2050	2100	1990	2000	2050	2100
Canada	1.7	1.7	1.6	1.6	1.7	1.8	1.6	1.5
USA	23.9	23.0	17.9	17.9	24.0	23.0	18.6	15.0
Central America	3.1	2.9	2.9	2.9	3.1	2.9	2.8	3.3
South America	7.3	7.2	7.3	7.3	7.3	7.2	7.1	7.4
Northern Africa	0.8	0.8	1.7	1.7	0.8	0.8	1.7	2.6
Western Africa	1.5	1.6	2.1	2.1	1.5	1.6	1.9	2.3
Eastern Africa	0.9	1.0	1.0	1.0	0.9	1.0	0.9	1.0
Southern Africa	1.3	1.4	1.8	1.8	1.3	1.4	1.7	2.7
OECD Europe	17.7	16.5	11.2	11.2	17.8	16.6	11.9	8.3
Eastern Europe	4.1	3.9	3.1	3.1	4.1	3.9	3.2	2.4
Former USSR	12.6	12.3	9.2	9.2	12.5	12.2	9.0	8.5
Middle East	1.9	2.4	5.4	5.4	1.9	2.3	5.3	7.2
South Asia	6.8	6.8	10.1	10.1	6.8	6.8	9.9	11.4
East Asia	7.1	8.5	14.4	14.4	7.0	8.4	14.3	17.0
South East Asia	4.6	5.1	5.9	5.9	4.6	5.0	5.6	6.1
Oceania	1.1	1.2	1.2	1.2	1.2	1.2	1.2	1.2
Japan	3.6	3.8	3.1	3.1	3.6	3.8	3.3	2.2
OECD90	48.2	46.2	35.1	35.1	48.3	46.4	36.6	28.2
EEUR & FSU	16.7	16.2	12.3	12.3	16.6	16.1	12.1	10.8
Asia	18.4	20.4	30.4	30.4	18.4	20.2	29.8	34.5
Africa & Lam	16.7	17.2	22.3	22.3	16.7	17.3	21.4	26.5
Annex-I	64.9	62.4	47.3	47.3	64.8	62.5	48.8	39.0
non-Annex I	35.1	37.6	52.7	52.7	35.2	37.5	51.2	61.0

IMAGE-AOS End-date-case	Evaluation-date 2050				Evaluation-date 2100			
	1990	2000	2050	2100	1990	2000	2050	2100
Canada	2.3	2.1	1.7	1.7	2.3	2.2	1.6	1.5
USA	23.3	22.2	17.3	17.3	23.1	22.1	17.4	14.5
Central America	2.0	2.2	2.8	2.8	2.1	2.3	2.7	3.3
South America	8.2	7.9	7.5	7.5	8.2	8.0	7.3	7.3
Northern Africa	0.8	0.9	1.8	1.8	0.9	0.9	1.9	2.8
Western Africa	1.6	1.9	2.2	2.2	1.7	2.0	2.1	2.3
Eastern Africa	1.0	1.2	1.1	1.1	1.1	1.3	1.0	1.1
Southern Africa	1.4	1.5	2.0	2.0	1.4	1.5	2.0	2.8
OECD Europe	17.1	15.6	10.6	10.6	17.2	15.8	10.7	7.7
Eastern Europe	4.4	4.1	3.1	3.1	4.4	4.1	3.1	2.3
Former USSR	13.1	12.4	8.9	8.9	12.6	12.1	8.2	7.7
Middle East	2.2	2.8	5.9	5.9	2.2	2.8	6.2	7.9
South Asia	4.6	4.9	9.8	9.8	5.0	5.2	10.2	11.8
East Asia	8.9	10.4	15.7	15.7	8.7	10.2	16.1	18.0
South East Asia	4.0	4.3	5.2	5.2	4.1	4.3	5.0	5.7
Oceania	1.9	1.8	1.3	1.3	2.0	1.9	1.4	1.2
Japan	3.2	3.5	3.0	3.0	3.0	3.4	3.1	2.1
OECD90	47.8	45.2	33.9	33.9	47.7	45.4	34.2	27.0
EEUR & FSU	17.5	16.5	11.9	11.9	17.0	16.1	11.3	10.0
Asia	17.5	19.6	30.7	30.7	17.8	19.7	31.3	35.5
Africa & Lam	17.1	18.6	23.4	23.4	17.5	18.8	23.2	27.5
Annex-I	65.3	61.7	45.9	45.9	64.7	61.5	45.5	37.0
non-Annex I	34.7	38.3	54.1	54.1	35.3	38.5	54.5	63.0

Table F.5 Regional contributions (%) to the global-mean surface temperature increase (as percentages of total temperature increase) for the **alternative scenario cases** for the evaluation dates: 2000 and 2050 (start-date: 1890 and end-date: 2100) for the ACCC (upper table) and IMAGE-AOS model (lower table).

ACCC-model Scenario-case	Evaluation-date 2050				Evaluation-date 2100			
	A1	A2	B1	B2	A1	A2	B1	B2
Canada	1.4	1.6	1.4	1.7	1.1	1.5	1.2	1.4
USA	15.3	17.9	16.2	18.6	12.4	15.0	13.6	15.1
Central America	3.2	2.9	3.4	2.5	3.3	3.3	3.8	2.6
South America	8.1	7.3	8.3	6.5	7.7	7.4	8.6	6.5
Northern Africa	2.2	1.7	2.2	1.5	3.0	2.6	3.1	2.1
Western Africa	2.3	2.1	2.5	2.0	3.9	2.3	4.0	2.9
Eastern Africa	1.0	1.0	1.2	1.0	1.8	1.0	2.0	1.3
Southern Africa	2.4	1.8	2.4	1.7	3.3	2.7	3.3	2.8
OECD Europe	10.4	11.2	11.0	12.0	8.3	8.3	9.3	9.8
Eastern Europe	2.8	3.1	2.9	3.0	2.1	2.4	2.4	2.6
Former USSR	8.4	9.2	8.4	9.0	6.8	8.5	7.3	8.0
Middle East	6.5	5.4	6.4	4.5	7.5	7.2	8.3	6.0
South Asia	11.5	10.1	10.4	10.7	14.7	11.4	12.0	12.8
East Asia	14.1	14.4	13.0	14.2	14.5	17.0	11.8	15.9
South East Asia	6.4	5.9	6.2	6.7	6.4	6.1	6.0	6.7
Oceania	1.0	1.2	1.1	1.2	0.9	1.2	0.9	1.1
Japan	2.8	3.1	2.9	3.3	2.2	2.2	2.3	2.3
OECD90	30.9	35.1	32.6	36.8	24.9	28.2	27.4	29.8
EEUR & FSU	11.2	12.3	11.2	12.0	9.0	10.8	9.7	10.6
Asia	32.1	30.4	29.6	31.6	35.6	34.5	29.8	35.5
Africa & Lam	25.8	22.3	26.6	19.7	30.5	26.5	33.1	24.1
Annex-I	42.1	47.3	43.9	48.8	33.9	39.0	37.1	40.4
non-Annex I	57.9	52.7	56.1	51.2	66.1	61.0	62.9	59.6

IMAGE-AOS Scenario-case	Evaluation-date 2050				Evaluation-date 2100			
	A1	A2	B1	B2	A1	A2	B1	B2
Canada	1.4	1.7	1.4	1.8	1.1	1.5	1.1	1.4
USA	14.3	17.3	15.2	18.1	11.2	14.5	11.9	14.3
Central America	3.3	2.8	3.5	2.4	3.3	3.3	4.1	2.6
South America	8.5	7.5	8.8	6.8	7.8	7.3	9.0	6.5
Northern Africa	2.4	1.8	2.4	1.6	3.3	2.8	3.6	2.3
Western Africa	2.5	2.2	2.8	2.2	4.3	2.3	4.7	3.1
Eastern Africa	1.2	1.1	1.4	1.2	2.1	1.1	2.3	1.4
Southern Africa	2.6	2.0	2.7	1.8	3.6	2.8	3.8	3.1
OECD Europe	9.6	10.6	10.1	11.3	7.3	7.7	8.0	9.0
Eastern Europe	2.8	3.1	2.8	3.0	1.9	2.3	2.3	2.6
Former USSR	7.9	8.9	7.9	8.5	5.9	7.7	6.1	7.3
Middle East	7.2	5.9	7.2	4.9	8.4	7.9	9.8	6.7
South Asia	11.5	9.8	10.1	10.3	15.8	11.8	12.6	13.4
East Asia	15.3	15.7	14.2	15.5	14.9	18.0	12.3	16.8
South East Asia	5.7	5.2	5.4	5.9	6.0	5.7	5.3	6.2
Oceania	1.2	1.3	1.2	1.4	0.9	1.2	1.0	1.3
Japan	2.7	3.0	2.7	3.2	2.0	2.1	2.0	2.1
OECD90	29.2	33.9	30.7	35.8	22.5	27.0	24.0	28.2
EEUR & FSU	10.7	11.9	10.7	11.5	7.8	10.0	8.4	9.8
Asia	32.5	30.7	29.8	31.8	36.7	35.5	30.2	36.4
Africa & Lam	27.7	23.4	28.9	20.8	32.9	27.5	37.4	25.6
Annex-I	39.8	45.9	41.4	47.4	30.3	37.0	32.4	38.0
non-Annex I	60.2	54.1	58.6	52.6	69.7	63.0	67.6	62.0

Table F.6 Regional contributions (%) to the global-mean surface temperature increase (as percentages of total temperature increase) for the **alternative end-date cases for different IPCC SRES emissions scenarios** for the evaluation date 2100 (start-date: 1890 and end-date: 2100) for the ACCC (upper table) and IMAGE-AOS model (lower table).

ACCC-model Scenarios	Evaluation-date 2100				Evaluation-date 2100				Evaluation-date 2100			
	IPCC SRES scenario A2				IPCC SRES scenario A1				IPCC SRES scenario B1			
End-date cases	1990	2000	2050	2100	1990	2000	2050	2100	1990	2000	2050	2100
	(REF)											
Canada	1.7	1.8	1.6	1.5	1.7	1.8	1.4	1.1	1.7	1.7	1.5	1.3
USA	24.0	23.0	18.6	15.0	24.0	23.1	16.2	12.4	24.2	23.3	18.0	15.9
Central America	3.1	2.9	2.8	3.3	3.1	2.9	3.3	3.3	3.1	3.0	3.4	3.6
South America	7.3	7.2	7.1	7.4	7.3	7.2	8.2	7.7	7.2	7.1	8.1	8.3
Northern Africa	0.8	0.8	1.7	2.6	0.8	0.8	2.2	3.0	0.8	0.8	2.0	2.5
Western Africa	1.5	1.6	1.9	2.3	1.5	1.6	2.1	3.9	1.5	1.6	2.3	3.1
Eastern Africa	0.9	1.0	0.9	1.0	0.9	1.0	1.0	1.8	0.9	1.0	1.1	1.5
Southern Africa	1.3	1.4	1.7	2.7	1.3	1.3	2.3	3.3	1.3	1.3	2.2	2.7
OECD Europe	17.8	16.6	11.9	8.3	17.8	16.7	11.1	8.3	17.9	16.8	12.4	11.0
Eastern Europe	4.1	3.9	3.2	2.4	4.1	3.9	2.9	2.1	4.0	3.9	3.1	2.8
Former USSR	12.5	12.2	9.0	8.5	12.5	12.2	8.2	6.8	12.0	11.9	8.9	8.2
Middle East	1.9	2.3	5.3	7.2	1.9	2.3	6.5	7.5	1.8	2.2	5.6	6.8
South Asia	6.8	6.8	9.9	11.4	6.8	6.8	11.3	14.7	7.5	7.4	9.8	11.0
East Asia	7.0	8.4	14.3	17.0	7.0	8.3	13.3	14.5	7.2	8.3	11.9	11.8
South East Asia	4.6	5.0	5.6	6.1	4.6	5.1	5.9	6.4	4.5	5.0	5.8	5.9
Oceania	1.2	1.2	1.2	1.2	1.1	1.2	1.1	0.9	1.1	1.2	1.1	1.0
Japan	3.6	3.8	3.3	2.2	3.6	3.8	3.0	2.2	3.4	3.6	3.0	2.7
OECD90	48.3	46.4	36.6	28.2	48.4	46.5	32.7	24.9	48.4	46.7	36.0	31.9
EEUR & FSU	16.6	16.1	12.1	10.8	16.6	16.1	11.2	9.0	16.0	15.7	11.9	11.0
Asia	18.4	20.2	29.8	34.5	18.4	20.2	30.6	35.6	19.2	20.7	27.5	28.7
Africa & Lam	16.7	17.3	21.4	26.5	16.6	17.2	25.6	30.5	16.4	16.9	24.6	28.4
Annex-I	64.8	62.5	48.8	39.0	65.0	62.7	43.9	33.9	64.4	62.4	47.9	42.9
non-Annex I	35.2	37.5	51.2	61.0	35.0	37.3	56.1	66.1	35.6	37.6	52.1	57.1

IMAGE-AOS Scenarios	Evaluation-date 2100				Evaluation-date 2100				Evaluation-date 2100			
	IPCC SRES scenario A2				IPCC SRES scenario A1				IPCC SRES scenario B1			
End-date cases	1990	2000	2050	2100	1990	2000	2050	2100	1990	2000	2050	2100
	(REF)											
Canada	2.3	2.2	1.6	1.5	2.4	2.2	1.4	1.1	2.3	2.2	1.3	1.1
USA	23.1	22.1	17.4	14.5	23.3	22.2	14.3	11.2	23.3	22.2	14.6	11.9
Central America	2.1	2.3	2.7	3.3	2.0	2.2	3.4	3.3	2.0	2.2	3.7	4.1
South America	8.2	8.0	7.3	7.3	8.2	8.0	8.7	7.8	8.2	8.0	9.2	9.0
Northern Africa	0.9	0.9	1.9	2.8	0.8	0.9	2.6	3.3	0.8	0.9	2.7	3.6
Western Africa	1.7	2.0	2.1	2.3	1.7	1.9	2.5	4.3	1.6	1.9	2.9	4.7
Eastern Africa	1.1	1.3	1.0	1.1	1.0	1.2	1.2	2.1	1.0	1.2	1.4	2.3
Southern Africa	1.4	1.5	2.0	2.8	1.4	1.5	2.6	3.6	1.4	1.5	2.9	3.8
OECD Europe	17.2	15.8	10.7	7.7	17.3	15.9	9.7	7.3	17.2	15.8	9.8	8.0
Eastern Europe	4.4	4.1	3.1	2.3	4.4	4.1	2.7	1.9	4.4	4.1	2.8	2.3
Former USSR	12.6	12.1	8.2	7.7	12.7	12.1	7.3	5.9	12.8	12.2	7.2	6.1
Middle East	2.2	2.8	6.2	7.9	2.2	2.8	7.6	8.4	2.2	2.8	7.9	9.8
South Asia	5.0	5.2	10.2	11.8	4.9	5.1	12.1	15.8	4.8	5.1	10.5	12.6
East Asia	8.7	10.2	16.1	18.0	8.7	10.2	14.7	14.9	8.8	10.3	14.0	12.3
South East Asia	4.1	4.3	5.0	5.7	4.1	4.3	5.4	6.0	4.1	4.3	5.1	5.3
Oceania	2.0	1.9	1.4	1.2	2.0	1.8	1.2	0.9	2.0	1.8	1.2	1.0
Japan	3.0	3.4	3.1	2.1	3.0	3.4	2.7	2.0	3.1	3.5	2.6	2.0
OECD90	47.7	45.4	34.2	27.0	47.9	45.5	29.2	22.5	47.9	45.5	29.6	24.0
EEUR & FSU	17.0	16.1	11.3	10.0	17.1	16.2	10.0	7.8	17.2	16.3	10.0	8.4
Asia	17.8	19.7	31.3	35.5	17.8	19.6	32.2	36.7	17.7	19.6	29.6	30.2
Africa & Lam	17.5	18.8	23.2	27.5	17.3	18.6	28.6	32.9	17.2	18.6	30.7	37.4
Annex-I	64.7	61.5	45.5	37.0	65.0	61.7	39.2	30.3	65.1	61.8	39.6	32.4
non-Annex I	35.3	38.5	54.5	63.0	35.0	38.3	60.8	69.7	34.9	38.2	60.4	67.6

Table F.7 Regional contributions (%) to the global-mean surface temperature increase (as percentages of total temperature increase) for the **alternative evaluation-date cases** (start-date: 1890 and end-date: 2000 and 2100) for the IPCC SRES A2 scenario for the ACCC (upper table) and IMAGE-AOS model (lower table).

ACCC model Evaluation-date- case	End-date: 2000			End-date: 2100		
	Evaluation dates			Evaluation dates		
	2000 (REF)	2050	2100	2000	2050	2100
Canada	1.7	1.7	1.8	1.7	1.6	1.5
USA	21.9	23.0	23.0	21.9	17.9	15.0
Central America	3.0	2.9	2.9	3.0	2.9	3.3
South America	7.2	7.2	7.2	7.2	7.3	7.4
Northern Africa	0.9	0.8	0.8	0.9	1.7	2.6
Western Africa	1.7	1.6	1.6	1.7	2.1	2.3
Eastern Africa	1.1	1.0	1.0	1.1	1.0	1.0
Southern Africa	1.4	1.4	1.4	1.4	1.8	2.7
OECD Europe	15.4	16.5	16.6	15.4	11.2	8.3
Eastern Europe	3.9	3.9	3.9	3.9	3.1	2.4
Former USSR	12.8	12.3	12.2	12.8	9.2	8.5
Middle East	2.3	2.4	2.3	2.3	5.4	7.2
South Asia	7.6	6.8	6.8	7.6	10.1	11.4
East Asia	9.1	8.5	8.4	9.1	14.4	17.0
South East Asia	5.4	5.1	5.0	5.4	5.9	6.1
Oceania	1.3	1.2	1.2	1.3	1.2	1.2
Japan	3.4	3.8	3.7	3.4	3.1	2.2
OECD90	43.7	46.2	46.4	43.7	35.1	28.2
EEUR & FSU	16.7	16.2	16.1	16.7	12.3	10.8
Asia	22.0	20.3	20.2	22.0	30.4	34.5
Africa & Lam	17.6	17.3	17.3	17.5	22.3	26.5
Annex-I	60.4	62.4	62.5	60.4	47.3	39.0
non-Annex I	39.6	37.6	37.5	39.6	52.7	61.0

IMAGE-AOS Evaluation-date- case	End-date: 2000			End-date: 2100		
	Evaluation dates			Evaluation dates		
	2000 (REF)	2050	2100	2000	2050	2100
Canada	2.1	2.1	2.2	1.7	1.6	1.5
USA	22.0	22.2	22.1	21.9	17.9	15.0
Central America	2.2	2.2	2.3	3.0	2.9	3.3
South America	8.0	7.9	8.0	7.2	7.3	7.4
Northern Africa	0.9	0.9	0.9	0.9	1.7	2.6
Western Africa	1.8	1.9	2.0	1.7	2.1	2.3
Eastern Africa	1.2	1.2	1.3	1.1	1.0	1.0
Southern Africa	1.5	1.5	1.5	1.4	1.8	2.7
OECD Europe	15.4	15.6	15.8	15.4	11.2	8.3
Eastern Europe	4.2	4.1	4.1	3.9	3.1	2.4
Former USSR	13.0	12.4	12.1	12.8	9.2	8.5
Middle East	2.5	2.8	2.8	2.3	5.4	7.2
South Asia	5.6	4.9	5.2	7.6	10.1	11.4
East Asia	10.3	10.4	10.2	9.1	14.4	17.0
South East Asia	4.4	4.3	4.3	5.4	5.9	6.1
Oceania	1.8	1.8	1.9	1.3	1.2	1.2
Japan	3.2	3.5	3.4	3.4	3.1	2.2
OECD90	44.5	45.2	45.4	43.7	35.1	28.2
EEUR & FSU	17.2	16.5	16.1	16.7	12.3	10.8
Asia	20.3	19.6	19.7	22.0	30.4	34.5
Africa & Lam	18.0	18.6	18.8	17.6	22.3	26.5
Annex-I	61.7	61.7	61.5	60.4	47.3	39.0
non-Annex I	38.3	38.3	38.5	39.6	52.7	61.0

Table F.8 Regional contributions (%) to the global-mean surface temperature increase (as percentages of total temperature increase) for the **alternative source cases** for the evaluation dates: 2000, 2050 and 2100 (start-date: 1890 and end-date: 2100) for the IPCC SRES A2 scenario for the ACCC (upper table) and IMAGE-AOS model (lower table).

ACCC model	Evaluation-date 2000			Evaluation-date 2050			Evaluation-date 2100		
	Fos CO2	Ant CO2	All GHG	Fos CO2	Ant CO2	All GHG	Fos CO2	Ant CO2	All GHG
Canada	2.2	1.7	1.7	1.7	1.6	1.6	1.4	1.4	1.5
USA	29.6	23.5	21.9	21.0	19.1	17.9	16.9	16.1	15.0
Central America	1.4	2.8	3.0	2.2	2.6	2.9	2.9	3.1	3.3
South America	2.3	7.2	7.2	4.8	7.0	7.3	5.4	6.5	7.4
Northern Africa	0.7	0.7	0.9	1.7	1.6	1.7	2.8	2.7	2.6
Western Africa	0.4	1.4	1.7	0.9	1.5	2.1	1.4	1.7	2.3
Eastern Africa	0.1	0.9	1.1	0.3	0.8	1.0	0.5	0.8	1.0
Southern Africa	1.3	1.3	1.4	1.7	1.7	1.8	2.4	2.3	2.7
OECD Europe	22.2	16.9	15.4	13.7	12.2	11.2	9.6	9.1	8.3
Eastern Europe	5.3	4.0	3.9	3.7	3.3	3.1	2.7	2.5	2.4
Former USSR	14.6	12.9	12.8	9.5	9.1	9.2	7.9	7.7	8.5
Middle East	2.5	2.2	2.3	6.0	5.5	5.4	8.2	7.8	7.2
South Asia	2.5	6.3	7.6	8.7	9.7	10.1	11.7	12.0	11.4
East Asia	8.4	7.9	9.1	15.7	14.4	14.4	17.9	17.0	17.0
South East Asia	1.4	5.1	5.4	3.5	5.6	5.9	4.7	5.8	6.1
Oceania	1.2	1.0	1.3	1.2	1.1	1.2	1.1	1.0	1.2
Japan	4.3	3.9	3.4	3.6	3.5	3.1	2.5	2.5	2.2
OECD90	59.3	47.0	43.7	41.2	37.4	35.1	31.6	30.1	28.2
EEUR & FSU	19.9	16.9	16.7	13.2	12.4	12.3	10.5	10.2	10.8
Asia	12.2	19.4	22.0	27.9	29.6	30.4	34.2	34.9	34.5
Africa & Lam	8.6	16.6	17.6	17.6	20.6	22.3	23.7	24.8	26.5
Annex-I	79.2	64.0	60.4	54.4	49.8	47.3	42.1	40.3	39.0
non-Annex I	20.8	36.0	39.6	45.6	50.2	52.7	57.9	59.7	61.0

IMAGE-AOS	Evaluation-date 2000			Evaluation-date 2050			Evaluation-date 2100		
	Fos CO2	Ant CO2	All GHG	Fos CO2	Ant CO2	All GHG	Fos CO2	Ant CO2	All GHG
Canada	2.2	2.2	2.1	1.7	1.6	1.7	1.4	1.4	1.5
USA	29.8	23.4	22.0	20.5	18.2	17.3	16.0	15.3	14.5
Central America	1.4	1.9	2.2	2.3	2.6	2.8	3.0	3.1	3.3
South America	2.3	8.1	8.0	5.0	7.3	7.5	5.6	6.5	7.3
Northern Africa	0.6	0.7	0.9	1.8	1.7	1.8	3.0	2.9	2.8
Western Africa	0.4	1.6	1.8	0.9	1.7	2.2	1.5	1.8	2.3
Eastern Africa	0.1	1.0	1.2	0.3	0.9	1.1	0.6	0.9	1.1
Southern Africa	1.3	1.4	1.5	1.7	1.9	2.0	2.5	2.5	2.8
OECD Europe	22.0	16.7	15.4	13.0	11.3	10.6	8.8	8.2	7.7
Eastern Europe	5.3	4.3	4.2	3.6	3.2	3.1	2.5	2.3	2.3
Former USSR	15.0	13.1	13.0	9.5	8.7	8.9	7.6	7.0	7.7
Middle East	2.4	2.5	2.5	6.2	6.1	5.9	8.6	8.5	7.9
South Asia	2.4	4.2	5.6	9.0	9.3	9.8	12.4	12.4	11.8
East Asia	8.1	9.5	10.3	16.1	16.0	15.7	18.4	18.2	18.0
South East Asia	1.4	4.0	4.4	3.7	4.8	5.2	4.8	5.4	5.7
Oceania	1.2	1.7	1.8	1.2	1.3	1.3	1.1	1.1	1.2
Japan	4.2	3.5	3.2	3.6	3.3	3.0	2.4	2.3	2.1
OECD90	59.4	47.6	44.5	40.0	35.7	33.9	29.7	28.3	27.0
EEUR & FSU	20.4	17.5	17.2	13.1	11.9	11.9	10.1	9.3	10.0
Asia	11.8	17.7	20.3	28.8	30.1	30.7	35.6	36.1	35.5
Africa & Lam	8.5	17.3	18.0	18.1	22.2	23.4	24.6	26.3	27.5
Annex-I	79.7	65.0	61.7	53.1	47.6	45.9	39.8	37.6	37.0
non-Annex I	20.3	35.0	38.3	46.9	52.4	54.1	60.2	62.4	63.0

Table F.9 Regional contributions (%) to the global-mean surface temperature increase (as percentages of total temperature increase) for the **non-linearity cases in attributing the CO₂ concentration** (i.e. Bern-TAR IRF, Bern-TAR single-turnover time IRF and IMAGE-AOS single-turnover time IRF) for the evaluation dates: 2050 and 2100 (start-date: 1890) for the IPCC SRES A2 scenario for end-date 2100 (upper table) and end-date 2000 (lower table).

Endate: 2100	Evaluation-date 2050								Evaluation-date 2100					
	IRF-4 lifetime		IRF-single lifetime				IRF-4 lifetime			IRF-single lifetime				
	Bern-TAR (REF)	Bern-Low	Bern-High	BERN-TAR single	Bern-Low	Bern-High	IMAGE-AOS	BERN-TAR	Bern-Low	Bern-High	BERN-TAR single	Bern-Low	Bern-High	IMAGE-AOS
Canada	1.7	1.6	1.8	1.8	1.6	1.8	2.1	1.8	1.6	1.8	1.8	1.7	1.9	2.2
USA	23.0	21.1	24.0	21.4	19.7	22.7	22.2	23.0	21.2	24.1	21.4	19.8	22.6	22.1
Central America	2.9	3.3	2.6	2.7	3.0	2.6	2.2	2.9	3.3	2.7	2.9	3.3	2.7	2.3
South America	7.2	8.7	6.3	7.2	8.6	6.4	7.9	7.2	8.7	6.4	7.4	8.6	6.5	8.0
Northern Africa	0.8	0.9	0.8	0.9	0.9	0.9	0.9	0.8	0.9	0.8	1.0	1.0	1.0	0.9
Western Africa	1.6	1.9	1.4	1.8	2.2	1.5	1.9	1.6	1.9	1.4	1.9	2.3	1.7	2.0
Eastern Africa	1.0	1.3	0.8	1.1	1.4	0.9	1.2	1.0	1.2	0.8	1.2	1.5	1.0	1.3
Southern Africa	1.4	1.4	1.3	1.4	1.5	1.4	1.5	1.4	1.4	1.3	1.5	1.5	1.4	1.5
OECD Europe	16.5	14.9	17.4	15.1	13.8	16.1	15.6	16.6	15.1	17.6	15.5	14.3	16.4	15.8
Eastern Europe	3.9	3.6	4.1	3.9	3.6	4.2	4.1	3.9	3.6	4.1	3.9	3.6	4.1	4.1
Former USSR	12.3	11.8	12.6	12.6	12.0	13.0	12.4	12.2	11.7	12.4	12.0	11.4	12.5	12.1
Middle East	2.4	2.3	2.4	2.8	2.7	2.8	2.8	2.3	2.3	2.4	2.6	2.5	2.7	2.8
South Asia	6.8	7.9	6.0	6.6	7.5	6.0	4.9	6.8	8.0	6.1	7.0	8.1	6.3	5.2
East Asia	8.5	8.4	8.6	9.6	9.4	9.6	10.4	8.4	8.2	8.4	9.3	9.1	9.4	10.2
South East Asia	5.1	6.3	4.5	5.7	7.0	4.9	4.3	5.0	6.1	4.4	5.3	6.3	4.7	4.3
Oceania	1.2	1.2	1.2	1.4	1.3	1.3	1.8	1.2	1.2	1.3	1.6	1.6	1.5	1.9
Japan	3.8	3.7	3.9	3.9	3.7	4.0	3.5	3.7	3.6	3.8	3.6	3.4	3.8	3.4
OECD90	46.2	42.4	48.4	43.6	40.1	46.0	45.2	46.4	42.7	48.6	43.9	40.8	46.1	45.4
EEUR & FSU	16.2	15.3	16.7	16.5	15.6	17.1	16.5	16.1	15.2	16.6	15.9	15.0	16.6	16.1
Asia	20.3	22.5	19.1	21.9	24.0	20.5	19.6	20.2	22.3	18.9	21.7	23.5	20.4	19.7
Africa & Lam	17.3	19.7	15.8	18.0	20.3	16.5	18.6	17.3	19.7	15.9	18.5	20.7	16.9	18.8
Annex-I	62.4	57.7	65.1	60.1	55.7	63.1	61.7	62.5	58.0	65.2	59.8	55.8	62.7	61.5
non-Annex I	37.6	42.3	34.9	39.9	44.3	36.9	38.3	37.5	42.0	34.8	40.2	44.2	37.3	38.5

Endate: 2000	Evaluation-date 2050								Evaluation-date 2100					
	IRF-4 lifetime		IRF-single lifetime				IRF-4 lifetime			IRF-single lifetime				
	Bern-TAR (REF)	Bern-Low	Bern-High	BERN-TAR single	Bern-Low	Bern-High	IMAGE-AOS	BERN-TAR	Bern-Low	Bern-High	BERN-TAR single	Bern-Low	Bern-High	IMAGE-AOS
Canada	1.7	1.6	1.8	1.8	1.6	1.8	2.1	1.8	1.6	1.8	1.8	1.7	1.9	2.2
USA	23.0	21.1	24.0	21.4	19.7	22.7	22.2	23.0	21.2	24.1	21.4	19.8	22.6	22.1
Central America	2.9	3.3	2.6	2.7	3.0	2.6	2.2	2.9	3.3	2.7	2.9	3.3	2.7	2.3
South America	7.2	8.7	6.3	7.2	8.6	6.4	7.9	7.2	8.7	6.4	7.4	8.6	6.5	8.0
Northern Africa	0.8	0.9	0.8	0.9	0.9	0.9	0.9	0.8	0.9	0.8	1.0	1.0	1.0	0.9
Western Africa	1.6	1.9	1.4	1.8	2.2	1.5	1.9	1.6	1.9	1.4	1.9	2.3	1.7	2.0
Eastern Africa	1.0	1.3	0.8	1.1	1.4	0.9	1.2	1.0	1.2	0.8	1.2	1.5	1.0	1.3
Southern Africa	1.4	1.4	1.3	1.4	1.5	1.4	1.5	1.4	1.4	1.3	1.5	1.5	1.4	1.5
OECD Europe	16.5	14.9	17.4	15.1	13.8	16.1	15.6	16.6	15.1	17.6	15.5	14.3	16.4	15.8
Eastern Europe	3.9	3.6	4.1	3.9	3.6	4.2	4.1	3.9	3.6	4.1	3.9	3.6	4.1	4.1
Former USSR	12.3	11.8	12.6	12.6	12.0	13.0	12.4	12.2	11.7	12.4	12.0	11.4	12.5	12.1
Middle East	2.4	2.3	2.4	2.8	2.7	2.8	2.8	2.3	2.3	2.4	2.6	2.5	2.7	2.8
South Asia	6.8	7.9	6.0	6.6	7.5	6.0	4.9	6.8	8.0	6.1	7.0	8.1	6.3	5.2
East Asia	8.5	8.4	8.6	9.6	9.4	9.6	10.4	8.4	8.2	8.4	9.3	9.1	9.4	10.2
South East Asia	5.1	6.3	4.5	5.7	7.0	4.9	4.3	5.0	6.1	4.4	5.3	6.3	4.7	4.3
Oceania	1.2	1.2	1.2	1.4	1.3	1.3	1.8	1.2	1.2	1.3	1.6	1.6	1.5	1.9
Japan	3.8	3.7	3.9	3.9	3.7	4.0	3.5	3.7	3.6	3.8	3.6	3.4	3.8	3.4
OECD90	46.2	42.4	48.4	43.6	40.1	46.0	45.2	46.4	42.7	48.6	43.9	40.8	46.1	45.4
EEUR & FSU	16.2	15.3	16.7	16.5	15.6	17.1	16.5	16.1	15.2	16.6	15.9	15.0	16.6	16.1
Asia	20.3	22.5	19.1	21.9	24.0	20.5	19.6	20.2	22.3	18.9	21.7	23.5	20.4	19.7
Africa & Lam	17.3	19.7	15.8	18.0	20.3	16.5	18.6	17.3	19.7	15.9	18.5	20.7	16.9	18.8
Annex-I	62.4	57.7	65.1	60.1	55.7	63.1	61.7	62.5	58.0	65.2	59.8	55.8	62.7	61.5
non-Annex I	37.6	42.3	34.9	39.9	44.3	36.9	38.3	37.5	42.0	34.8	40.2	44.2	37.3	38.5

Table F.10 Regional contributions (%) to the global-mean surface temperature increase (as percentages of total temperature increase) for the **non-linearity cases in attributing the radiative forcing** for the evaluation dates: 2050 and 2100 (start-date: 1890 and end-date: 2100) for the IPCC SRES A2 scenario for the ACCC (upper table) and IMAGE-AOS model (lower table).

ACCC model Non-linear radiative forcing attribution cases	Evaluation-date 2000		Evaluation-date 2050		Evaluation-date 2100	
	Linear radiative	Non-linear radiative	Linear radiative	Non-linear radiative	Linear radiative	Non-linear radiative
Canada	1.7	1.7	1.6	1.7	1.5	1.5
USA	21.9	22.1	17.9	18.4	15.0	15.8
Central America	3.0	3.0	2.9	3.0	3.3	3.2
South America	7.2	7.2	7.3	7.3	7.4	7.4
Northern Africa	0.9	0.9	1.7	1.7	2.6	2.4
Western Africa	1.7	1.7	2.1	2.1	2.3	2.3
Eastern Africa	1.1	1.1	1.0	1.0	1.0	1.0
Southern Africa	1.4	1.4	1.8	1.8	2.7	2.5
OECD Europe	15.4	15.6	11.2	11.7	8.3	9.1
Eastern Europe	3.9	3.9	3.1	3.1	2.4	2.5
Former USSR	12.8	12.7	9.2	9.5	8.5	8.8
Middle East	2.3	2.2	5.4	5.1	7.2	6.7
South Asia	7.6	7.7	10.1	9.8	11.4	10.9
East Asia	9.1	8.9	14.4	13.8	17.0	16.2
South East Asia	5.4	5.3	5.9	5.8	6.1	6.0
Oceania	1.3	1.3	1.2	1.2	1.2	1.2
Japan	3.4	3.4	3.1	3.1	2.2	2.4
OECD90	43.7	44.1	35.1	36.1	28.2	29.9
EEUR & FSU	16.7	16.6	12.3	12.6	10.8	11.4
Asia	22.0	21.8	30.4	29.4	34.5	33.1
Africa & Lam	17.6	17.5	22.3	21.9	26.5	25.6
Annex-I	60.4	60.7	47.3	48.7	39.0	41.3
non-Annex I	39.6	39.3	52.7	51.3	61.0	58.7

IMAGE-AOS Non-linear radiative forcing attribution cases	Evaluation-date 2000		Evaluation-date 2050		Evaluation-date 2100	
	Linear radiative	Non-linear radiative	Linear radiative	Non-linear radiative	Linear radiative	Non-linear radiative
Canada	2.1	2.1	1.7	1.8	1.5	1.5
USA	22.0	22.2	17.3	18.0	14.5	15.4
Central America	2.2	2.2	2.8	2.8	3.3	3.1
South America	8.0	8.0	7.5	7.6	7.3	7.4
Northern Africa	0.9	0.9	1.8	1.7	2.8	2.5
Western Africa	1.8	1.8	2.2	2.2	2.3	2.3
Eastern Africa	1.2	1.2	1.1	1.1	1.1	1.1
Southern Africa	1.5	1.4	2.0	1.9	2.8	2.6
OECD Europe	15.4	15.7	10.6	11.2	7.7	8.6
Eastern Europe	4.2	4.2	3.1	3.2	2.3	2.5
Former USSR	13.0	12.8	8.9	9.3	7.7	8.3
Middle East	2.5	2.4	5.9	5.5	7.9	7.2
South Asia	5.6	5.7	9.8	9.2	11.8	11.0
East Asia	10.3	10.0	15.7	15.0	18.0	17.2
South East Asia	4.4	4.5	5.2	5.2	5.7	5.5
Oceania	1.8	1.8	1.3	1.4	1.2	1.3
Japan	3.2	3.1	3.0	3.0	2.1	2.3
OECD90	44.5	44.9	33.9	35.3	27.0	29.1
EEUR & FSU	17.2	17.0	11.9	12.4	10.0	10.8
Asia	20.3	20.2	30.7	29.4	35.5	33.7
Africa & Lam	18.0	17.9	23.4	22.9	27.5	26.4
Annex-I	61.7	61.9	45.9	47.7	37.0	39.9
non-Annex I	38.3	38.1	54.1	52.3	63.0	60.1